Effects of *Cercospora* leaf spot disease on sugar beet genotypes with contrasting disease susceptibility

Simone Schmittgen

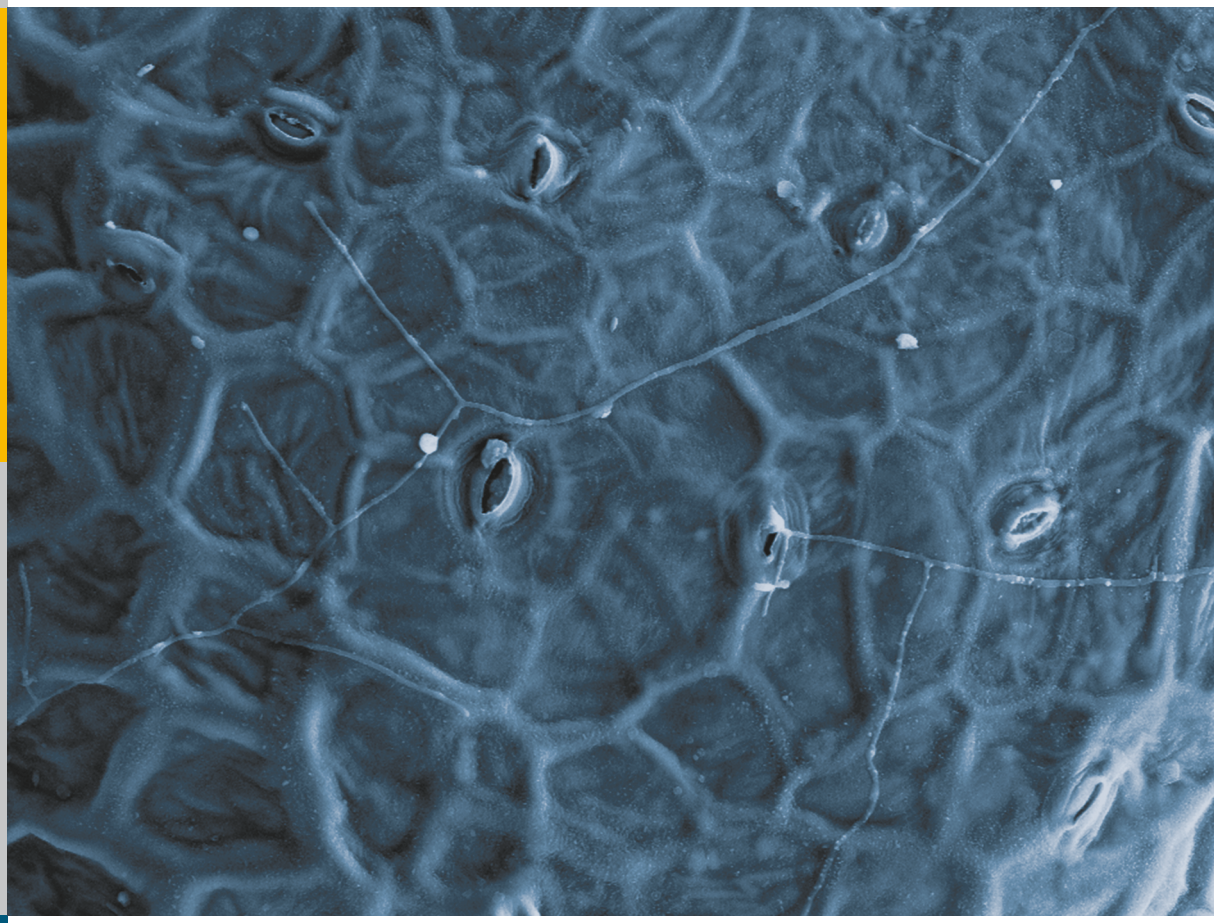

Member of the Helmholtz Association

Energie & Umwelt / Energy & Environment
Band / Volume 244
ISBN 978-3-95806-021-0

JÜLICH FORSCHUNGSZENTRUM

Schriften des Forschungszentrums Jülich
Reihe Energie & Umwelt / Energy & Environment Band / Volume 244

Forschungszentrum Jülich GmbH
Institut für Bio- und Geowissenschaften
Pflanzenwissenschaften (IBG-2)

Effects of *Cercospora* leaf spot disease on sugar beet genotypes with contrasting disease susceptibility

Simone Schmittgen

Schriften des Forschungszentrums Jülich
Reihe Energie & Umwelt / Energy & Environment Band / Volume 244

ISSN 1866-1793 ISBN 978-3-95806-021-0

Bibliographic information published by the Deutsche Nationalbibliothek.
The Deutsche Nationalbibliothek lists this publication in the Deutsche Nationalbibliografie; detailed bibliographic data are available in the Internet at http://dnb.d-nb.de.

Publisher and Distributor: Forschungszentrum Jülich GmbH
Zentralbibliothek
52425 Jülich
Tel: +49 2461 61-5368
Fax: +49 2461 61-6103
Email: zb-publikation@fz-juelich.de
www.fz-juelich.de/zb

Cover Design: Grafische Medien, Forschungszentrum Jülich GmbH

Printer: Grafische Medien, Forschungszentrum Jülich GmbH

Copyright: Forschungszentrum Jülich 2015

Schriften des Forschungszentrums Jülich
Reihe Energie & Umwelt / Energy & Environment, Band / Volume 244

D 61 (Diss. Düsseldorf, Univ., 2014)

ISSN 1866-1793
ISBN 978-3-95806-021-0

The complete volume is freely available on the Internet on the Jülicher Open Access Server (JuSER) at www.fz-juelich.de/zb/openaccess.

Neither this book nor any part of it may be reproduced or transmitted in any form or by any means, electronic or mechanical, including photocopying, microfilming, and recording, or by any information storage and retrieval system, without permission in writing from the publisher.

Selbstständigkeitserklärung

Ich versichere an Eides statt, dass die Dissertation von mir selbständig und ohne unzulässige fremde Hilfe unter Beachtung der „Grundsätze zur Sicherung guter wissenschaftlicher Praxis an der Heinrich-Heine-Universität Düsseldorf“ erstellt worden ist. Diese Dissertation wurde bisher in dieser oder ähnlicher Form noch bei keiner anderen Institution eingereicht. Ich habe bisher keine erfolglosen Promotionsversuche unternommen.

Jülich, den

Simone Schmittgen

Carpe diem!

Horaz (65 v. Chr. - 8 v. Chr.)

Abstract

The fungal pathogen *Cercospora beticola* causes the most destructive foliar disease of sugar beet, namely *Cercospora* leaf spot (CLS), which results in economically important yield losses. Current breeding efforts aim at developing sugar beet lines with lower fungal susceptibility as well as high productivity to ensure reduced fungicide applications in the context of integrated pest management. However, the main challenge remains to select sugar beet genotypes that produce the required yield quality and quantity, and to quantify their defense ability. Well-established visual disease scoring can be supported and supplemented by new techniques that enable earlier disease detection and genotype resistance classification. In this thesis, visual disease scoring was combined with novel invasive and non-invasive techniques to analyze shoot and root disease responses to *Cercospora* infection.

The fungal growth within the sugar beet leaf tissue was quantified using molecular analysis of the fungal calmodulin gene. This allows for the pre-selection of resistant genotypes before disease symptoms were visible. It could be shown that plants with high susceptibility (HS) allowed a stronger fungal colonization in the leaf tissue than ones with low susceptibility (LS). These results correlated with the respective disease severity. The HS genotypes consistently displayed more severe disease symptoms than LS plants. In particular, the moderately susceptible (MS) genotype seemed to be a promising candidate according to its variable response indicating a more adaptable reaction to changing environmental conditions. Therefore, this MS genotype might produce more yield under low-to-moderate disease pressure compared with HS plants, which would be comparatively more strongly infected and deliver reduced yield.

The cuticle forms a barrier between the plant and the environment and therefore provides resistance against pathogens. Cuticular wax may affect host-pathogen recognition and conidia adhesion on the leaf surface. In this study, LS plants were found to contain larger amounts of cuticular waxes. Mature leaves, which showed reduced fungal colonization, also had higher wax levels than immature leaves. Further experiments are needed to investigate the precise role of sugar beet cuticular waxes on *C. beticola* infections.

Field evaluations are essential for the characterization and selection of sugar beets with increased resistance, because controlled greenhouse experiments differ from agricultural growth conditions. In this regard, spectral sensors are the interface between field and greenhouse. They can be used to monitor disease progression non-invasively before and after symptom development, and to quantify leaf damage with the use of vegetation indices in a breeding scenario. In a field experiment of this study, the leaf signatures of infected sugar beet genotypes were quantified at a progressed disease stage. It could be shown that vegetation indices for quantifying canopy greenness (NDVI – Normalized Difference Vegetation), leaf water content (LWI) and *Cercospora* leaf spot disease (CLSI) correlated significantly with plant susceptibility. Laboratory measurements of leaf transmittance using the new

HyperART-system, which is developed in a complementary PhD project at IBG-2, enables leaf absorbance quantification and provides insight into the signature changes at the first signs of CLS.

Detailed time-courses of foliar disease effects on taproot development were monitored and quantified by Magnetic Resonance Imaging (MRI). An early growth reduction within two weeks after inoculation was investigated during a low foliar symptom expression phase according to initial measurements of cell damage caused by fungal colonization and ramification in the leaf tissue. Plants displayed an increased growth of cambial rings that were connected to new, non-inoculated leaves. This response partly compensated for the reduced growth of cambial rings that were associated with inoculated leaves. The sugar beet genotypes showed different taproot growth after CLS infestation. These plant responses on root performance could be associated with susceptibility. For resistance breeding, these might be potential traits to select candidate genotypes and to elucidate the physiologically underlying mechanisms to ensure both yield quantity and quality.

Using a combination of invasive and non-invasive methods, this study revealed plant responses above and below the ground during foliar infection at different disease stages. Moreover, a full picture of sugar beet responses to *Cercospora* leaf spot was obtained. In addition to visual disease scoring, plant resistance can be verified with novel detection systems such as MRI, molecular analysis and spectral imaging, which provide a more detailed view of disease progression. Therefore, the new techniques can assist breeders to identify sugar beet varieties with increased fungal resistance. In particular, the early detection of reduced taproot growth with MRI has the potential to facilitate the discovery of traits associated with enhanced resistance.

Zusammenfassung

Die *Cercospora*-Blattfleckenkrankheit kann weltweit zu erheblichen ökonomischen Ernteverlusten an Zuckerrüben führen. Durch die im Rahmen des integrierten Pflanzenschutzes geforderte Chemikalienreduktion gewinnt der Aspekt der pflanzlichen Pathogenresistenz an Bedeutung. Aufgrund dessen sind insbesondere Genotypen mit geringer Anfälligkeit und zeitgleich hohem Ernteertrag für die Züchtung gefragt. Bei der Auswahl geeigneter Genotypen spielen Selektionsmethoden wie die klassische Bonitur der Befallsstärke eine wesentliche Rolle. Eine Ergänzung ist durch moderne Methoden möglich, durch die eine frühzeitigere Krankheitserkennung und Klassifizierung von Genotypen in Resistenzklassen erzielt werden kann. In dieser Dissertation wurden Pflanzenreaktionen im Spross- und Wurzelwachstum verschiedener Zuckerrübengenotypen während des Blattkrankheitsverlaufes mittels invasiver sowie nicht invasiver Methoden quantifiziert.

Die Quantifizierung des Pilzwachstums im Blattgewebe erlaubt bereits vor Auftreten der ersten Krankheitssymptome eine Einstufung der Zuckerrübengenotypen in Resistenzklassen. Mit Hilfe der quantitativen real-time PCR Analyse des *C. beticola* Calmodulingens zeigte sich, dass Pflanzen mit erhöhter Anfälligkeit eine größere Pilzmenge im Blattgewebe aufwiesen. Diese dem Pathogen gegenüber anfälligeren Pflanzen zeigten eine reproduzierbare Antwortreaktion, die ein erhöhtes Pilzwachstum und eine höhere Befallsstärke beinhaltete. Insbesondere der moderat anfällige Genotyp zeigte eine variable Reaktion, die auf eine bessere Anpassung an vorherrschende Umwelteinflüsse hindeutete und diesen als vielversprechenden Kandidaten der Resistenzzüchtung erschienen ließ. Bei einem gering bis mäßig starkem Krankheitsdruck wäre zum einen der stark anfällige Genotyp bereits stärker befallen und in Biomasse reduziert und zum andern der weniger anfällige Genotyp noch nicht vergleichbar schnell gewachsen, um einen erhöhten Ernteertrag aufweisen zu können.

Die Kutikula bildet eine Barriere zwischen Pflanze und Umwelt und verleiht Resistenz gegen Pathogene. Kutikuläre Wachse können sich auf die Pflanze-Pathogen-Erkennung sowie auf die Sporenanhaftung auf der Blattoberfläche auswirken. In dieser Studie wies der weniger anfällige Genotyp eine erhöhte Wachsmenge auf. Auch ausgewachsene Blätter zeigten neben einem geringen Pilzwachstum eine erhöhte Wachsmenge. Weitere Untersuchungen sind diesbezüglich notwendig, um den möglichen Einfluss der Wachsschicht auf die pflanzliche Abwehr und die Pflanze-Pathogen Erkennung zu ermitteln.

Feldevaluierungen sind für die Auswahl und Charakterisierung von Genotypen mit verstärkter Resistenz unerlässlich, da sich die Bedingungen im kontrollierten Gewächshaus und auf agrarwirtschaftlichen Flächen unterscheiden. Diesbezüglich stellen Spektrometer aufgrund ihres breiten Anwendungsbereiches eine Schnittstelle zwischen Gewächshaus und Feld dar. Basierend auf der Blattsignatur ermöglichen diese eine Überprüfung des Krankheitsverlaufes vor und nach Sichtbarwerden von

Blattsymptomen. Die aus dem Feldversuch gewonnenen Vegetationsindices des Chlorophyllgehaltes (NDVI – Normalized Difference Vegetation), des Wassergehaltes (LWI - Leaf Water Index) und der *Cercospora*-Befallsstärke (CLSI - *Cercospora* Leaf Spot Index) zeigten eine signifikante Korrelation mit den Resistenzklassen der einzelnen Genotypen. Unter Laborbedingungen kann die in einer parallelen Dissertation am IBG-2 entwickelte HyperART-Station möglicherweise dazu genutzt werden die Krankheitsentwicklung vor Auftreten der Blattsymptome zu detektieren, da zusätzlich zum reflektierten auch das transmittierte Licht erfasst wird.

Detaillierte Zeitverläufe des Rübenkörperwachstums während der Krankheitsentwicklung zeigten bereits zwei Wochen nach Inokulation einen mit Magnetresonanz Imaging (MRI) quantifizierbaren Reduktionseffekt, der bei einem bis dahin geringen Blattschaden von unter 1% befallener Blattfläche auftrat. Inokulierte Pflanzen wiesen ein verstärktes Wachstum der Kambienringe auf, die mit neugebildeten, nicht inokulierten Blättern versorgt wurden. Dies kompensierte teilweise das reduzierte Wachstum der unzureichend versorgten, mit infizierten Blättern verbundenen Kambienringe. Die Genotypen zeigten Unterschiede im Rübenkörperwachstum sowie in der krankheitsinduzierten Reaktion. Diese Unterschiede im Wurzelwachstum ließen sich mit der Genotypenanfälligkeit in Verbindung setzen. Hierdurch lassen sich möglicherweise neue Selektionseigenschaften erschließen, die sowohl Anwendung in der Resistenzzüchtung finden als auch physiologischen Untersuchungen der zugrundeliegenden Mechanismen dienen könnten.

In dieser Studie wurden Effekte der Blattfleckenkrankheit in Spross- und Wurzelentwicklung während verschiedener Krankheitsstadien mit invasiven und nicht invasiven Methoden quantifiziert. Darüber hinaus konnte ein Gesamtbild krankheitsinduzierter Reaktionen gewonnen werden. Der Anfälligkeitsgrad der Genotypen wurde auf verschiedenen Ebenen mittels klassischer Bonitur sowie modernen Detektionssystemen wie MRI, molekularer Analyse und spektralen Messungen erfasst, wodurch ein detaillierter Einblick in die Krankheitsentwicklung ermöglich werden konnte. Diese Methoden eignen sich demnach für die Resistenzzüchtung von Zuckerrüben, um Genotypen mit geringer Anfälligkeit gegenüber *C. beticola* zu charakterisieren. Insbesondere die frühe und folglich fortschreitende Reduktion des Rübenkörperwachstums bietet Gelegenheit bestimmte Wurzel- oder Wachstumseigenschaften zu ermitteln, die als Selektionsfaktoren in die Zuckerrübenresistenzzüchtung einfließen können.

Contents

Abbreviations

The alipathic compounds of wax analysis were described with a simplified nomenclature. For example the Hexacosanol, or Hexacosan-1-ol (IUPAC) with the structure formula $C_{26}H_{54}O$, is described as C_{26} alcohol.

BSTFA	N,O-Bis(trimethylsilyl)trifluoroacetamide
CLS	*Cercospora* Leaf Spot
CTAB	Cetyltrimethylammoium bromide
DNA	Desoxyribonucleic acid
Dpi	Days post inoculation
EDTA	Ethylenediaminetetraacetic acid
ETR	Electron transport rate
F_m	Maximal fluorescence in the dark adapted state
$F_{m'}$	Maximal fluorescence in the light adapted state
F_0	Minimal fluorescence in the dark adapted state
F_v	Variable fluorescence
FOV	Field of View
GC	Gas chromatography
GC-MS	Mass spectrometer
GC-FID	Flame ionization detector
HK	Hexokinase
HS	Highly susceptible
Inv	Invertase
G6PDH	Glucose-6-phosphate dehydrogenase
ITS	Internal Transcript Spacer Region
LS	Lowly susceptible
MS	Moderately susceptible
NADPH	Nicotinamide adenine dinucleotide phosphate
PCR	Polymerase Chain Reaction
PGI	Phosphoglucoisomerase
PVP	Polyvinylpyrrolidone
PR	Pathogenesis-related
PSII	Photosymstem II
RNA	Ribonucleic acid
rRNA	Ribosomal Ribonucleic acid
ROS	Reactive oxygen species
Sems	Spin echo multi slice
TE	Echo time
TR	Repetition time
SE	Standard error
Y(II)	Actual quantum yield of PSII

1 Introduction

Cercospora leaf spot (CLS) is one of the most destructive foliar diseases of sugar beet (*Beta vulgaris L. ssp. vulgaris*) and can lead to economically important yield losses (Malandrakis et al., 2006; Skaracis et al., 2010; Weiland and Koch, 2004). Crop losses of sugar beet can reach 40% and result in complete yield loss in the absence of fungicide treatments (Rossi et al., 2000; Shane and Teng, 1992). Current disease management practices are based on a combination of crop rotation, fungicide application, and cultivation of resistant sugar beet cultivars (Shane and Teng, 1992). However, due to increasing fungal resistance to different chemical classes of fungicides (Weiland and Koch, 2004) and the demand for integrated pest management, fungal resistance of sugar beet plays an increasingly important role in the preventive control of CLS epidemics (Rossi, 1995).

1.1 Host crop *Beta vulgaris*

Beta vulgaris L. ssp. vulgaris belongs to the *Amaranthaceae* family of angiosperms. Sugar beet is cultivated worldwide in moderate climatic zones being harvested usually 5 to 9 months after sowing depending on seasonal climate conditions. During the growing season 2012/13 for example, 1.6 million hectares of cropland were used for sugar beet cultivation in Europe[1]. With more than 4 x 10^5 ha of field area, Germany was the leading sugar beet cultivation country in Europe, followed by France, Poland and Great Britain. The worldwide sugar production amounts annually to ca. 145 million tons with an average consumption of 24 kg per capita[2] provided by sugar beet for approximately 25% and sugar cane (*Saccharum officinarum L.*) for about 75%. Chemical application to plants can result in the rapid development of pathogen resistance. Previously, extensive application of certain fungicides, such as benzimidazoles, sterol biosynthesis inhibiting triazoles und strobilurines, led to a more frequent appearance of resistant *Cercospora* isolates and to a total loss of disease control in the early 1970s (Karaoglanidis et al., 2000; Malandrakis et al., 2006; Weiland and Koch, 2004). Integrated plant protection aims to balance agricultural, ecological and toxicological application methods in order to prevent yield losses - damage thresholds (“Schadensschwelle”) (Hallmann et al., 2009). The European guideline (91/414/ECC) of integrated pest management (IPM) is generally defined as “the careful consideration of all available pest control techniques and subsequent integration of appropriate measures that discourage the development of pest populations and keep pesticides and other interventions to levels that are economically justified and reduce or minimize risks to human health and the environment. IPM emphasizes the growth of a healthy crop with the least possible

[1] www.zuckerverbaende.de/zuckermarkt/zahlen-und-fakten/eu-zuckermarkt/ruebenanbau.html
[2] www.zuckerverbaende.de/zuckermarkt/zahlen-und-fakten/weltzuckermarkt/erzeugung-verbrauch.html

disruption to agro-ecosystems and encourages natural pest control mechanisms."[3]. Significant increase of yield quantity and quality could be achieved by a combination of crop rotation, fungicide application, mineral fertilization and cultivation of resistant sugar beet cultivars (Hallmann et al., 2009; Li et al., 2011; Shane and Teng, 1992). Forecasting models and public services support the decision of chemical application based on the current infection status in Germany and other producing countries. For example, the infection epidemiology model of Wolf et al. (1998) calculated a tolerance limit of 5% necrotic leaf area at season ending. Below this disease threshold, sufficient product quantity and quality is achieved (Wolf et al., 1998).

Cultivated sugar beets are biennial plants requiring an overwintering (vernalization) period to start their reproductive phase leading to stem elongation and flowering initiation (bolting phase). Early bolting can lead to decreased sugar content and mechanical problems during harvesting and sugar extraction (Boudry et al., 1994; Longden and Goddard, 1987). Bolting is influenced by light, temperature and internal physiological mechanisms (Lexander, 1980), and is regulated by the major bolting gene B (Boudry et al., 1994). The bolting locus B represents a master switch distinguishing between an annual and a biannual plant life cycle. This locus is absolutely necessary for flowering according to its regulatory response to long days (photoperiod) and cold periods (vernalisation) (Pin et al., 2012). During the domestication process, sugar beets were selected to have a loss-of-function allele of locus B, leading to reduced sensitivity to the photoperiod and the biennal life cycle (Bradshaw et al., 2010). In addition, breeding methods in France lead to a rapid increase in sugar yield (Bradshaw et al., 2010; McFarlane, 1971). Further improvement was achieved using better optimized plant cultivation methods such as soil management, fertilization and plant protection (Bradshaw et al., 2010). Cultivation costs were reduced while sugar yields increased. The adoption of molecular-assisted breeding methods and the introduction of hybrid lines allowed an annual increase of sugar yield per hectare of about 1.4% in European countries (Bradshaw et al., 2010; Draycott, 2008).

The anatomy of sugar beet can be divided into a shoot part, the leaf rosette, and a root part, the sugar storage taproot, separated by a crown and neck, which are the epi- and hypo-cotyl, respectively (Fig. 1 A). Cross-sections show a varying number of concentric cambial rings (Fig. 1 B), usually between eight to fourteen depending on cultivar and developmental stage (Artschwager, 1930; Bradshaw et al., 2010). The sugar beet specific secondary thickening of the taproot results from the additional xylem and phloem production of each cambial ring. Each mature cambial ring shows a vascular xylem and a parenchymatic phloem region which are separated by a cambium meristem. Sugar is stored in the phloem parenchyma of each ring. Due to cell division and enlargement, each ring increases in thickness over time. Ring thickening starts with the inner cambial rings, whereas outer ones become visible

[3] www.fao.org/agriculture/crops/core-themes/theme/pests/ipm/en/

later in development (Artschwager, 1926). As described by Zamski and Azenkot et al. (1981), the first cambial ring develops from the procambium located between the primary phloem and xylem and from the pericycle and interfascicular parenchyma of the diarch root. The secondary cambial ring develops from this primary phloem. Subsequently, each ring originates from the previous, inner core cambium and differentiates in the outermost parenchyma.

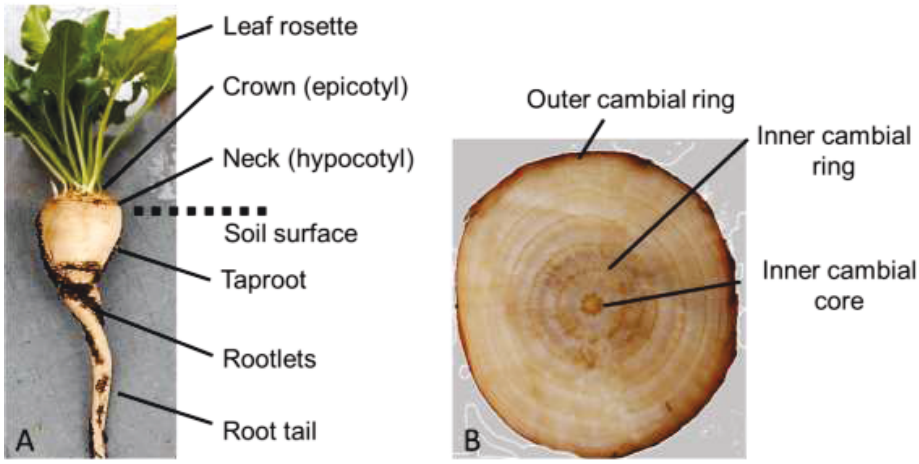

Fig. 1: Sugar beet anatomy. (A) Image of an excavated sugar beet. (B) Image of a taproot in cross-section cut at the position representing the thickest cross-sectional diameter.

Invasive studies of the vascular system of sugar beet showed that successive cambial rings were provided with photoassimilates from different leaves that were connected to the root system by several vascular traces. Besides the cotyledons, which showed two vascular traces, and the first true (mature) leaves with seven traces, all following leaves are connected to the taproot with eight to ten vascular traces (Zamski and Azenkot, 1981). It could be shown that the first three, true leaves supplied the first cambial ring. The first four leaves supplied the second cambial ring. Therefore, it was concluded that each true leaf provided at least two cambial rings with photoassimilates (Zamski and Azenkot, 1981). During seasonal secondary thickening of the taproot, sucrose is simultaneously and continuously accumulated in the storage parenchyma (Milford, 1973; Trebbi and McGrath, 2009). In sugar beets photoassimilates are transported from the source leaves to the storage tissue in the taproot that represents the sink organ (Fieuw and Willenbrink, 1990; Schneider et al., 2002). Biotic stress can result in the down-regulation of photosynthetic gene expression (Berger et al., 2004) and altered source-sink metabolism. Instead of storing incoming photoassimilates, sink resources were reduced to activate defense responses (Leal and Lastra, 1984). It could be shown that pathogen attack of leaves

resulted in co-regulated changes of defense, sink strength and photosynthesis gene expression *in planta* (Berger et al., 2004). This study indicates that plants respond 24 h after foliar infestation with an increased expression of the sink-specific extracellular invertase as well as two days after inoculation with a reduced sugar content in the leaves. Based on chlorophyll fluorescence imaging, inhibition of photosynthetic electron transport was shown to be restricted to the infection site, while the photosynthesis of the remaining leaf area did not change at this stage (Berger et al., 2004). It had been shown that some pathogens increase (Robert et al., 2006; Scholes, 1992) and others decrease the photosynthesis of undamaged leaf parts (Berger et al., 2004; Rabbinge et al., 1985), whereas other studies showed no pathogen effect on photosynthesis (Van Oijen, 1990; Waggoner and Berger, 1987). For *Cercospora* infection on sugar beet in laboratory conditions, it has been shown that photosynthesis was reduced shortly before and after disease onset using chlorophyll fluorescence imaging (Chaerle et al., 2007) and after a disease severity of 3-6% using pulse-amplified modulation (PAM) fluorometer (Levall and Bornman, 2000). It is therefore unclear, how rapidly sugar beet taproot growth and regulation of sink strength reacts to CLS to fluctuating levels of solar radiation in greenhouse.

Pathogens can invade plants by penetrating the cuticle, the largest interface between plants and the environment, through wounds or its stomatal openings (Agrios, 1997; Pool and McKay, 1916). Stomatal density changes throughout plant developmental stages until leaf maturity. Furthermore, the number of stomata on upper and lower surfaces can differ between sugar beet leaves depending on foliage color, size and thickness (Artschwager, 1926). However, it is unclear if higher stomatal densities result in an increased fungal penetration (Solel and Minz, 1971). The cuticle provides protection thanks to its chemical composition and physical structure. It comprises two main components, first the intracuticular waxes, and second the soluble lipids, also known as epicuticular waxes (Fig. 2; Bargel et al., 2006).

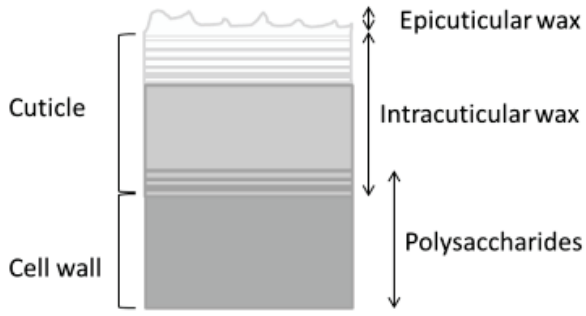

Fig. 2: Hypothetical scheme of the plant cuticle structure and its main components (modified after Bargel et al. 2006).

The cuticle is hydrophobic and protects plants from water loss due to transpiration (King and von Wettstein-Knowles, 2000). Furthermore, it represents a physical barrier to biotic stresses (Bargel et al., 2006; Campbell et al., 1980; Gniwotta et al., 2005; Kolattukudy, 1970; Kunst and Samuels, 2003). Plant waxes are a complex mixture of long-chain alipathic and aromatic compounds. Main component classes are usually hydrocarbons (*n*-alkanes), wax esters, free fatty alcohols and fatty acids (Kolattukudy, 1970). Wax composition can be analyzed by gas chromatography (GC) combined with either mass spectroscopy (MS) or flame ionization detection (FID) (Jetter et al., 2008; Koch and Ensikat, 2008). The majority of resembling derivates of n-acyl alkanes with chain length from C_{20}-C_{40} can be substituted by several functional groups (-hydroxyl, -carboxyl, -ketoyl) to fatty acids, primary alcohols, aldehydes, β-diketones and secondary alcohols (Jetter et al., 2008). Cuticular waxes form complex and varied three-dimensional crystalline microstructures, e.g. platelets, rodlets and tubules (Baker and Hunt, 1981), which crystal types are based on chemical wax composition and on self-assembly processes (Koch et al., 2006a; Von Wettstein-Knowles, 1974). The epicuticular wax layer plays an important defense role on the leaf surface due to its water-repelling properties and host-pathogen recognition. According to microstructures of the cuticle such as wax crystals and trichomes, there is a reduced contact area and reduced adhesion (interfacial tension) of droplets on the leaf surface (Barthlott and Neinhuis, 1997; Neinhuis and Barthlott, 1997). Some fungi such as *C. beticola* depend on wet host interface for conidia germination (Allen et al., 1991; Campbell et al., 1980; Gniwotta et al., 2005). Therefore, the anti-adhesive properties and the cleaning feature, termed “lotus effect”, control the amount of contaminating spores which exist on the leaf surface at a given time. Attaching pathogens can be washed off in droplets rolling off the leaf surface (Campbell et al., 1980; Singh, 2005). Besides repellency, it also represents a physical barrier to pathogen penetration (Bargel et al., 2006; Campbell et al., 1980; Kolattukudy, 1970; Kunst and Samuels, 2003). Cuticular compounds are also important signals in host-pathogen and insect recognition (Gniwotta et al., 2005; Nielsen et al., 2000). Antifugal proteins purified from the intercellular washing fluid of sugar beet leaves were found to reduce culture growth of *Cercospora beticola* in laboratory experiments (Kristensen et al., 2000; Nielsen et al., 1996). Yet, little is known about the influence of leaf waxes on the interaction of sugar beet and *Cercospora beticola* under greenhouse and field conditions. In this study, the analysis of sugar beet genotypes revealed larger total wax amounts in lowly susceptible plants as well as in mature leaves, which were less infected than immature ones.

To cope with both biotic and abiotic challenges, plants had to develop defense strategies such as the cuticle, which provides passive protection against water loss and pythopathogen invasion. Generally, for a successful infestation the compatibility between host plant and phytopathogen is essential (Agrios, 1997). Plants show a basic resistance against pathogens classifying them as unsuitable host or non-host (Heath, 1991). A successful infection results from the interaction of a host plant and

with a compatible pathogen (Prell, 1996). When pathogens are able to overcome the basal host resistance, plant invasion can only be prevented by pathogen-specific resistance genes. Using this secondary defense response, pathogens can be contained (De Wit, 2007; Prell, 1996). Preformed barriers, e.g. cuticular and its wax composition, prevent pathogen attachment on the leaf surface and penetration into the leaf tissue. Expression of specific pathogenesis-related (PR) genes was shown to be involved in pathogen defense during compatible interactions. Weltmeier et al. (2011) showed that under severe disease pressure, polygenic resistant cultivars had two-fold higher defense gene expression compared with the susceptible cultivar. Therefore, in sugar beet a high number of defense genes as well as an early response in gene expression seem to be important to reduce a severe *C. beticola* infestation.

1.2 Pathogen *Cercospora beticola*

The plant pathogen *Cercospora beticola* is a filamentous imperfect fungus not passing a known sexual developmental stage with fruiting body (Duffus and Ruppel, 1993; Lartey et al., 2010; Weiland and Koch, 2004). Needle-shaped conidia are multiseptated and reach lengths of 50 to 200 µm that are produced by conidiophores for reproduction. After the penetration of germinating tube of appressoria-attached conidia through the stomata, the fungus propagates and colonizes biotrophically the intercellular space. After producing the non-host toxins cercosporin and beticolin (Daub and Ehrenshaft, 2000; Fajola, 1978; Goudet et al., 2000), it changes to a necrotrophic stage (Fig. 3). The photosenzitiser cercosporin, a perylenequinon, is activated by photons raising this molecule to an energy-rich triplet status. Excess energy is released to oxygen molecules in form of electrons, thus forming reactive oxygen species (ROS), e.g. $^1O_2$ + $^{\cdot}O_2^-$ (Daub and Ehrenshaft, 2000). ROS can very rapidly (milliseconds) oxidize nucleic acids and membranes leading to the destruction of plant cells if their production exceeds the capacity for metabolic quenching. Beticolin, the second non-host specific toxin, was shown to inhibit the ATP depending H^+-transporter of pea (Macri et al., 1983) and depolarize tabacco membranes (Gapillout et al., 1996). In general, beticolins are able to form ion channels with multiple conductance states and permeability levels. Otherwise, an antioxidant effect was postulated due to its $^{\cdot}O_2^-$ trapping capability (Goudet et al., 2000). In the plant tissue, toxins lead to the release of soluble nutrients to the hyphae resulting in cell and further leaf destruction. Leaf symptoms start with characteristic brown necrotic spots with 0.5 to 6 mm diameter. Mature lesions show a red margin resulting from betacyanine accumulation in sugar beet leaves following a plant wounding reaction (Skaracis et al., 2010). Furthermore, spots coalesce to extended lesions leading to the complete collapse of leaf tissue. The production of conidiophores protruding from the stomata of invaded leaves is induced by temperatures between 27 to 32°C at day and 17°C at night, and humidity of 90% (Skaracis et al., 2010). Conidiophores are

septate, light brown structures producing conidia. After a maturation period, conidia can infect new leaves. This infection cycle can re-occur several times in a growing season. Ultimately, this cycle can result in the destruction of the whole photosynthetically active canopy. Affected sugar beets have to grow new leaves depending on the re-allocation of available sugar from the taproot, which leads to overall loss of yield (Holtschulte et al., 2010; Rossi et al., 2000; Saito, 1966).

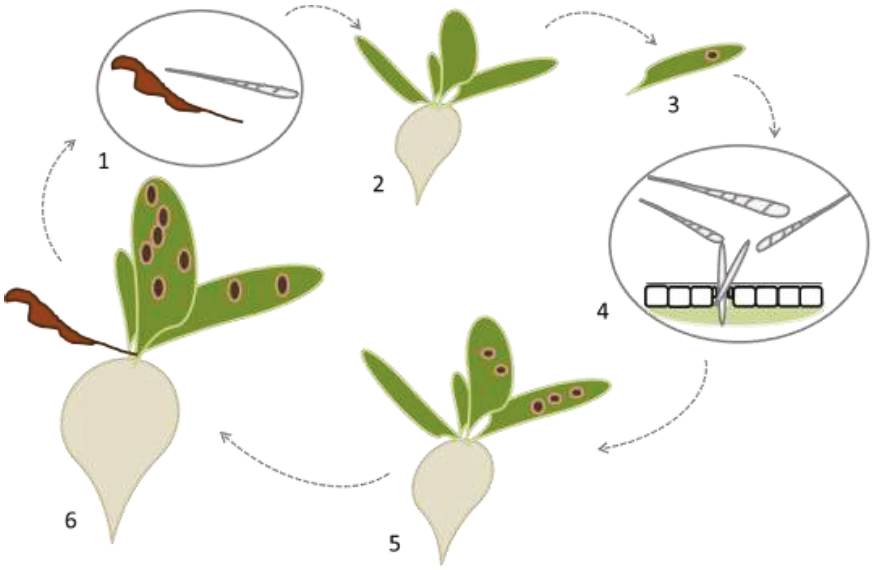

Fig. 3: Scheme of *Cercospora* life cycle on sugar beet. Conidia survive in soil or dried infected leaf material (1) infecting young plants (2). (3) Leaf symptoms develop and new conidia are produced (4) infecting new leaves (5) and leading to the loss of photosynthetically active leaf area (6). This life cycle can re-occur multiple times in environmental conditions favorable to fungal development, such as warm day temperatures and high humidity (modified after Jones and Windels, 1991).

The host range of *C. beticola* includes the families *Chenopodiaceae* and *Amaranthacease* (Weiland and Koch, 2004). Besides the genus *Beta* and other weed species, e.g. *Amaranthus*, *Atriplex*, *Chenopodum*, *Cyclamen*, *Plantago*, *Malva*, *Limonium*, several crop plants can be infected, for example spinach (*Spinacia*), lattuce (*Lactuca*) and celery (*Apium*) (Groenewald et al., 2006; Lartey et al., 2003; Lartey et al., 2010).

1.3 Breeding for Plant Resistance

Plants have always been used for food, feed and energy production. Desirable plants have high yield quantity and quality (Helback, 1959), and tolerance and resistance to biotic and abiotic stresses (Freytag and Hahlbrock, 1992). Phytopathogens can cause severe yield losses in susceptible plants. The most prominent example is the epidemic of potato blight in Northern Europe in 1845 leading to total loss of potato cultivation. The Great Famine in Ireland was caused by rapid and wide propagation of the fungus *Phytoptora infestans* (Agrios, 1997). Already in 1886, von Thümen first mentioned CLS as the most destructive disease of sugar beets in Germany (Von Thümen, 1886).

Genetic variability and resources are the foundation of plant resistance breeding. Within 2 to 4 years of experimental selection, promising parental lines are selected and crossed (Fig. 4). For official registration, the final evaluation of prospective hybrids takes between 8 to 11 years. Several key issues have to be considered in CLS resistance breeding. Candidate cultivars need to produce high yield both under CLS pressure and in the absence of the disease. The combined resistance to several pathogens is requested. Also, plant quality needs to meet the demands and tolerance limits of sugar producers. Furthermore, there is an increasing public and political pressure to reduce pesticide application for plant protection (Holtschulte et al., 2010).

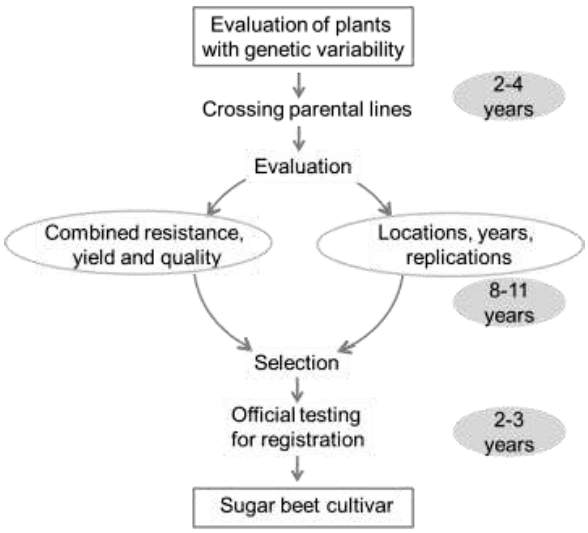

Fig. 4: Scheme of sugar beet breeding process. Breeding process starts with the initial evaluation of parental plants, which display genetic variability, to officially registrated cultivars (modified after Holtschulte et al, 2010).

The selection of putative parental lines can be conducted by classical approaches, such as visual disease scoring and invasive quantification of white sugar yield. Nevertheless, selection experiments have to be conducted under high and low CLS pressure, and in the absence of the disease *i*) at different locations, *ii*) in different years and *iii*) with several replications. Therefore, novel approaches offer the possibility to accelerate breeding processes. Molecular approaches such as marker-assisted selections allow the identification of resistance genes in the genome of sugar beet lines, which can be introduced in backcrossing programs. Monitoring of plant performance has been improved in recent years allowing the detection of foliar diseases non-invasively (Bock et al., 2010; Fiorani et al., 2012; Fiorani and Schurr, 2013; Mahlein et al., 2013). Root performance can be investigated non-invasively in soil using X-ray computed tomography (CT) and Magnetic Resonance Imaging (MRI) (Jahnke et al., 2009; Jansen et al., 2014; Zhu et al., 2011).

During the domestication process, selection mainly favored high yield traits, while *Cercospora* resistance traits seem to have been negatively selected (Schäfer-Pregl et al., 1999; Smith and Campbell, 1996; Smith and Ruppel, 1974). Wild relatives such as *Beta vulgaris spp. maritima* generally show lower susceptibility (Coons et al., 1955) and serve as donor germplasm for the introduction of CLS resistance in modern sugar beet breeding lines. Taguchi et al. (2011) highlighted the importance of four quantitative trait loci (QTL) on four chromosomes of the sugar beet genome, in accordance with previous studies, that also detected at least four major QTLs (Nilsson et al., 1999; Schäfer-Pregl et al., 1999; Setiawan et al., 2000). The aforementioned QTLs contain pathogenesis-related (PR) proteins such as the enzymes chitinase and β-1,3-glucanase. Molecular biology approaches could elucidate the correlation between genes, which are responsible for resistance and for the inheritance of yield productivity. In the study of Weltmeier et al. (2011), the defense response of a polygenic resistant cultivar was based on the defense strength and on the gene pool activated 15 days after inoculation in comparison with a susceptible cultivar. The resistant cultivar expressed significantly higher levels of genes directly acting against pathogens and important for signal perception and signaling, for example, receptor-like proteins and ubiquitin ligases (Weltmeier et al., 2011). Besides the preferred quantitative, horizontal CLS resistance, total resistance was described in one specific pathogen-host interaction. The sugar beet line “FC 702/2” has the *Cb* gene providing total resistance to the *C. beticola* race “C2” (Whitney and Lewellen, 1976). The *Cb* gene triggers a hypersensible reaction in leaves preventing fungal infection (Weltmeier et al., 2011). Because this gene-for-gene resistance can be overcome quicker than quantitatively inherited resistance, it is not included in sugar beet breeding programs (Skaracis and Biancardi, 2000; Weiland and Koch, 2004). Resistant or lowly susceptible sugar beet cultivars showed reduced foliar infection and foliar damage leading to a reduced biomass loss of both shoot and root. Nevertheless, after minor infestations, such resistant genotypes produce less biomass and sugar yield compared with highly susceptible lines (Rossi et al., 1999; Shane and Teng, 1992). The current breeding goal is to combine high

yield with moderate CLS resistance to achieve desirable sugar beet production under both high and low disease pressure (Lartey et al., 2010). This is particularly important as climate changes may lead to an increased frequency of fungal favorable conditions, such as high night humidity and warm day temperatures (Holtschulte et al., 2010; Rathaiah, 1976). In this study, fungal growth performance in sugar beet leaves was investigated by molecular detection of the fungal calmodulin gene and by spectral analysis in order to evaluate the applicability of these methods for the selection of genotypes with low susceptibility.

1.4 Disease Detection

Besides the conventional visual disease scoring, major progress in non-invasive shoot phenotyping has been achieved with imaging sensors (Bock et al., 2010; Fiorani and Schurr, 2013). Spectral, thermographic and Magnetic Resonance Imaging (MRI), enable precise observations of plant performance (Fiorani et al., 2012; Hillnhütter and Mahlein, 2008; Rascher et al., 2011). The traditional scoring of disease severity is based on time consuming, visual estimation performed by well-trained personnel. Optical measurements show the advantage of objective and precise scoring (West et al., 2003). Imaging spectroscopy include hyper- and multispectral sensors with a growing number of applications, for both field and greenhouse conditions.

1.4.1 Imaging spectroscopy

Imaging spectroscopy is based on reflected light from leaves, either coming from the sun or from artificial sources of radiation. Spectral signals can be collected by ground level and airborne measurements (Rascher et al., 2009) based on the detection of reflected light or chlorophyll fluorescence of the canopy. The reflected radiation in the visible, near and far infrared range gives information about morphological and physiological condition of the vegetation (Buschmann and Nagel, 1993).

The reflected light from the leaf surface is influenced by surface properties and physiological features, for example trichomes, epicuticular waxes and leaf pigment composition (Buschmann and Nagel, 1993; Gamon and Surfus, 1999). Pigments such as chlorophyll, anthocyanins and carotenoids absorb the incoming light in the visible region (400- 700 nm), whereas light of the near-infrared region (700 – 1200 nm) and further region (1200 – 2500 nm) is absorbed by water, proteins and other molecules (e.g. lignin). Incident light is usually reflected in the near infrared range (700 – 1200 nm), according to multiple light scattering on the interface between air and leaf cells. Therefore a healthy leaf displays a low reflection in the visible range, but high reflection in the near infrared range. Differences in the reflectance signature can be caused by changes in the pigment composition, surface morphology and

plant density on the field (West et al., 2003). Such changes can be referred to drought stress, nutrient lacking and plant diseases, respectively (Bock et al., 2010; Rascher et al., 2011; West et al., 2003). Incident light can be reflected on, absorb by or transmitted through the leaf surface (Fig. 5). About 10-15% of incoming light is reflected. A small amount is absorbed by pigments and tissue structures. Whereas a certain amount of radiation crosses epidermis, palisade and sponge parenchyma, and goes through the leaf, thus it is transmitted. Photons can be reflected diffusely in the mesophyll, palisade, and sponge parenchyma. Measurement methods become more complex when diffuse scattered light is considered.

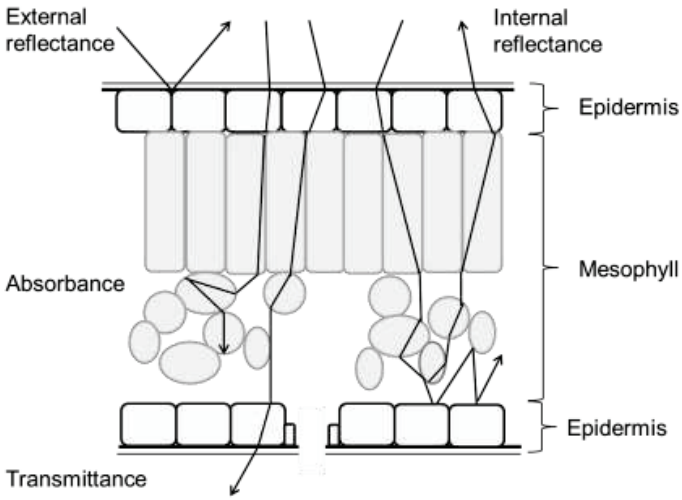

Fig. 5. Schematic figure of incident light scattering on leaf cross section. The pathway of transmittance, external and internal reflectance are shown through epidermis and mesophyll (modified after Buschmann and Nagel, 1993).

Spectral sensors give insight into the quality of the reflected or transmitted light spectrum regarding the intensity of each wavelength. Devices such as the spectroradiometer FieldSpec (ASD Inc., Boulder, USA) average the spectral signature of a respective spherical area (point measurement). Otherwise, cameras provide spectral signature of each image pixel. Referring the wavelength signature of each pixel (Z component) to the leaf area image (2D format of X and Y component), this leads to a three-dimensional hypercube. Multispectral sensors only detect parts of electromagnetical radiation, so called wideband channels, instead of the whole spectrum. Generally, the challenge of this image generating spectroscopy is the processing of huge data files. Data compression and algorithm selection can facilitate the processing of raw data (Fiorani et al., 2012; Plaza et al., 2006); Rumpf et al. (2010).

Based on spectral signatures, temporal or spatial changes can be analyzed. The intensity of specific wavelengths can be taken into account to calculate vegetation indices that provide information about plant properties (Gamon and Surfus, 1999; Huete, 1988), e.g. the widely used Normalized Differenced Vegetation Index (NDVI) and the Leaf Water Index (LWI). Additionally, plant-pathogen interactions were described by spectral imaging. In this respect, the *Cercospora* Leaf Spot Index (CLSI), based on reflected spectra, allowed the detection of fungal infection on sugar beet leaves (Mahlein et al., 2013). An early detection of CLS on sugar beet was based on support vector machines and spectral vegetation indices revealing disease onset three days after inoculation (Rumpf et al., 2010). The transmitted spectra through leaves might provide further spectral information revealing property changes at a earlier point in time, than it would be possible with just the reflected spectra. Combining the reflectance and transmittance signal of *Cercospora* inoculated leaves might offer the opportunity to identify and quantify fungal disease progression in a more detailed fashion at an early disease stage.

1.4.2 Magnetic resonance imaging

MRI has become an increasingly important tool to image plants organs non-invasively (Borisjuk et al., 2012). MRI techniques enable the study stems and root anatomy in soil, along with their leaf water content and transport (Van As, 2007; Van As et al., 2007). In particular, monitoring of soil-grown plants is feasible for imaging roots (Jahnke et al., 2009; Rascher et al., 2011). Quantitative application of advanced proton MRI methods allow high-resolution 3D imaging of root responses to environmental factors (Borisjuk et al., 2012; Fiorani and Schurr, 2013; Rascher et al., 2011) including sugar beet (Hillnhütter et al., 2011; Jahnke et al., 2009). This technique is used to study the 3D root anatomy and to observe developmental changes and active water uptake from soil (Pohlmeier et al., 2008). Traditional approaches to observe root systems include destructive digging, weighing and scanning (Box and Ramsuer, 1993; Samson and Sinclair, 1994; Trebbi and McGrath, 2009), and prohibit the observation of the same specimen at different developmental stages. X-ray computed tomography (CT) can take 2D cross-sectional images that can be reconstructed into 3D models of the root system. The disadvantages of this method are associated with a low contrast between plant material and the surrounding substrate (Zhu et al., 2011) and different plant tissues (Jung et al., 2012). According to a larger selection of parameters for tissue or organ segmentation, MRI can properly distinguish roots from the surrounding soil, and other tissue structures (Jahnke et al., 2009; Jansen et al., 2014; Metzner et al., 2014, submitted). Recently, similar MRI protocols were used to analyze specific plant-pathogen interactions. Hillnhütter et al. (2011) presented the first non-destructive study of belowground symptoms of cyst nematode infestation (*Heterodera schachtii*) on the sugar beet root system. Furthermore, the imaging of metabolites during photosynthesis can be tracked by ^{11}C allocation with positron emission tomography

(PET) in combination with structural MRI imaging of the respective plant organ (Jahnke et al., 2009). MRI also allows the detection of sugars and lipids by the use of ^{1}H Chemical Shift Imaging (CSI) (Glidewell, 2006). It is well known that leaf infestation reduces taproot growth and yield, yet there is still limited understanding of morphological and anatomical responses and their development during extended vegetation periods (days to weeks and months). Furthermore, quantitative variation between genotypes, previously characterized by a different resistance level, has not yet been analyzed in order to verify morphological responses. In this study, MRI measurements of taproot development under progressing canopy infestation reveal how early taproot effects are detectable and how long-term dynamics of taproot growth are changed.

1.5 Research objectives of this thesis

CLS is considered to be the most destructive foliar disease of sugar beet. Due to the societal demand to reduce fungicide application, exploiting natural plant resistance plays an important role in sugar beet breeding. In addition to classical approaches, novel phenotyping methods might accelerate the selection of promising breeding lines. Therefore, the combinations of invasive and non-invasive methods were conducted to investigate plant responses above and below the ground during foliar infection at different disease stages. In this study, the aim was to quantify plant responses of sugar beet lines with different CLS susceptibility. Plant defense responses were explored by monitoring fungal growth, leaf waxes, spectral leaf signatures and root growth, in order to identify novel traits of importance for sugar beet breeding. An early response of sugar beet to CLS was detected in the taproot highlighting the rapid effects on yield reduction at the very beginning of disease. Low genotype susceptibility was associated with low fungal growth in the leaf tissue and low disease severity as well as low signature changes of leaves. These aspects of reduced disease progression and sugar beet traits, such as taproot volume and the thickness of specific cambial rings, might improve pre-selection of potential candidate genotypes in the greenhouse for resistance breeding.

1. Taproot anatomical and physiological responses during disease progression

The aim of this thesis was to investigate the effect on root biomass and growth with MRI during foliar disease development to reveal how early taproot effects are detectable and how long-term growth dynamics are changed. Which factors do trigger the response in taproot growth?

2. Responses at the shoot level

In order to verify plant defense ability against this pathogen, the fungal growth in inoculated leaf tissue was quantified by the establishment of a molecular biological analysis based on the fungal calmodulin gene. Furthermore, disease severity was quantified in order to evaluate plant resistance ability. How does the fungus develop in the leaf tissue? How strong are sugar beet defenses against *Cercospora*? How does the environment influence plant defense susceptibility?

3. Leaf and canopy level changes in spectral signatures

An attempt was made to bridge field trails and lab-based experiments in order to quantify disease severity non-invasively with spectrometry. At an progressed disease stage, vegetation indices correlated significantly with visual disease scoring. To determine, how early fungal infestation would be detectable, laboratory experiments were conducted using hyperspectral imaging. Does hyperspectral imaging improve disease detection and constitute a considerable advantage compared with non-imaging spectrometry?

4. The importance of cuticular waxes for fungal establishment

To investigate the impact of leaf waxes on the fungal establishment on the leaf surface, the amount of cuticular waxes in sugar beet genotypes with contrasting susceptibility to CLS were analyzed using gas chromatography. Do waxes affect fungal invasion effectiveness?

2 Materials and Methods

2.1 Plant genotypes

Sugar beet genotypes (*Beta vulgaris L. spp. vulgaris*) with different susceptibility to *Cercospora* leaf spot were obtained from KWS SAAT AG (Einbeck, Germany). The classification of susceptibility was provided by KWS, based on prior knowledge deriving from the sugar beet breeding program at company.

Table 1: **List of Sugar Beet Genotypes**

Genotype	Susceptibility to CLS classified by KWS	Identification number (KWS)
STD HS	High	8RF5006
STD MS	Moderate	2S_1141
STD LS	Low	6S_1541
BL 20	High	8VK1692
BL 18	Moderate	2VK1505
BL 17	Moderate to low	8AS0528
BL 8	Low	1JF6265

2.2 Chemicals

Chemicals were purchased from Sigma Aldrich Chemie GmbH (Taufkirchen, Germany), Duschefa (Brüssel, Belgium), Carl Roth GmbH & Co. KG (Karlsruhe, Germany), Analytik Jena AG (Jena, Germany) as stated in the text.

2.3 Equipment

The technical equipment used for this dissertation is listed in Table 2.

Table 2. Technical equipment list

Equipment	Type	Manufacturer	Location
Laboratory			
Ball mill	Type MM200	RETSCH	Haan, Germany
Centrifuge	Mircofuge 16	Beckman Coulter GmbH	Krefeld, Germany
Climate chamber	Model MIR-254	SANYO North America Corporation	San Diego, USA
DNA concentration determination	NanoDrop 1000	NanoDrop products	Wilmington, USA
Electrophoresis system	PowerPac™ Basic Power Supply	Bio-Rad Laboratories GmbH	Munich, Germany
Light microscope	Axiophot 2	Carl Zeiss Microscopy GmbH	Göttingen, Germany
Mobile microscope	DigiMicro mobile	DNT Entwicklungs- und Vertriebs GmbH	Dietzenbach, Germany
Real-time PCR Detection system	Single-Color Real-Time PCR Detection System	Bio-Rad Laboratories GmbH	Munich, Germany
Spectrophotometer	Synergy 2	BioTek Instruments	Winooski, VT, USA
Sensor systems			
Chlorophyll fluorometer	Monitoring PAM	Heinz Walz GmbH	Effeltrich, Germany
Gas chromatography	Agilent 6890 with quadropole MS detector 5973N or FID	Agilent Technologies	Böblingen, Germany
MRI-Tomograph	4.7T, bird cage quad 100	Agilent Technologies	Oxford, UK Palo Alto
Multispectral camera	Agriculture Digital Camera	Tetracam	Chatsworth, California, USA
RGB camera	D 3000	Nikon GmbH	Düsseldorf, Germany
HyperART system	Patent DE 10 2012 005 477.7; PS-Camera (350-1000 nm), SWIR Camera (1000 -2500 nm)	Forschungszentrum Jülich GmbH Specim	Jülich, Germany Oulu, Finland
Scanning Electron Microscopes	SEM Gemini 1550VP	Carl Zeiss Microscopy GmbH	Jena, Germany
Spectroradiometer	FieldSpec	ASD Inc.	Boulder, USA

2.4 Software programs

Software programs used in this work are listed in Table 3.

Table 3: List of software programs

Software	Type	Manufacturer	Location
MeVisLab	Image processing and analysis	MeVis Medical Solutions AG	Bremen, Germany
Mircosoft Office	Programs for text editing, calculation, presentation	Microsoft Corporation	Redmond, Washington, USA
Pixel Wrench	Image processing and analysis	Tetracam, Inc.	Chatsworth, California, USA
RS3 Software	Analyses of light spectrum	ASD Inc.,	Boulder, Colorado, USA
SigmaPlot	Graph creation and statistical analysis	Systat Software GmbH	Erkrath, Germany
VnmrJ	Image acquisition (MRI)	Varian Inc.	Oxford, UK
WinControl-3	Data acquisition	Heinz Walz GmbH	Effeltrich, Germany

2.5 Cultivation of biological material

2.5.1 Plant cultivation

Plants were grown in 1L pots (Rosentopf, Soparco, Condé-sur-Huisne, France) filled with soil mixture of Hawita Dachstaudensubstrat and Pikiererde (1:1, v/v) to achieve appropriate plant cultivation conditions regarding soil pH (<7.5) and soil depth for taproot growth (Table 4). The photoperiod was set to 16h light/ 8h dark cycle with additional illumination (200 µmol m^{-2} s^{-1}, Master SON-T Pia Agro 400W, Philips Deutschland GmbH, Hamburg, Germany) in the greenhouse, when plants were not provided with enough sun light due to season. Greenhouse temperature was set to minimal 15°C (Fan heater STH9T, Helios Ventilatoren, Villingen-Schwenningen, Germany) with 55 - 76% humidity at night and reached on average 26°C with 27-67% at day.

Table 4: Plant cultivation equipment list

Equipment	Type	Manufacturer	Location
Fertilizer	Hakaphos Blau 15+10+15(+2)	COMPO GmbH & Co. KG	Münster, Germany
Soil	Dachstaudensubstrat (Sondermischung)	HAWITA GRUPPE GmbH	Vechta, Germany
Soil	Einheitserde Typ P Pikier	Balster Einheitserdewerk GmbH	Frödenberg, Germany

The automated watering system in the greenhouse (costum-made, Hellmuth Bahrs GmbH & Co. KG, Brüggen-Bracht, Germany) was adjusted to keep plants watered sufficiently during seasonally changing temperature conditions. Plants were provided weekly with an amount of NPK-nutrition solution (Table 4). Fertilization started at plant age of two weeks after emerging. The amount of nutrient solution (0.2%) was increased with developmental stage (Table 5) applied with a dispenser (Ceramus classic, Hirschmann Laborgeräte GmbH & Co. KG, Eberstadt, Germany).

Table 5: Fertilization of sugar beet genotypes. Plants in soil pots based on experimentally determined amounts for optimal nutrient supply during plant development.

Plant age (weeks after sowing)	Developmental stage (BBCH)	Fertilizer amount (mL plant^{-1})
2-4	< 12	60
5-7	< 16	80
8-10	> 17	100

Plants for MRI measurements were grown in PVC tubes (internal 8.1 cm diameter and 40 cm length) in a mixture of homogenized agricultural topsoil and coarse sand (1:2; v/v) under the aforementioned greenhouse conditions. The agricultural topsoil (gleyic cambisol) was collected by removing the top 30 cm from a farmer's field (Kaldenkirchen, Germany). The air-dried soil was pulverized and homogenized in a Drum hoop mixer (J. Engelsmann, Ludwigshafen, Germany), sieved through a 2 mm mesh and freed of ferromagnetic particles by moving it in a thin layer on a conveyor belt through a perpendicular magnetic field provided by rare earth magnets. Coarse quartz sand (grain size of 0.71 to 1.4 mm; Quartzwerke Witterschlick, Alfter, Germany) was freed of magnetic particles by the same process. For drainage and aeration the tubes had 8 mm bottom holes, which were covered with a nylon mesh (grid size 200 µm) to prevent substrate loss and roots outgrowth (Metzner et al., 2014, submitted). Water (15 mL per application) and NPK nutrient supply (Table 6)

was adjusted stepwise to the BBCH development stage and applied with an automated watering system (GARDENA Manufacturing GmbH, Ulm, Germany). These growth conditions were applied to all plants of the three MRI-experiments.

Table 6: Fertilizsation of sugar beets in MRI pots. Nutrient applications of three experiments are listed.

Plant age (weeks after sowing)	Fertilizer concentration (%)	Frequency (times per day)	Sugar beet genotypes
1-3	0.01	1-2	STD HS/ LS
3-7	0.03	3-4	In Exp. 7
7-8	0.05	4	
8-12	0.07	4	
> 12	0.12	3	
1-2	0.01	1	STD HS
2-5	0.01	2	In Exp. 8
5-7	0.03	2	
7-8	0.03	3	
8-10	0.03	4	
> 12	0.05	5	
1-2	0.03	1	BL 20/ 8
2-12	0.05	1	In Exp. IX
> 12	0.05	2	

2.5.2 Chemical plant protection

Chemical plant protection was necessary against the possible infestation of powdery mildew (*Erysiphe betae*), dark-winged fungus gnates (*Sciaridae*), spider mites (*Tetranychidae*) and thrips (*Thysanoptera*). To prevent powdery mildew infection, sugar beets were treated with wettable sulphur washed away one day in advance of *Cercospora* inoculation (Netzschwefel, Agrostulln GmbH, Stulln, Germany).

2.6 Fungal material and propagation

Cercospora beticola Sacc. (isolate Herensen) was provided from KWS SAAT AG (Einbeck, Germany). The fungus was grown on 50% vegetable juice (Gemüsemix, Eckes-Granini Deutschland GmbH, Nieder-Olm, Germany) agar plates (1.5% agar) dosed with antibiotics Timentin and Streptomycin and adjusted to pH 6.8 with sodium hydroxide solution (8.0 M), as personally communicated with KWS SAAT AG. For

long-term storage, the fungus was cultivated on agar plates for a few days at room temperature and then mycelia fragments were frozen at -20°C. Frozen stock material was renewed every six months by obtaining new conidia from infected leaves, which were kept for 24 h under 90 - 100% humidity. For propagation, frozen material was transferred onto agar plates (stage 1) and allowed to proliferate in a climate chamber (Table 2) at 60% humidity and 26°C for 1-2 weeks. Mycelia fragments were transplanted (stage 2) onto new plates and cultivated at 26°C and 60% RH for 1 week before the agar, overgrown by fungal mycelium, was removed from petri dishes and homogenized together with sterile water using a kitchen hand mixer. The water-mycelia pulp was distributed on plates (stage 3) and grown in a climate chamber under 8h/16h UV light photoperiod for 3 days for sporulation enhancement (Table 7).

Table 7: Treatment of fungal material

Fungus	Temperature	Duration	UV light level/ hours day^{-1}
Mycelia fragments	-20°C	< 6 months	-
1 Stage	26°C	1-2 weeks	-
2 Stage	26°C	1 week	-
3 Stage	26°C	2-3 days	3 (5 lamps) for 8h, 1 (1 lamp) for 16h

2.7 Inoculation procedure

2.7.1 Inoculum preparation

Conidia were carefully scraped from plates with a slide (5 - 10 mL water per plate), bigger mycelia fragments were filtered with a kitchen sieve and a piece of gauze bandage (amicus aluskin, Fritz Oskar Michallik GmbH & Co, Mühlacker, Germany). The conidia-water solution concentration was set to 3 x 10^4 conidia mL^{-1} (unless otherwise stated in the text) using a hemocytometer (Thoma chamber, Carl Roth GmbH + Co. KG, Karlsruhe, Germany). For higher conidia adhesion on the leaf surface 0.1% Tween20 was added (Wicke et al., 1993). Control plants were mock-inoculated with water-Tween20 (0.1%) solution to simulate inoculation procedure.

2.7.2 Inoculation approach

Plant inoculation was conducted as described in Schmidt et al. (2008). Following the conidia application, plants were kept for one week under 80 - 100% relative humidity and temperatures between 15°C (night) and 35°C (day) in plexiglass boxes at light intensity of 300 µmol m^{-2} s^{-1} at leaf level (Master SON-T Pia Agro 400W, Philips Deutschland GmbH, Hamburg, Germany) that was added 24 h after inoculation. After

the inoculation procedure, plants were kept again under greenhouse conditions. Inoculation of plants was conducted at the developmental stage BBCH 14 to 16 classified according to the BBCH scale (Hess et al., 1997; Meier, 2001), when four to six mature leaves were developed.

2.8 Measurements of leaf area

Photosynthetically active (green) leaf area was measured manually by multiplying ruler-measured length and width of each leaf with the specific leaf area factor (0.7014) of sugar beet leaves. A leaf factor was computed by correlating manually measured (length x width) and weighed sheet templates shaped like leaves (Schmittgen et al., 2011). The average leaf area per genotype was calculated as the mean of plants per treatment (mean ± SE).

2.9 Harvesting of plant material

Harvesting of shoot and taproot was carried out at respective time points after inoculation. The shoot was cut with a garden scissor just above the hypocotyl and the taproot was cleaned from soil by washing. The shoot material was weighed and dried in paper bags for at least one week before dry weight measurements. The shoot material was dried at 70°C and the root material at 50°C, avoiding caramelization of sucrose at higher temperatures. To compare disease effects on plant biomass, ratios were calculated by dividing fresh weight of the inoculated by the non-inoculated treatment ($FW_{inoculated}$ $FW_{non\text{-}inoculated}^{-1}$). Error bars were determined by calculating the propagation of error (Eq. 1; Barlow, 1989).

$$y = y(x1, x2, \dots) \Rightarrow \Delta y = \frac{\partial y}{\partial x1}\Delta x1 + \frac{\partial y}{\partial x2}\Delta x2 + \cdots \quad \text{(Eq. 1)}$$

Δy: failure of F_y
Δx_i: failure F_i of x_i
$\Delta x_i/x_i$: relative failure f_i of x_i
$\Delta y_i/y_i$: relative failure f_y of y

2.10 Digital photography

Pictures were taken with a RGB camera (Table 2) to image several disease stages at the leaf and root level.

2.11 Microscopy

Fungal material was imaged using a light microscope (Table 2). The attached leaves of infected plants were imaged with a digital mobile microscope. Structure electron microscopic images were taken from dried leaf samples that were covered with a thin gold layer (**Table 2**) and carried out by Dr. Walter Schröder at the SEM facility (PGI, Forschungszentrum Jülich GmbH, Jülich, Germany).

2.12 Visual disease scoring

Visual disease scoring is a well-established method to quantify disease progression based on visible infected and destroyed leaf area. Additionally, plant developmental stages were recorded based on the BBCH scale (Meier, 2001). Foliar disease severity was scored visually and given as percentage of infected leaf area. The percentage of infected leaf area from 0 to 3% was classified with a modified scale based on Shane and Teng (1992). The percentage of infected leaf area from 3 to 100% (Fig. 6) was estimated according to the scale of Rossi and Battilani (Rossi and Battilani, 1989). Mean values of disease severity were calculated by pooling all leaves of one genotype (all plants per treatment) divided by the number of plants. Leaves were included at the time point of first visible symptoms. Disease severity was cumulated over time, leaves scored with 100% infected leaf area were included in leaf pool of further scoring time points. The number of symptomatic leaves per plant (Eq. 2) increased within days post inoculation (dpi).

$$\text{Leaves per plant (n)} = \frac{\text{all leaves per genotype}}{\text{number of plants per genotype}} \qquad \text{(Eq. 2)}$$

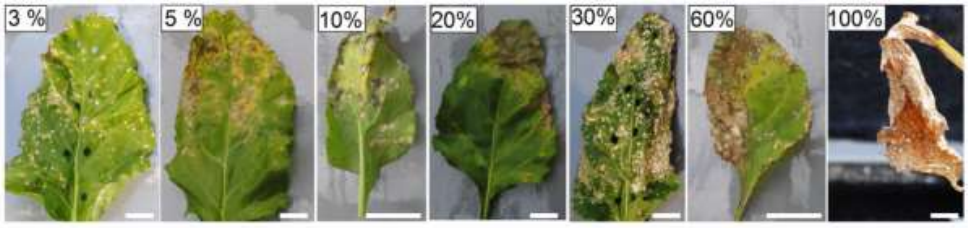

Fig. 6: Representative leaf samples of visually scored disease severity. Different disease severities (% infected leaf area) are represented. The scale of the leaves is indicated by the white line (2 cm).

2.13 Leaf wax analysis

Leaf waxes were analyzed using gas chromatography (GC). The analyses were carried out at the Department of Ecophysiology (IZMB, University of Bonn, Germany) under the supervision of Prof. Dr. Lukas Schreiber.

2.13.1 Harvesting of plant material

Single leaves (experiment 1 and 3) or leaf discs of 1.25 cm diameter (experiment 2) were harvested at respective leaf maturity. Discs of leaves of the first leaf pair (old, mature) and of the second, third or fourth leaf pair (young, immature) were harvested (and dried) in advance of wax extraction (Table 8). Epicuticular waxes were removed by covering the adaxial leaf surface with cellulose acetate (5% in acetate) and stripping the dried papery layer (Powell et al., 1999).

Table 8: Experimental conditions of wax analysis of breeding lines. Leaf waxes of the BL 20 and BL 8 plants were analyzed. Wax extraction took place at a plant age of 6 weeks after sowing. The measurement parameters are summarized, e.g. plant age, leaf number sample type and extracted leaf area.

Objective	BBCH	Leaves		Wax extraction	Sample type	Leaf area (cm^2)
		mature	immature			
Pretest	18	3/ 4	9/ 10	adaxial	Fresh leaves	12.3
Test	16	3/ 4	7/ 8	adaxial abaxial	Dried leaf discs	7.9
Combined with fungal growth	14	3/ 4	5/ 6	adaxial	Fresh leaves	3.1

2.13.2 Sample preparation

Samples were analyzed as previously described (Hauke and Schreiber, 1998). Leaf dics were either immersed 10 s in chloroform or leaf surface was covered with chloroform ten-times for 1 s. Hydroxylic groups were derivatized using 20 µL of BSTFA [N, O – bis (trimethylsilyl) trifluroacetamide with 1% trimethylchlorosilane; Pierce, Rockford, IL] and 20 µL of pyridine at 70 °C for 40 min. In a further step, the sample volume was reducted to 20 µL by chloroform evaporation in a stream of nitrogen gas. Then samples were transferred to auto sampler vials and analyzed by gas chromatography (GC).

2.13.3 Measurement parameters

Wax quantity and identification were determined by gas chromatography flame ionization detector (GC-FID) and gas chromatography mass spectrometry (GC-MS), respectively. Wax components were identified by MS spectra (70 eV, m/z 50–70) after separation by capillary GC [DB-1, 30 m × 0.32 mm, 0.1 µm (J & W), on-column injection at 50°C, oven 2 min at 50°C, 10°C min^{-1} to 150°C, 1 min at 150°C, 3°C min^{-1} to 310°C, 30 min at 310°C, and the carrier gas at 2 mL min^{-1}] on an gas chromatograph combined with a quadropole mass-selective detector (Table 2). Sample extracts (each 1 µL) were injected via auto sampler. For the quantitative analysis the samples were run on an identical GC system with a flame ionization detector (FID) based on the internal standard.

2.13.4 Compound identification and quantification

One representative GC-MS peak diagram was used to identify single compounds based on specific composition of alcohols, acids or esters and an internal software library (Agilent Technologies, Oxford, UK). The specific compounds were identified and peak areas of the GC-FID chromatogram were integrated to determine the quantity of monomers.

2.14 Taproot carbohydrate analysis

2.14.1 Harvesting of plant material

Tissue sections of the taproot were taken from inoculated and non-inoculated plants at 35 dpi or 85 das. One quarter per taproot was cut out, weighted, frozen in liquid nitrogen and stored at -80°C for further analysis.

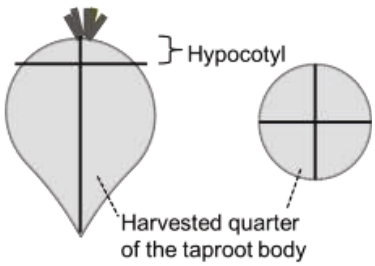

Fig. 7: Scheme of taproot harvest. During the harvest taproots were cut in quarters, one quarter was analyzed for carbohydrate content in the enzymatic assay.

2.14.2 Sample and enzyme preparation

Samples were grounded in cooled hardened steel vessels (Vol. 10 mL) with two aluminium balls (10 mm), in a ball mill (Table 2) for 2 min at a speed of 30 Hz.

Soluble carbohydrates were extracted from the grounded material that were about 200 mg. An aliquot of the sample extract was analyzed in the enzymatic assay. The enzymes glucose-6-phosphate dehydrogenase (G6PDH), Hexokinase (HK), phospho-glucoisomerase (PGI) and invertase (Inv) were prepared prior to the analysis. Each enzyme G6PDH (0.32 mL; 5.6 U), HK (0.48 mL; 6 U) and PGI (0.24 mL; 10 U) (Roche Diagnostic GmbH, Mannheim, Germany) was centrifuged for 4 min at 13000 rpm at room temperature. Pellets were dissolved in 0.4 mL Tris buffer (100mM Tris, 10mM MgCl2, pH 8.1). About 0.25 mL (corresponding to ¼ the volume of 2 mL eppendorf reaction tube) of Inv (Sigma-Aldrich Chemie GmbH, St. Louis, MO, USA) was suspended in 0.25 mL TRIS buffer.

2.14.3 Enzymatic carbohydrate analysis

Soluble carbohydrates such as glucose, fructose, and sucrose were analyzed by a coupled enzyme assay (Jones et al., 1977) using a micro plate spectrophotometer (Table 2) according to Walter et al. (2002). The quantification of soluble carbohydrates is based on the optical density (OD) increase of $NADPH+H^+$ at 340 nm (1 µmol $NADPH + H^+$ mL^{-1} = 6.22 OD) that is produced in the first enzymatic reaction from glucose-6-phosphate to 6-phosphogluconate catalyzed by the enzyme G6PDH. During the following three reactions HK, PGI and Inv were added to the extract to assess glucose, fructose and sucrose concentration (Fig. 8).

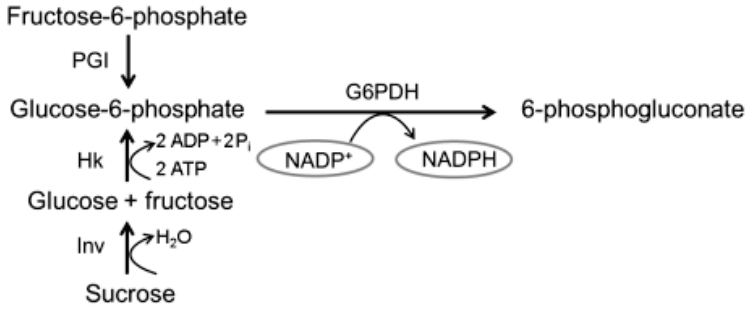

Fig. 8: Enzymatic reaction of the carbohydrate analysis. The amount of glucose, fructose and sucrose were quantified based on the optical density of NADPH + H^+ at 340 nm in a spectrophotometer. Reactions were catalyzed by the enzymes glucose-6-phosphate dehydrogenase (G6PDH), hexokinase (HK), phosphoglucoisomerase (PGI) and invertase (Inv) that were added subsequently to the sample (adapted from Jones et al., 1977).

Thereby, NADPH + H^+ corresponds to hexose in a ratio of 1 to 1 and to sucrose in a ratio of 2 to 1, because one molecule of sucrose produces two NADPH + H^+. Each well of a 96-well-microtiter plate contained 20 µl of sample (aliquot) and 160 µL master mix consisting of 10.5 mL imidazole buffer (100mM imidazole, 5mM MgCl2,

pH 6.9), 315 µL ATP (60 mg mL^{-1}), 315 µL $NADP^+$ (36 mg mL^{-1}) and 140 µL G6PDH. After the determination of glucose-6-phosphate concentration in the aliqout, the enzymes HK, PGI and Inv (2 µL) were subsequently added and the optical density at the steady state (plateau of reaction) was used to analyze the amount of carbohydrates.

2.14.4 Data analysis

Based on the equation (Eq.3) carbohydrate concentrations were calculated. The sucrose concentration was calculated by dividing c_{hexose} by 2.

$$C_{hexose}\ \left(\frac{\mu mol}{gFW}\right) = \frac{\left(\Delta OD\,\frac{Vextract\,\mu L}{Valiquot\,\mu L}\right)}{\left(\varepsilon NADPH\frac{mL}{\mu mol\,cm}\,F microplate\,\frac{cm}{mL}\,mgFW\right)} \qquad \text{(Eq. 3)}$$

ε: extinction coefficient of NADPH, $6.22\,\frac{mL}{\mu mol\,cm}$

F: correction factor of microplate, $2.85\,\frac{cm}{mL}$

To calculate the relative sucrose content of taproots (%), in a first step, the sucrose content (µmol g_{FW}^{-1}) was multiplied with the molar mass of sucrose (342 g mol^{-1}) and with the sample amount (mg_{FW}) to calculated the absolute sucrose amount (mg) of the sample. In a second step, the absolute sucrose amount was then correlated with the sample amount to analyze the relative sucrose content of the taproot (%).

2.15 Fungal growth analysis

2.15.1 Harvesting of plant material

Single leaves or leaf discs of 1.25 mm diameter were harvested at respective time intervals after inoculation. Leaves were cut with a knife, the midvein was removed and fresh weight was measured. Samples were frozen directly in liquid nitrogen and stored at -80°C until further sample preparation.

2.15.2 Sample preparation

Samples were ground in a ceramic mortar and pestle cooled with liquid nitrogen until a fine powder was achieved. About 100 mg of powder was weighed in an Eppendorf

vessel (Eppendorf AG, Hamburg) and used for DNA extraction. Leaf discs were ground in 2 mL Eppendorf vessels with one aluminium ball (5 mm), 200 µL of s-lysis-solution and 25 µL protein kinase K (innuPREP Plant DNA kit, Analytik Jena AG, Jena) in a ball mill (Table 2) for 60 sec at a speed of 30 Hz. The aluminium ball was removed after washing with additional 200 µL SLS that was added to the sample.

2.15.3 DNA isolation

In a preliminary experiment, fungal DNA was isolated using the cetyltrimethylammonium bromide (CTAB) protocol (Zhang et al., 2000). After sample grinding and buffer extraction (2% CTAB, 1.4 M NACl, 100 mM Tris-HCl (pH 8), 20 mM EDTA, 2% polyvinylpyrrolidone (PVP) and 2% β-mercaptoethanol), the sample was dissolved in a mixture of chloroform: isoamylalcohol (24:1). DNA was withdrawn from the chloroform phase and precipitated with 0.6 vol isopropanol (100%). After ethanol washing, DNA pellet was dissolved in TE buffer (10 mM Tris-HCl, 15 mM NaCl, pH 7.5) and RNA was removed over night at 4°C using RNAse (10 µg mL^{-1}).

For the quantitative real-time PCR determination, total genomic DNA of fungal and plant material was isolated using the innuPREP Plant DNA kit (Analytik Jena AG, Jena) following the manufacturer's guidelines, except two sample adaptations. The evaluation volume was reduced to 100 µL and evaluation time was extended to ≤ 3 minutes. Genomic DNA concentrations were measured with the NanoDrop spectrometer (Table 2) measuring the extinction of the sample and the 260 nm absorbance of nucleotides, respectively.

2.15.4 Gel extraction

To check degradation of RNA, DNA samples were separated on a 1.5% agarose gel in 1 x TAE buffer (40mM Tris, 18 mM acetic acid, 1mM EDTA) with a Bio-Rad PowerPac System (Table 2). Based on gel size of 80 to 120 mL, gel running conditions varied between 80 to 160 V and 20 to 30 min. The fragment size of nucleic acids was compared with a 100 bp DNA Ladder (New Enfland Biolabs, Ipswich, Massachusetts, USA) visualized by ethidium bromide staining.

2.15.5 PCR reactions

Primer for molecular approaches were obtained from Eurofins MWG Operon (Ebersberg, Germany) listed in Table 9. The fungal calmodulin gene (EMBL-EBI, DQ026493) and the Internal Transcript Spacer (ITS) region (Gardes et al., 1991; Weiland and Sundsbak, 2000) were amplified under the three steps PCR conditions described in Table 10. All reaction mixtures (in total 50 µL per well) consisted of 1.0 µL DNA starting material (50 ng µL-1), 2.5 µL primer (ITS 1 and 4; CercoCal, 1:10 dilution), 0.4 µL dNTPs, 1 µL BSA, 34.4 µL sterile water, 5 µL buffer (KCl), 3 µL $MgCl_2$ and 0.2 µL *Taq* polymerase (Fisher Scientific - Germany GmbH, Schwerte, Germany).

Table 9: List of primers

Name	Target gene	Sequence	
		Primer (‘5 → ‘3)	Amplified length (bp)
ITS 1/4	rRNA region	(1)TCC GTA GGT GAA CCT GCG G/ (4) TCC TCC GCT TAT TGA TAT GC	550
CercoCal	*C. beticola* calmodulin (cmdA)	(F) CAA GGA CGG CGA TGG TAT G/ (R) TTC GGT CGA GGT TAG TTC AGT ACA	298
Cal	*C. beticola* calmodulin (cmdA)	(F) GCC TTC TCT CTC TTC GTA CGT ACA G/ (R) GCG AAT GTA CTG AAC TAA CC T CGA CC	229

2.15.6 Real-time PCR

The optical real-time PCR detection system of BioRad was used to quantify the amount of the fungal calmodulin gene (Table 2). Starting DNA concentration per sample (well) was adjusted to 8 µg total DNA. With the use of a standard curve of respective fungal DNA amounts, fungal DNA per sample could be calculated. Fungal DNA of the standard curve was adjusted to 1 pg – 10 ng. Fungal calmodulin gene was amplified using three step real-time PCR conditions described in Table 10. All reaction mixtures (in total 20 µL per well) consisted of 0.6 µL Cal primer (F: 725 pM and R: 553 pM, 1:10 dilution, Table 9); 10 µL SYBR Green (Qiagen, Hilden, Germany), 0.8 µL sterile water and 8 µL DNA sample (8 µg DNA in total). Further, a melting curve was acquired to check purity of PCR amplification regarding the presence of primer dimers. The melting peak (at 88°C) was analyzed to assess purity of the amplification of the calmodulin gene.

Table 10: Quantitative real-time PCR conditions for Cal, ITS and CercoCal primer

	Length (min)	Temperature (°C) [Cal/ ITS/ CercoCal]	
Denaturation	5	94	
Denaturation	1	94	↑
Annealing	1	63/ 58/ 65	40 cycles
Elongation	1	72	↓
Final elongation	1	72	

2.15.7 Data analysis

In the internal optical system software (Bio-Rad Laboratories GmbH, Munich, Germany) the cycle threshold (C_t) of each run was adjusted depending on individual PCR performance, usually around 120 PCR Base Line Subtracted CF RFU. Based on the C_t value of each sample and the parameters of the fungal standard curve (y-intercept and slope) the fungal amount per well was calculated (Eq. 4). Under consideration of sample dilution per well (300 ng_{DNA} in total per well, vol. 8 µL), sample DNA concentration and fresh weight, fungal amount could be calculated for each leaf sample (Eq. 4), as previously described for *Aspergillus* fungi (Johnson et al., 2013).

$$\text{Fungal DNA } \left(\frac{pg}{mgFW}\right) = \frac{e^{\frac{\text{Ct} - \text{y-intercept}}{\text{slope}}}}{\text{mgFW}} \frac{\text{cDNA}}{d} \qquad \text{(Eq. 4)}$$

d: dilution factor per well, $\frac{300\ ng\ DNAtotal}{8\ \mu L\ well\ vol.}$

c_{DNA}: DNA concentration, $\frac{ng}{\mu L}$

2.16 Magnetic Resonance Imaging (MRI)

Measurements were conducted at the MRI-system facility of IBG-2 Plant Science, Forschungszentrum Jülich, using a vertical bore 4.7T magnet equipped with gradient coils providing 300 mT m^{-1}(Varian, Oxford, UK).

2.16.1 Measurement principle

The measurement principle of MRI is the excitation of protons (^1H) and detection of the rotation of their magnetic moments that allows to visualize the root system non-invasively.

MRI is based on nuclear magnetic resonance (NMR), in contrast to NMR techniques, it is based on an inhomogenous magnetic field resulting from magnetic field gradients which allow spatial location of emitted proton spin signals (Weishaupt et al., 2009). Nuclei with un-even number of neutrons or protons possess a nuclear spin measureable with nuclear resonance spectroscopy (Hornak, 1996). With a nuclear spin precession, protons adjust their spins in the direction of the applied magnetic field (B_0). In such a homogeneous external magnetic field all spins of one chemical

species (e.g. hydrogen) precess with the same frequency. This specific evasion movement is called Larmor frequency and results in a longitudinal magnetization (M_z) in direction of the applied magnetic field. For detecting and localization of protons, high frequency (HF) pulses are applied by a transmitter coil. These HF pulses are applied in 90° in the XY layer matching with the appropriate Larmor frequency to induce spin precession. Due to the precession in the XY layer, protons (the sum vector) induce a transversal magnetization (alternating voltage) in the receiver coil. After increasing the magnetization signal by an intensifier, it can be proceeded in a computer imaging.

Two processes are important for the decrease of the transversal magnetization and therefore crucial for MRI signals. The T_1 and T_2 relaxation releases energy to surrounding area (spin-grid relaxation) and to surrounding spins (spin-spin relaxation), respectively. The spin-grid relaxation T_1 occurs according to spin relaxation back to its initial state. The spin-spin relaxation T_2 is based on the interference between spins dephasing according to their differing Larmor frequency. The energy is not emitted to the grid, but is divided between spins (Weishaupt et al., 2009). Imaging contrast of MRI images is determined by proton density per volume unit, T_1 and T_2 relaxation time. With a decrease of proton density, the MRI signal intensity also decreases. The T_1 time indicates the time spins need to return to their initial state and to be stimulated again. The T_2 images indicate how fast MRI signal decreases after dephasing. T_1 and T_2 relaxation time are varying in different tissues, according to differing proton density tissue types can be differed visually (Weishaupt et al., 2009).

There are two factors, the repetition (TR) and the echo time (TE) important for resolving MRI images. Depending on the repetition time (temporal length between inductions) T_1 or T_2 weighted images are obtained. Tissue, displaying a fast spin-grid relaxation $T_{1,}$ can be induced more frequently, because protons return earlier to the initial state, indicating a short repetition time. Protons of tissue, displaying a long spin-spin relaxation $T_{2,}$ need longer to return to the initial state, indicating a long repetition time. The echo time represents the time slot between the RF pulse induction and the measurement of the MRI signal. To achieve a maximum MRI signal intensity, a long repetition time (spin-grid relaxation) and a short echo time (spin-spin relaxation) was chosen. To obtain 3D images, multiple inductions of protons with 90° HF pulses are needed. In the process of signal localization and image acquisition Fourier transformations are used. The Fourier transformation allows the conversion from frequency to time domain (Hornak, 1996). Therefore, slices have to be induced several times with spatial encoding. To determine slice thickness and localization, phase encodes the Y direction and frequency encodes the X direction. For efficient imaging of root systems spin echo multi slice (sems) measurements can be used. The application of these method on sugar beet is specified in Jahnke et al. 2009. In this study, sems measurements were conducted with parameters listed in Table 11.

Table 11: MRI measurement parameter

Parameter	Value
TE	5.4 ms/ 12 ms
TR	2 s
Slice number	64
Slice thickness	1.5 mm
Field of View	70 x 70/ 100 x 100 mm²
Pixel size	273 x 273 µm²

2.16.2 Image analysis

Images were acquired and analyzed with the software package MeVisLab (MeVis Medical Solutions AG, Bremen, Germany) in combination with Matlab (Mathworks, Ismaning, Germany) and the open source Matlab toolbox AEDES (www.aedes.uef.fi). To extract taproot signal from the background, signal had to be segmented from noise and unwanted sources of signal (e.g. water in soil pores, petioles) by manually setting an intensity threshold minimizing background noise and maximizing sample signal under visual control. 3D Images of the region of interest had a spatial resolution of 0.273 x 0.273 x 1.5 mm³.

2.16.3 Measured taproot parameters

Taproot parameters as volume, length, width and ring thickness were analyzed and mean values (mean ± SE) were calculated per treatment. Relative growth rate (RGR) of taproot volume (cm³) was calculated for the first 14 days after inoculation (Eq. 5) as previous described (Walter and Schurr, 1999).

$$\mathrm{RGR}\left(\frac{\%}{\mathrm{day}}\right) = 100\ \frac{\ln\frac{Vt2}{Vt1}}{(t2-t1)} \qquad \text{(Eq. 5)}$$

t_1: first time point (0 dpi)
t_2: second time point (14 dpi)
V_{t1}: volume of taproot at t_1
V_{t2}: volume of taproot at t_2

2.17 Photosynthetic efficiency analysis

The photosynthetic efficiency (Y(II)), the electron transport rate (ETR) and the photosynthetic active radiation (PAR) were measured by chlorophyll fluorescence with commercial Monitoring-PAM fluorometers (Table 2) under greenhouse conditions.

2.17.1 Measurement parameters of greenhouse experiment

The apparent rate of photosynthetic ETR of photosystem (PS) II was obtained by the PAM devices and the actual quantum yield of PSII (YII) was calculated for dark-adapted leaves as (F_v F_m^{-1}) and for leaves during the day as ($F_{m'}$ − F′) ($F_{m'}$)$^{-1}$, as previously described (Rascher et al., 2009). The Monitoring-PAMs were adjusted at mature leaves (leaf 8) before and continuously after inoculation and measured repeatedly at 10-minute intervals 24 h per day after applying a saturating flash of 3500 µmol m^{-2} s^{-1}.

2.17.2 Data analysis of the Monitoring-PAM fluorometer

For data analysis, fitting curves were used to exclude outlier that lay beyond the prediction bands of a 95% confidence (SigmaPlot, Systat Software GmbH, Erkath, Germany). The ETR data were fitted using a positive exponential function with a rise to maximum (single, two parameters) and the Y(II) data were fitted using a negative exponential function (single, two parameters) of light intensity (Rascher et al., 2012). Corrected data were then plotted in graphs.

2.18 Spectral Imaging

Spatial and temporal resolution of canopy signature was measured by a spectroradiometer (FieldSpec), a multispectral camera (Tetracam) and by a newly developed hyperspectral sensor system, the hyperspectral absorption-reflectance-transmittance imaging (HyperART) system (Patent DE 10 2012 005 477.7).

2.1.1. Measurement principle

In the principle of hyperspectral measurements, light has to be scattered into its wavelength spectrum in order to get the intensity of each single wavelength. The reflected light of an object is focused by a collimator and a lens. The light is then scattered through a diffraction grating and detected by a digital sensor, e.g. CCD chip (Bock et al., 2010). The information of the detected spectrum can be given in wavelength spectra of integrated areas and in form of multispectral or hyperspectral images where each pixel includes a single spectrum.

2.1.2. Measurement parameters of field experiment

The field experiment of *Cercospora*-infected sugar beet breeding lines (BL 20, 18, 17 and 8) was conducted in Plattling (Bavaria) during two cloudless sunny days in August 2012 with two different spectral devices, the Tetracam and the FieldSpec (Table 2). Multispectral images of the Tetracam consist of three bands with a spectral range from 350 - 2500 nm. The FieldSpec averages the hyperspectral signature of a spherical area. The hyperspectral cameras have a resolution of 3 nm at 700 nm and 8 nm at 1400 and 2100 nm with a sampling interval of 1.4 nm in the range from 350 to 1050 nm and 2 nm in the range from 1000 to 2500 nm. The hyperspectral FieldSpec data were normalized to relative values using the spectra of a white reference panel (Spectralon, Labsphere Inc., North Dutton, New Hampshire, USA). Multispectral images were acquired holding the Tetracam approximately 2 m above the canopy in the time frame from 2 p.m. to 4 p.m. The FieldSpec data were acquired holding the optic pistol grip approximately 1.5 m above the canopy in the time frame of 11 to 12 a.m.

2.18.3 The HyperART system

Hyperspectral images were acquired by Sergej Bersträsser (Forschungszentrum Jülich GmbH, Jülich, Germany). In the CROP.SENSe project (number 315309), sub-project ZS1, founded by the BMBF (Bundesministerium für Bildung und Forschung). He developed a new sensor system allowing simultaneous measurement of reflected and transmitted light (Patent DE 10 2012 005 477.7). The HyperART system setup is a prototype developed for non-invasive evaluation of leaf properties and enables the detection of reflectance and transmittance, thus allowing the calculation of absorbance. The working principle of the HyperART-system relies on the upward redirection of (emitted and reflected) light of a plant sample towards two line scanners (Fig. 9). The leaf, still connected to the plant, is placed into the custom-made rectangular clip, which consists of two frames that are connected at the top. With a frame net of fishing lines, leaves are fixed in a clip frames that can host samples up to 560 cm². The clip poses the (horizontal) plane at a 90° angle. The leaf, kept Inside the clip, is illuminated from either side, while it is positioned between two mirrors at an angle of 45° (Fig. 9). One mirror redirects the reflected light to the line scanners (i.e., upwards), while the other mirror does the same for the transmitted light. The distance of the upper mirror edge to the two line scanner, offering a spectral range of 400 to 2500 nm (Table 2), is 85 cm. The two line scanners were fixed above a slide bar moving the leaf clip through the mirrors. The first line scanner (spectral camera PS V10E, Spectral Imaging Ltd., Oulu, Finland) is sensitive in the 400 to 1000 nm range and offers a spatio-spectral resolution of 1392 × 1040 pixels with nominal spectral resolution of 2.72 nm. The second line scanner (SWIR, Spectral Imaging Ltd., Oulu, Finland) is sensitive to the spectral range of 1000 to 2500 nm. The sensor can acquire 320 spatial pixels and 256 spectral bands' images with a nominal spectral resolution of 10 nm.

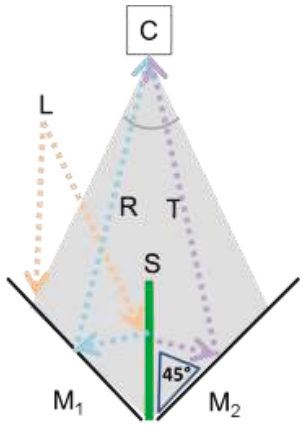

Fig. 9: Setup scheme of the HyperART system (Patent DE 10 2012 005 477.7). System parts are indicated by letters: C (hyperspectral camera), M1 and M2 (mirror 1 and 2), S (leaf clip sample), L (light source), R (reflected light) and T (transmitted light). The camera range (angle) is shown in gray.

2.18.4 Measurement parameters of the HyperART system

Sample illumination consists of two lamps (12V 50 Watt Osram, Munich, Germany) with aluminium reflector and diffused with frosted glass. To determine the incoming electromagnetic radiation a 99% reflective white standard (Spectralon, Labsphere Inc., North Dutton, New Hampshire, USA) were measured before and following measurements of each leaf sample.

2.1.3. Vegetation indices

Single wavelengths were used to calculate vegetation indices listed in Table 12. The NDVI indicates biomass and leaf area, the LWI indicates water content, the CLSI and CDI, experimentally developed by S. Bergsträsser, allows to classify CLS.

Table 12: **List of vegetation indices**

Index	Formula	Reference
NDVI, normalized difference vegetation index	$(R800 - R670) \times (R800 + R670)^{-1}$	Rouse et al., 1973
LWI, leaf water index	$R1300 \times R1450^{-1}$	Seelig et al., 2008
CLSI, *Cercospora* leaf spot index	$(R698 - R570) \times (R698 + R570)^{-1} + R734$	Mahlein et al., 2013
PRI, photochemical reflectance index	$(R531-R570) \times (R531+R570)^{-1}$	Gamon and Surfus, 1992
CDI, *Cercospora* detection index	$(712-561) \times (712+561)^{-1}$	Experimental index

2.1.4. Data analysis of multispectral camera

The multispectral images of the Tetracam were analyzed with the software Pixel Wrench (Table 3). Calculated indices received values between -1 and 1. Index values ≥ 0.1 represented vegetation and < 0.1 soil.

2.1.5. Data analysis of the spectroradiometer

The hyperspectral FieldSpec data were detected with the software RS3 converted to Excel (Table 3). Leaf spectrum was normalized to relative values using the spectra of a white reference and appropriate wavelength values were chosen to calculate indices according to the formulas shown in Table 12.

2.1.6. Data analysis of the HyperART system

Hyperspectral images were processed using ENVI 4.8 (Exelis Visual Information Solutions, Inc., Boulder, Colorado, USA) and MatLab R2012b (MathWorks®, Natick, Massachusetts, USA) Software. Firstly, the dark frame image was subtracted from both the sample and white reference images (Fastspec extension of ENVI). In the next step, the corrected sample image with relative values was cut to separate reflection and transmittance image. In each case, the size of the white reference image was adjusted to the sample image size. Secondly, each pixel of the image was divided by the corresponding pixel within the white reference image to achieve relative values and correct for possible illumination differences (Spectral Math tool of ENVI). In general, the absorbance can be calculated (Absorbance = 1 - (Reflectance + Transmittance)). This would include that the transmittance image is flipped to overlay the reflection image and rectified by corresponding points to correct displacements produced by image acquisition.

2.19 Summary of conducted experiments

Experiments of this dissertation are listed in Table 13, Table 8 and Table 15. In Table 13, all inoculation experiments are listed with objectives concerning measurement methods such as disease scoring, quantifying fungal growth (fungal gr.) in leaves, harvested plant biomass (biomass), quantifying leaf waxes (wax), monitoring taproot growth (Root gr. MRI) and determining the sucrose content of taproots (taproot sugar). Further objectives were foliar spectral signature (Spec. sig.) measurements of FieldSpec and Tetracam, and with hyperspectral imaging (HI image). The photosynthetic efficiency (Photo) of photosystem II and the electron transport rate were measured using commercial Monitoring-PAM fluorometers.

Table 13: List of all sugar beet inoculations with *Cercospora*. Experimental conditions and measurement objectives are listed. Plants were inoculated with concentration of 3 x 10^5 conidia mL_{-1}, * with 6 x 10^5 conidia mL^{-1}.

Exp.	Objective		Date of inoculation	Genotypes	BBCH
	Disease scoring	others			
1 *	X	Taproot sugar	08.03.12	STD HS/MS/LS	15
2	X		27.07.12	STD HS/MS/LS	16-18
3	X	Harvest, Fungal gr.	13.07.12	STD HS/MS/LS	14
4	X	Fungal gr.	31.08.12	STD HS/LS	16-18
5	X	Biomass	28.09.12	STD HS/LS	14
6		Fungal gr.	15.01.13	STD HS/LS	16-18
7	X	Root gr. (MRI)	10.05.13	STD HS/LS	18
8	X	Root gr. (MRI)	05.12.12	STD HS	16-17
field	X	Spec. sig.	20.08.12	BL 20/18/17/8	
9	X	Fungal gr.	11.04.13	BL 20/8	14
10	X	Biomass	18.10.13	BL 20/18/8	16
11	X	Biomass	12.03.13	BL 20/18/17/8	14
12		Fungal gr., HI image	21.05.13	BL 20/8	16
13		Fungal gr., HI image	07.06.13	BL 20/18/8	14
14		Fungal gr.	02.04.13	BL 20/18/8	13-14
15	X	Fungal gr., Wax	09.12.13	BL 20/8	16
16	X	Root gr. (MRI)	20.12.13	BL 20/18/8	16
17		Photo	20.05.14	BL 20	18

Table 14: Experimental conditions in the greenhouse. Temperature and humidity during the day and the night were measured by internal sensors in the greenhouse and values were averaged for the experimental time. Light intensity was measured with external sensors outside of the greenhouse. During six experiments the external sensors did not detect illuminance. Field data were obtained from a private weather station[4] 50 km away from the experimental field in Plattling, Bavaria.

Exp.	Date of inoculation	Temperature (day/ night)	Humidity (day/ night)	Illuminance (kilo lux)
1	08.03.12	24/ 16	40/ 57	9.4
2	27.07.12	30/ 19	40/ 71	14.2
3	13.07.12	28/ 18	43/ 73	11.8
4	31.08.12	25/ 16	48/ 66	10.0
5	28.09.12	22/ 16	55/ 66	7.4
6	15.01.13	17/ 15	37/ 38	1.6
7	10.05.13	21/ 19	57/ 60	---
8	05.12.12	17/15	47/ 48	2.1
Field	20.08.12	25/ 20	43/ 60	---
9	11.04.13	23/ 18	45/ 59	---
10	18.10.13	20/ 19	46/ 47	5.6
11	12.03.13	20/ 15	44/ 45	---
12	21.05.13	23/ 18	55/ 65	---
13	07.06.13	26/ 21	56/ 74	12.1
14	02.04.13	20/ 16	49/ 49	---
15	09.12.13	20/18	34/ 36	4.5
16	20.12.13	20/ 19	32/ 35	3.3

[4] www.wetter-eggerszell.de/j2012.htm

In Table 5, molecular analysis and measurement parameters are mentioned, e.g. efficiency and R^2 of standard curves of the real-time PCR approaches, sample number (n), sample type and leaf symptoms developed at sampling time point. The quantification of fungal growth was also combined with other methods, e.g. hyperspectral imaging with the HyperART system (Spec) and wax analysis of leaves (wax).

Table 15: List of molecular experiments. The measurement parameters for the experiments with standard genotypes (HS, MS, LS) and breeding lines (20, 18, 17, 8) are listed.

Exp.	Objective	Date	Standard curve qRT-PCR		Geno -type	dpi	Disease severity (%)
			Efficiency (%)	R^2			
3	Comparison between leaf halves	13.07.12	89.96	0.9996	HS MS LS	7 14	0/0/0 1-10/ 0.5-10/ 0.5-5
4	Comparison between leaf halves	31.08.12	103.54	0.9312	HS LS	3 10	0/0 0.2-5 0.1-0.2
6	Standard genotypes	15.01.13	90.7	0.997	HS LS	3 6 10	0 0 0.2-0.5
9	Breeding lines	11.04.13	76.1	0.9966	20 8	1 4 6	0 0 0
12	Combination with Spec	21.05.13	78.4	0.997	20 8	4 6 8	0 0 0.01-0.1
13	Combination with Spec	07.06.13	75.8	0.9932	20 18 8	4 8	0 0
14	Breeding lines	02.04.13	92.2	0.997	20 18 8	3 6 10	0 0 0.01-0.2
15	Combination with wax	09.12.13	85.3	0.9982	20 8	3	0

2.20 Statistical data analysis

All data were statistically tested by using SigmaPlot (SYSTAT Software GmbH, Erkrath, Germany). Analysis of variance (ANOVA) One-Way and Two-Way (Holm-Sidak) as well as t-tests were used for comparing data of the different genotypes and the two treatments of inoculated and non-inoculated plants.

3 Results

This study investigated the influence of *Cercospora* leaf spot (CLS) on above and belowground sugar beet growth. The aim was to test novel methods to identify and plants with increased resistance and to quantify their ability to cope with this pathogen in order to improve the selection process for breeding purposes. Conventional methods were used to compare disease development, leaf symptom progression and biomass loss of standard genotypes (STD) and breeding lines (BL). Moreover, advanced invasive and non-invasive methods were compared to well-established ones. The influence of cuticular waxes on plant resistance and fungal growth in inoculated leaves was detected invasively. Non-invasive measurements of shoot and root by spectral imaging and magnetic resonance imaging (MRI) allowed the observation of dynamic changes in plant organs in order to gain a full picture of plant responses to CLS and to get a better understanding of the relation between the infected shoot and the affected root system. In this study, low genotype susceptibility was associated with reduced fungal growth in the leaf tissue, low disease severity and slight changes in leaf signature. For the first time the reduction of taproot growth was quantified at the very beginning of disease onset as well as during foliar disease progression by the use of MRI. Genotype susceptibilities could be verified indicating that these methods might be convenient to quantify the ability of genotypes to defend against CLS. These results indicate that greenhouse experiments might be appropriate for the selection of candidate genotypes in breeding programs.

3.1 Disease development in controlled environment and in the field

To gain insight into the disease development, fungal growth and symptoms were investigated in controlled environments and in the field.

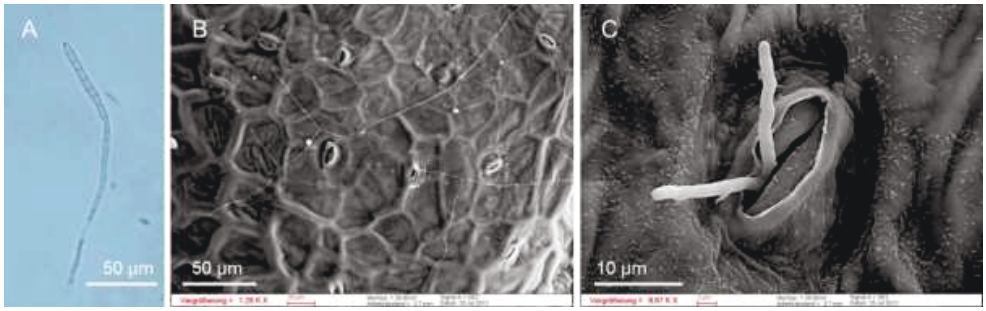

Fig. 10: Microscopic images of *Cercospora* conidia. (A) Light microscopic image of hyaline conidium. (B) Structure electron microscopic images of hyphae growing on leaf surface and (C) conidiophores growing out of stomata during conidia release. (B, C) Leaf samples were vaporized with gold particles by scanning electron microscopy.

After *in vitro* inoculation of leaves with conidia of *Cercospora beticola* (Fig. 10 A), fungal growth on leaf surfaces could be detected (Fig. 10 B). During infestation development, the fungus produced conidiophores protruding out of stomata to release new conidia (Fig. 10 C). Fungal toxin production led to the appearance of first small necrotic spots appearing 7 to 10 dpi (Fig. 11 A). Small spots began to coalesce leading to the collapse of leaf tissue (Fig. 11 B).

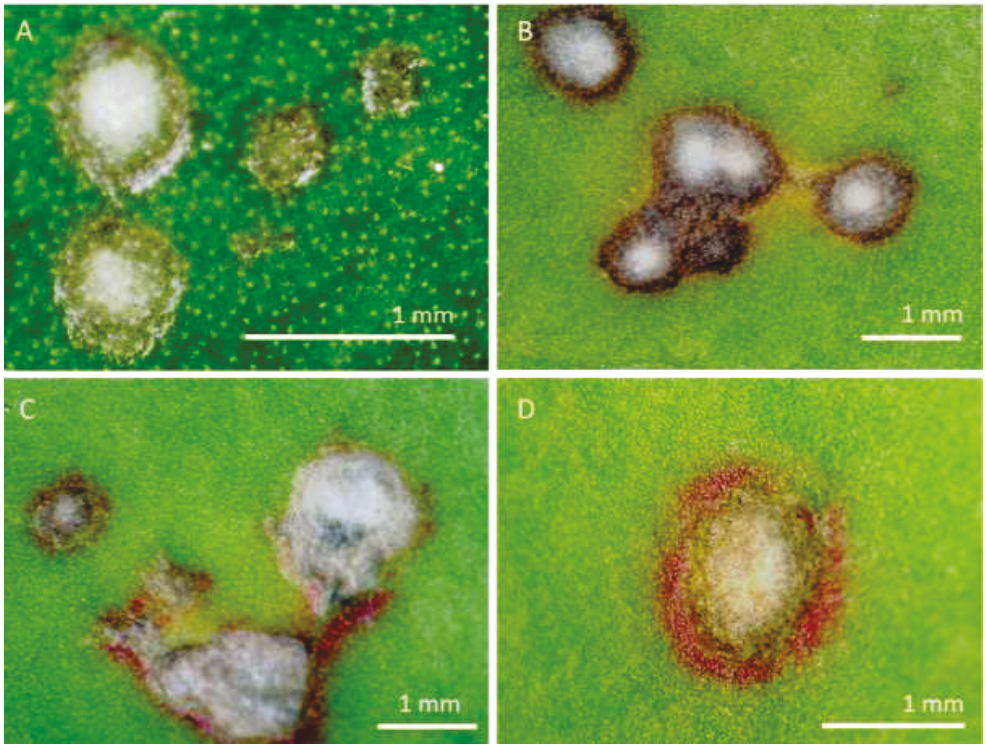

Fig. 11: Microscopic images of infected sugar beet leaves. (A) First appearing small brown spots with whitish middle part at the infection site. (B) Maturing spots with brownish margin, which progressively darkens and starts to coalesce. (C) Mature spot characterized by red margins. (D) Close-up of fully developed spot and red margin. Images were taken with the DigiMirco mobile microscope.

As described in literature (Lartey et al., 2010; Weiland and Koch, 2004), sugar beets accumulated betacyanines according to the wounding of leaf tissue visible as red margin around the lesions (Fig. 11 C, D). The brightness of the red color depends on the sugar beet genotype. Based on his crossings of forage beets with wild beets, Beta maritima, Schmidt (1928) described an increased red margin formation depending on the strength of the genetic maritima background. Moreover, the development of a cork layer around the fungal infection sites was discovered

(Schmidt, 1928). During the following symptoms development, an increasing leaf area became necrotic. Leaf necrosis started to enlarge from single infected leaf parts to larger leaf sections and usually led to a complete leaf loss (Fig. 12 A, B and C). Sugar beet genotypes were classified into resistance groups based on the visually estimated disease severity that had been shown previously by representatively infected leaves (Fig. 6).

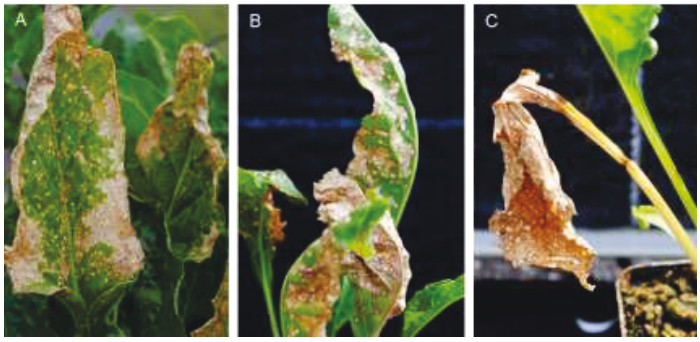

Fig. 12: Symptomatic sugar beet leaves infected with CLS. (A) Leaves with 25% infected area. (B) Curled, drying leaves due to infection. (C) Terminal leaf damage (100% infected leaf area)

In this study, sugar beet genotypes characterized by low susceptibility to CLS showed slow lesion formation and a low terminal disease severity compared with highly susceptible genotypes. Foliar disease severity was estimated visually and related with the terminal biomass loss of taproots.

3.2 Disease progression and effect on biomass development

Cercospora Leaf Spot causes sugar beet leaf damage, which can be classified by visual scoring (Shane and Teng, 1992). Differences in disease severity are indicators of plant physiological responses and defense ability allowing to classify the resistance level of genotypes. Different genotypes were scored after fungal inoculation to verify their resistance classes. Standard genotypes (STD) and breeding lines (BL) were examined showing high (HS), moderate (MS) and low (LS) susceptibility to CLS. The BLs of the KWS breeding program were scored in the KWS experimental field in Plattling (Bavaria, Germany) in August 2012. Breeding line 20 (BL 20) was scored as highly susceptible, BL 8 as lowly susceptible and BL 18 and 17 as moderately susceptible in the field experiment. In the greenhouse experiments of this thesis, plants showed variable disease severities and numbers of infected leaves depending on the season. The greenhouse conditions could not be controlled completely leading to seasonal differences in temperature, humidity and light intensity (Table 14). However, sugar beet genotypes characterized by low susceptibility to CLS usually showed a low terminal disease severity compared with highly susceptible genotypes. Therefore, the resistance classes of the genotypes could be verified by visual disease scoring.

3.2.1 Disease progression

In the first four experiments, the highly (HS), moderately (MS) and lowly susceptible (LS) standard (STD) genotype were inoculated and compared in order to verify their resistance classes by visual disease scoring. The HS plants showed 14% increased disease severity at 35 dpi compared with LS plants. The MS plants reached 53% infected leaf area at 35 dpi (Fig. 13 A). In experiment 2, HS plants showed a 20% increased disease severity at 27 dpi compared with LS ones (Fig. 13 B). The MS plants reached the highest infected leaf area with 71%, which was 29% increased compared with the HS ones. In experiment 3, HS plants showed a 12% increased disease severity at 27 dpi compared with LS plants (Fig. 13 C). The MS plants displayed a similar infected leaf area with 35% at 27 dpi (Fig. 13 C). In experiment 4, the HS plants reached 44% infected leaf area at 35 dpi, while the LS plants displayed 63% (Fig. 13 C).

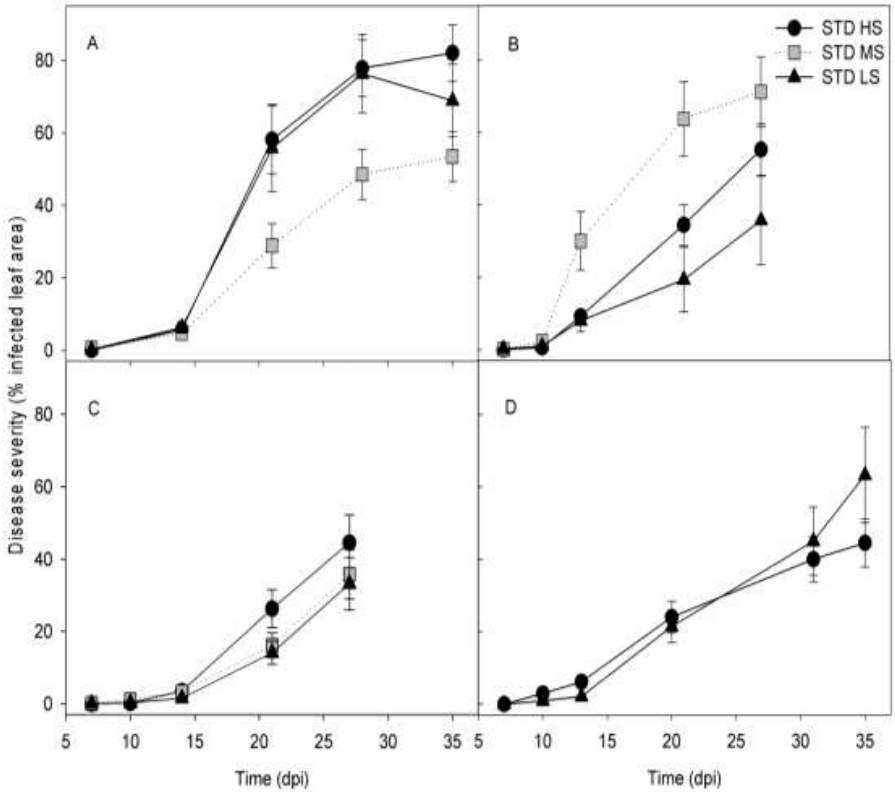

Fig. 13: Scoring of disease severity of standard genotypes. Disease severity (percentage of infected leaf area) of STD HS, MS and LS showed increasing numbers of symptomatic leaves (n_{HS}/ n_{MS}/ n_{LS}) from 0 dpi to 27, 28 or 35 dpi, respectively. (A) Experiment 1 (n = 5-19/ 19-43/ 11-20). (B) Experiment 2 (n = 24-25/ 3-16/ 5-15). (C) Experiment 3 (n = 7-34/ 2-35/ 4-35) and (D) Experiment 4 (n = 1-20/ 3-23). In the four experiments, the disease severity of genotypes was scored visually at leaf level. Mean values ± SE were calculated from disease onset (7 dpi) to plant harvest (27-35 dpi).

In experiment 9 to 11, the HS (BL 20), MS (BL 17 and 18) and LS (BL 8) breeding lines were inoculated and compared in order to verify their resistance classes by visual disease scoring. In experiment 9, the BL 20 plants showed 33% infected leaf area at 28 dpi compared with BL 8 plants (44%; Fig. 14 A). In experiment 10, BL 20 plants showed 39% infected leaf area at 42 dpi compared with BL 8 plants (25%; Fig. 14 B). The BL 18 plants reached 48% infected leaf area at 42 dpi. In experiment 11, BL 20 plants showed 12% infected leaf area at 28 dpi compared with BL 8 plants (6%; Fig. 14 C). The BL 17 and 18 plants reached 20% and 5% infected leaf area at 28 dpi.

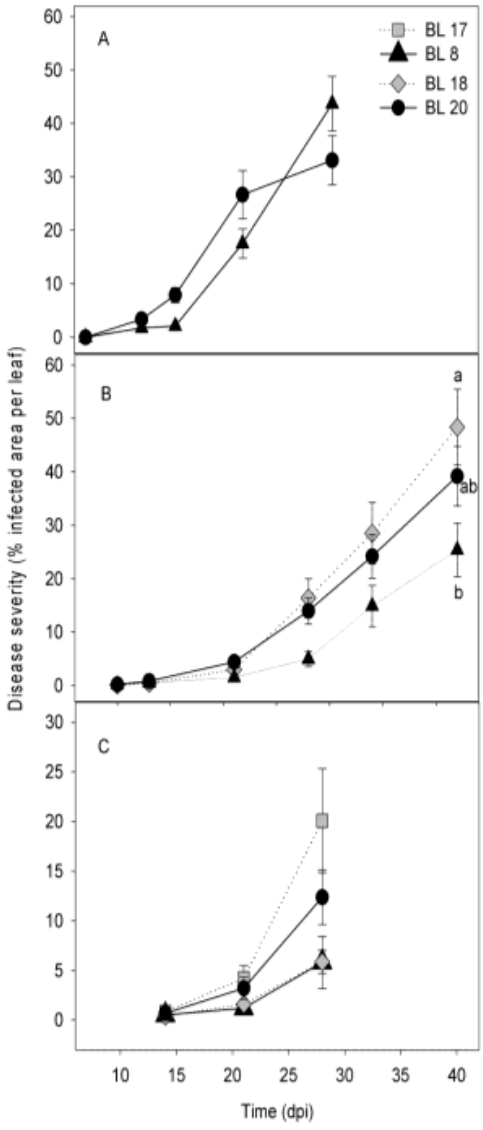

Fig. 14: Scoring of disease severity of breeding lines. Disease severity (percentage of infected leaf area) of BL 20, BL 18, BL 17 and BL 8 showed increasing numbers of symptomatic leaves (n_{BL20}/ n_{BL18}/ n_{BL8}/ n_{BL17}) from 0 dpi to 27, 28 and 42 dpi. (A) Experiment 9 (leaves per plant n = 7-77/ 1-74/ -). (B) In experiment 10 (n = 37-48 / 21-35 / 30-47/ -) a significant difference between the BL 8 and BL 18 genotype was measured at 42 dpi (One-Way ANOVA, $P<0.05$). (C) Experiment 11 (n = 34-37 / 31-33/ 33.37/ 32-38). Mean values ± SE were calculated from disease onset (7 – 14 dpi) to plant harvest (27 – 42 dpi).

In summary, the LS genotypes (STD LS and BL 8) usually showed a low terminal disease severity compared with HS genotypes (STD HS and BL 20), whereas the HS genotypes (STD MS and BL 17/ 18) displayed a variability in disease severity between the experiments. Generally, plants were more severely affected in experiments conducted during the late spring and summer season than during the winter and early spring period, indicating an influence of warm day temperature and high night humidity on the foliar infestation (Table 14).

3.2.2 Effect on taproot biomass and sucrose content

To investigate the influence of CLS on the biomass of sugar beets, plants were harvested 3 to 4 weeks after inoculation. Sugar beet genotypes were compared in order to quantify plant responses in taproot biomass and sugar accumulation during foliar disease development. The accumulation of shoot biomass was also quantified, but this section focuses only on the sugar storage organ, the taproot. Sugar beet genotypes of the aforementioned experiment 3, 4, 10 and 11 (Fig. 13; Fig. 14; Table 13) were compared based on the ratio of taproot biomass of both treatments ($FW_{inoculated}$ $FW_{non\text{-}inoculated}^{-1}$). A decreased ratio indicates biomass reduction due to fungal infection.

In experiment 3 and 4, the taproot biomass of the HS, MS and LS standard genotypes was compared to quantify the growth reduction caused by fungal infestation. The taproot biomass of HS plants (ratio 0.53) was more affected by fungal infection than the LS ones (ratio 0.89), while plants showed disease severity of 45% and 33% infected leaf area at 27 dpi (Fig. 15 A). The MS plants showed similar reduction in biomass (ratio 0.87) as LS plants with 35% infected leaf area. In experiment 4, the taproot biomass of HS plants (ratio 0.65) was more affected by fungal infection than the LS ones (ratio 0.81), while plants showed disease severity of 72% and 75% infected leaf area at 35 dpi (Fig. 15 B).

In experiment 10 and 11, the taproot biomass of the breeding lines BL 20, BL 18, BL 17 and BL 8 were compared to quantify the growth reduction caused by CLS infestation. In experiment 11, the taproot biomass of BL 20 plants (ratio 0.72) was more affected by fungal infection than the BL 8 ones (ratio 0.76), while plants showed disease severity of 12% and 20% infected leaf area at 28 dpi (Fig. 15 C). The BL 17 plants showed similar reduction in biomass (ratio 0.77) with 6% infected leaf area, while the BL 18 plants displayed the lowest reduction (ratio 0.81) with 6% (Fig. 15 C). In experiment 10, the taproot biomass of BL 20 plants (ratio 0.74) was similarly affected by fungal infection compared with the BL 8 ones (ratio 0.74), while plants showed disease severity of 39% and 25% infected leaf area at 28 dpi (Fig. 15 D). The BL 18 plants showed the lowest biomass reduction (ratio 0.85) with 48% infected leaf area (Fig. 15 D).

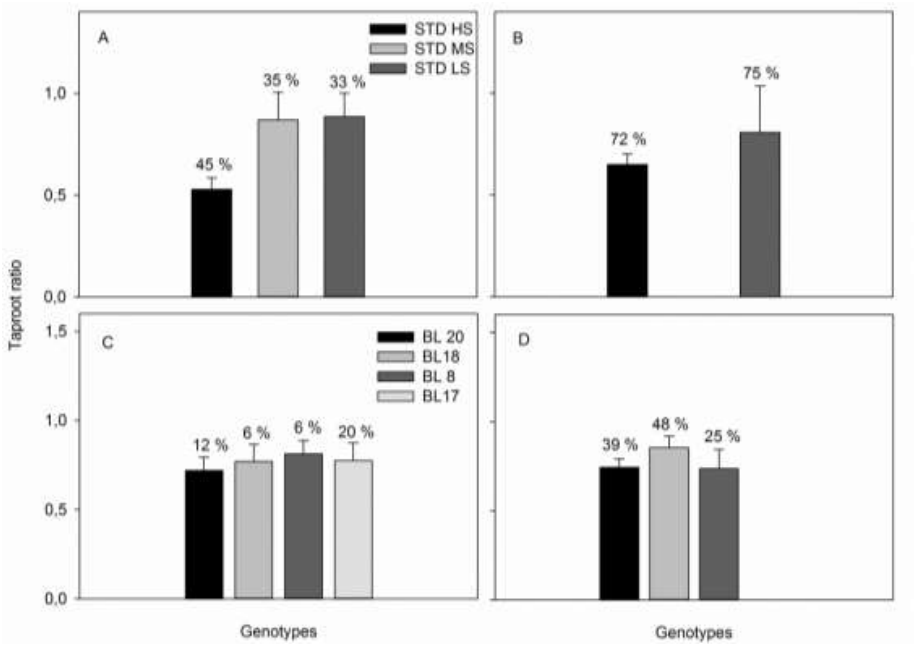

Fig. 15: Taproot ratio of sugar beet genotypes. Taproot ratio ($FW_{inoculated}$ $FW_{non\text{-}inoculated}^{-1}$) with percentage of disease severity in (A) experiment 3 at 27 dpi (71 das) and in (B) experiment 5 at 27 dpi (64 das), and of breeding lines in (C) experiment 11 at 28 dpi (64 das) and (D) experiment 10 at 42 dpi (87 das). Mean values of n = 5 (A, C, D) and n = 8 (B) plants per treatment. The variation of each treatment was calculated according to the propagation of error.

In experiment 1, the impact of CLS on the taproot sucrose content (µmol g_{FW}^{-1}) and on the relative sucrose content (%) was analyzed. In this experiment, that had been described previously regarding the progression of disease severity (Fig. 13 A), the taproot sugar amount of the HS, MS and LS standard genotypes were analyzed at 35 dpi (85 das). The HS plants showed the lowest taproot sucrose content and relative sucrose content in the inoculated as well as in the non-inoculated treatment (Fig. 16). The LS plants displayed the highest values in both treatments, whereas the MS plants had lower values compared with the LS plants.

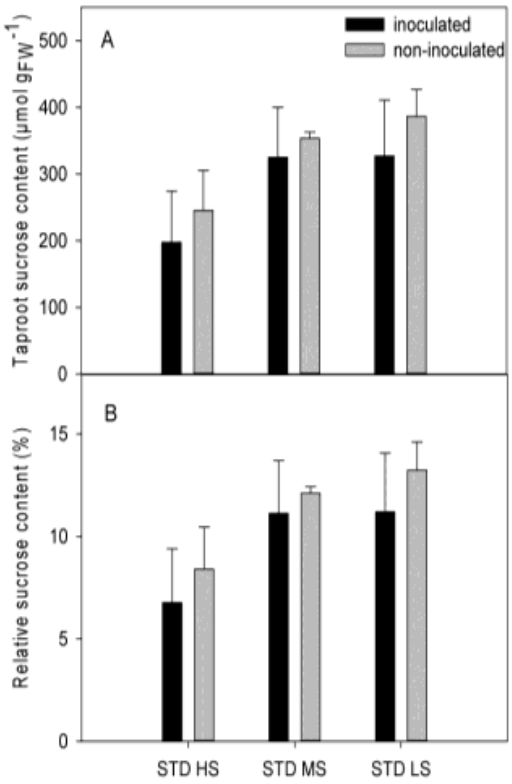

Fig. 16: Taproot sucrose amounts of standard genotypes. (A) Taproot sucrose content (µmol gFW^{-1}) and (B) relative sucrose content (%) of STD HS, MS and LS quantified by a coupled enzyme assay that was analyzed in a spectrophotometer. Plants were harvested at a plant age of 85 das and 35 dpi. Mean, non-inoculated plants n = 3 (HS) and n = 2 (MS; LS), and inoculated plants n=5 (HS; LS) and n = 6 (MS) ± SD.

To summarize, the HS genotypes (STD HS, BL 20) showed the highest reduction in taproot biomass due to fungal infection. While the MS (STD MS, BL 18) and LS (STD LS, BL 8) plants showed a similar or an increased disease severity compared with the HS plants, the taproot biomass of HS plants was lower. This indicates that plants characterized by a low susceptibility were able to defend more effectively against CLS compared with plants displaying a high susceptibility. The measurement of taproot sucrose revealed a reduction in the inoculated treatments of all three genotypes compared to the respective non-inoculated treatment. Even though it is widely known, that CLS reduces the sugar content of sugar beet (Lartey et al., 2010; Shane and Teng, 1992), the data of sucrose measurements should be interpreted with care, because only a low number of taproot samples were analyzed in this study. However, the LS genotype displayed the highest sucrose content indicating a high disease pressure, because HS genotypes were described to produce an increased biomass and sugar content under low disease pressure (Smith and Ruppel, 1974).

3.2.3 Effects of disease progression on biomass

In summary, highly susceptible genotypes (STD HS and BL 20) were more severely infected, more strongly reduced in growth and had a lower sugar content of the taproot compared with lowly susceptible ones (STD LS and BL 8). Moderately susceptible genotypes (STD MS, BL 18 and BL 17) varied in disease strength under experimental conditions and displayed variable reaction in biomass reduction. Disease severity did not correlate linearly with biomass reduction. Overall, lower biomass reduction was measured in genotypes with increased resistance. According to the visual differences in disease response and in taproot weight, these genotypes were used for further experiments in order to investigate the fungal establishment on the leaf surface and its growth in the leaf tissue as well as its effect on leaf signature and taproot growth dynamics.

3.3 Influence of leaf waxes on plant resistance

Conidia have to adhere to the leaf surface prior to plant infestation. The leaf surface, or the plant cuticle, represents a physical barrier that has to be overcome by pathogens. The water-repelling property of leaf waxes represents a challenge to pathogens. After adhesion, some fungi depend on wet host interface for conidia germination (Carver and Gurr, 2008). Wax components are also crucial for the host recognition of some fungi and thus, the germination of their conidia (Tsuba et al., 2002). Therefore, the amount and composition of leaf waxes, and subsequently wax crystals and their structure on the leaf surface may influence fungal infection success (Carver and Gurr, 2008). The cuticular waxes of two genoytypes were analyzed in three experiments to investigate, if they contribute to plant resistance (Table 8). In the third wax experiment, leaves were inoculated and analyzed to correlate the leaf wax amount with the fungal growth in the leaf tissue (Table 13, experiment 15). Additionally to the comparison of the lowly susceptible (BL 8) and the highly susceptible (BL 20) genotype, mature and immature leaves were compared, because faster disease onset of younger (immature) leaves had been described previously (Lartey et al., 2010). In these three experiments, it could be shown that the LS genotype and mature leaves had higher total wax amounts than the HS genotype and the respective immature leaves.

In a preliminary wax experiment, one sample per genotype and leaf age was analyzed to verify differences between these two factors. One sample was averaged of two leaves (one leaf per plant). It could be shown, that BL 8 plants had higher total wax amounts in mature (2.9 µg cm^{-2}) and immature (2.1 µg cm^{-2}) leaves compared with BL 20 leaves, which showed 2.1 µg cm^{-2} (mature) and 1.7 µg cm^{-2} (immature). The main wax compound, primary alcohols, displayed a similar trend.

In the first wax experiment, the aforementioned differences in the total wax amount of the preliminary experiment could be verified between the BL 20 and BL 8 genotype in regard to plant susceptibility and leaf age. Highly significant differences could be detected in the total wax amount between the two breeding lines (Fig. 17 A, One-Way ANOVA, Holm-Sidak, $P<0.001$). Mature HS leaves reached 3.4 µg cm^{-2} total wax amounts, while immature ones showed 2.2 µg cm^{-2}. Compared with the respective HS leaves, mature LS ones had a 26% and immature leaves a 15% increased wax amount. Comparing the leaves of each genotype showed that mature leaves displayed significantly more waxes than their respective immature ones. The HS matures leaves had a 44% and the LS matures ones had a 35% higher total wax amount compared with the respective immature ones (Fig. 17 B, One-Way ANOVA, $P<0.05$). The main component of sugar beet waxes of both genotypes and leaf ages were primary alcohols, followed by acids and esters. Mature HS leaves showed 2.5 µg cm^{-2} and immature leaves 1.9 µg cm^{-2} primary alcohols, whereas mature LS leaves reached higher amounts. The wax composition of immature leaves was

similar between genotypes, 93 to 94% primary alcohols, 2% acids and 5% esters (Table 16). With leaf maturity this composition changed and differences between genotypes appeared (Fig. 17 B, C). Mature LS leaves displayed decrease of primary alcohol by 4%, increase of acids by 3% and of ester by 1% amount compared to HS ones (Table 16). The main wax component of both genotypes and leaf ages was the C_{26} alcohol representing the main difference in total wax amount.

Table 16: Wax composition of breeding lines. Mature and immature leaves of HS (BL 20) and LS (BL 8) plants consisted of primary alcohols, acids and esters (% of total wax amount).

	HS		LS	
	mature	immature	mature	immature
primary alcohols	79	93	83	94
acids	7	2	4	2
esters	14	5	13	5

Compared with the respective HS leaves, mature LS ones had 31% and immature ones 22% higher C_{26} alcohol amounts (Fig. 17 B). Comparing the leaves of each genotype showed that mature leaves accumulated significantly more C_{26} alcohol than their respective immature ones. The HS matures leaves had 26% and the LS matures ones 34% higher C_{26} alcohol amounts compared with the respective immature leaves (Fig. 17 B, t-test, $P<0.001$). The main fatty acids component of mature leaves were C_{26} and C_{28} acids, whereas C_{30} acids was represented in similar amounts in mature and immature ones (Fig. 17 D). The main wax ester component of mature leaves were C_{40} and C_{42} esters, whereas immature ones had very low amounts of wax esters (Fig. 17 E). Compared with other increased compounds in mature leaves, β-Sitosterol was increased in immature leaves representing an important membrane compound stabilizing phospholipids of cell membranes in plants (Raven et al., 2006).

In summary, the LS plants showed an significantly increased total wax amount compared to the HS plants of the preliminary and first experiment. For both genotypes, mature leaves displayed significantly higher total wax amounts compared with their respective immature leaves.

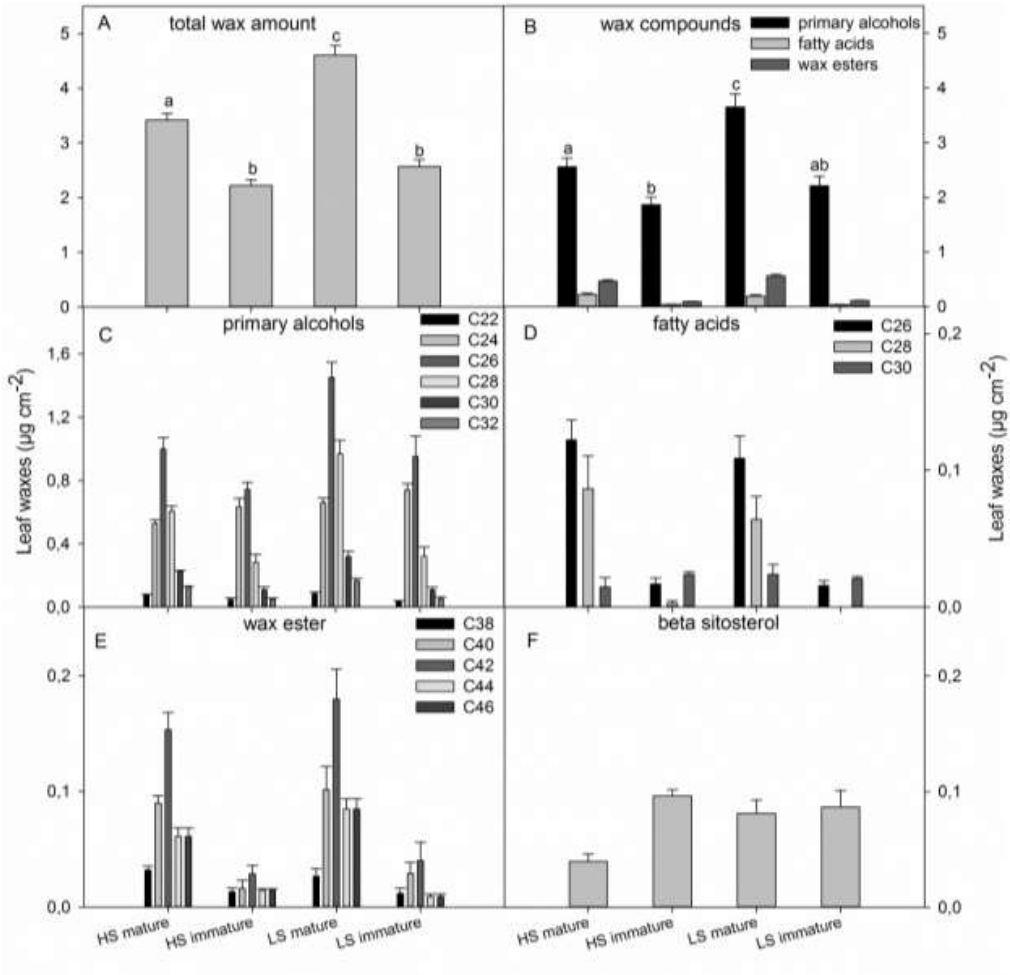

Fig. 17: Cuticular waxes of breeding lines. Summed wax amount of the adaxial and abaxial leaf surfaces of the HS (BL 20) and LS (BL 8) genotype in the first wax experiment. (A) Total wax amount. (B) Wax composition consisting of primary alcohols, fatty acids and wax ester. (C) Primary alcohols, (D) fatty acids. (E) Wax esters. (F) Amount of β-Sitosterol. (A, B) Significant difference in total wax amount and primary alcohols between genotypes and leaf age were detected by GC-MS and analyzed by a One-Way ANOVA, Holm-Sidak, $P<0.001$ (A) and $P<0.05$ (B). Waxes were quantified with GC-FID of mature (leaf 3 and 4) and immature (leaf 7 and 8) leaves; wax components were identified by GC-MS. Mean ± SE, n = 5.

In the second wax experiment (Table 8; equivalent to experiment 15 in Table 13), the impact of leaf waxes on the pathogen establishment was investigated to correlate the total wax amount with the fungal growth in the leaf tissue. In this context, sugar beet leaves of the HS and LS genotype were inoculated and were analyzed at two time points, one and three days after inoculation, in regard to the amount of leaf waxes and fungal biomass.

At 1 dpi, the LS leaves showed a significantly increased total wax amount compared to the immature HS leaves (Fig. 18 A, One-Way ANOVA, Holm-Sidak, P<0.05). At 3 dpi, immature leaves of both genotypes had significantly increased total wax amounts compared with the respective mature leaves (Fig. 18 B, One-Way ANOVA, Holm-Sidak, P<0.05). In comparison to the first experiment, the total wax amount of this experiment was about two-fold lower, probably because only the waxes of one leaf side were analyzed.

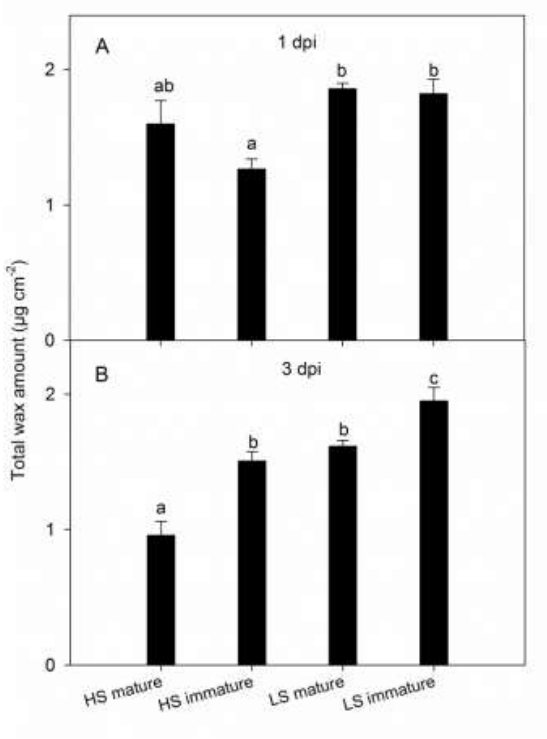

Fig. 18: Cuticular waxes of breeding lines after fungal inoculation. Total wax amount of the adaxial leaf surface of the HS (BL 20) and LS (BL 8) genotype 1 and 3 days after inoculation (dpi) in the second wax experiment. (A) Total wax amount at 1 dpi. (B) Total wax amount at 3 dpi. Significant difference in total wax amount of mature (leaf 3 and 4) and immature (leaf 5 and 6) leaves were detected by GC-MS and analyzed by a One-Way ANOVA, Holm-Sidak, P<0.05. Mean ± SE, n=4.

Besides the leaf wax analysis, leaves were also analyzed regarding the fungal growth within the leaf tissue. The analysis of fungal growth at 3 dpi revealed that immature leaves of both genotypes showed a higher fungal amount compared with mature leaves (Fig. 19). Comparing the two genotypes, the LS plants showed higher fungal amounts than the HS genotype.

The second wax experiment investigated not only the fungal growth on an "untreated" leaf surface (Fig. 19), but also on leaf surfaces that were stripped with cellulose acetate. Leaves were bisected at the middle lamella to analyze one untreated and one stripped leaf half. At 1 and 3 dpi, the total wax amount did not differ between untreated and stripped leaf surfaces, indicating that the wax removal was not sufficient. Because there were also no differences in the fungal growth between the two treatments, just the data of the untreated leaf surface were shown (Fig. 18; Fig. 19).

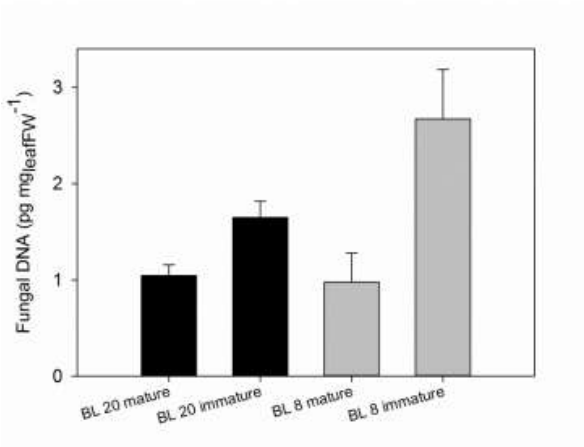

Fig. 19: Fungal amount of inoculated leaves of breeding lines. Fungal amounts of the HS (BL 20) and LS (BL 8) genotype were detected by qRT-PCR based on the *C. beticola* calmodulin gene. In the second wax experiment (equivalent to experiment 15), leaf discs of mature and immature leaves were sampled at 3 dpi of (A) BL 20 and (B) BL 8. Mean, n=5 ± SE.

To summarize the preliminary and the first wax experiment, LS plants and mature leaves had higher total wax amounts compared to HS plants and immature leaves. The main component of sugar beet leaf waxes was C_{26} primary alcohol, which decreased in wax composition during leaf maturing. The removal of epicuticular waxes had no effect on total wax amount, fungal growth and symptom development (data not shown). Contradictory to the preliminary and the first experiment, mature leaves of the second experiment did not showed higher wax amounts compared with immature leaves. An explanation for this investigation could be that the ascribed "immature" leaves of the second experiment were further developed compared with immature leaves of the preliminary and second experiment. Furthermore, sugar beets of the second experiment were delayed in growth during the winter season compared to the plants of the other two experiments (Table 13; Table 8). Regarding the total amount of waxes, the adaxial leaf surface seemed to have higher amounts than the abaxial one, because higher wax amounts were measured in the first experiment that includes both leaf surface sides.

3.4 Fungal growth in leaf tissue

After invading through the stomata fungal hyphae start to grow within the intercellular space of the leaf tissue (Steinkamp et al., 1979). However, depending on their resistance level, plants can inhibit further fungal spreading. The fungal growth in sugar beet leaves of HS and LS genotypes was quantified by quantitative real-time PCR (qRT-PCR) amplification to analyze genotype-specific responses against *C. beticola* and to enable an early detection of *Cercospora* leaf spot.

First, to test if the DNA extraction of fungal mycelia worked properly, standard primers were used for fungal gene amplification. The analysis of the nucleic sequence of the 5.8S rRNA gene and nearby ITS- region (Internal Transcribed Spacer) allows species-specific identification of fungi (Gardes et al., 1991). The ITS region of *C. beticola* showed an amplified length of about 550 bp (Fig. 20 A), as described previously (Weiland and Sundsbak, 2000).

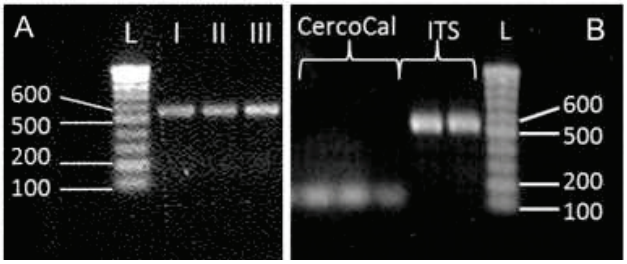

Fig. 20: Agarose gel electrophoresis of fungal DNA. (A) Testing the protocol for optimized DNA extraction of pure *Cercospora* mycelia and the amplification of the ITS region from two samples, I to III. (B) Comparison of amplified ITS and calmodulin region of pure fungal DNA with ITS 1 and 4, and CercoCal primers. Each PCR reaction contained 50 ng_{DNA} starting material and fragment sizes were compared with a 100 bp DNA Ladder (New Enfland Biolabs, Ipswich, Massachusetts, USA).

For amplifying the calmodulin gene of *C. beticola,* specific primers were used (De Coninck et al., 2011). These CercoCal primers allowed the amplification of a 298 bp fragment of the calmodulin gene in a PCR approach (Fig. 20), but did not work properly in the qRT-PCR analysis based on SYBR Green detection dye. Besides the specific melting curve peak of calmodulin at 88°C, a second fragments was amplified. The CercoCal primers were developed for the TaqMan detection method requiring an additional probe between primers for amplifying accurately. Therefore, new primers were developed also based on the *C. beticola* calmodulin gene (EMBL-EBI, DQ026493) for qRT-PCR reactions with the single fluorescence dye SYBR Green. Primer sequences were selected based on a Basic Local Alignment Search Tool (BLAST) comparing *C. beticola* and *C. apii* (EMBL-EBI, AY840414.1) that are both able to infect sugar beets. The forward primer was designed for the DNA regions with five distinct differences between the two species (See attachments, Chapter 10.1). To test the qRT-PCR analysis, samples were spiked with an additional amount of

fungal DNA to verify sensitivity of this detection system. An additional amount of pure fungal DNA (30 ng_{DNA}) spiked into a leaf sample, which had a DNA concentration of 300 ng_{DNA} (fungal and plant DNA), reduced the cycle thresholds (Ct) value from 27 to 19.3. Thus, a 10% increase of fungal DNA led to distinct lowering of the C_t value. Furthermore, non-infected leaves were introduced as controls resulting in high C_t values beyond the fungal standard curve meaning that plant DNA did not intervene with the fungal detection.

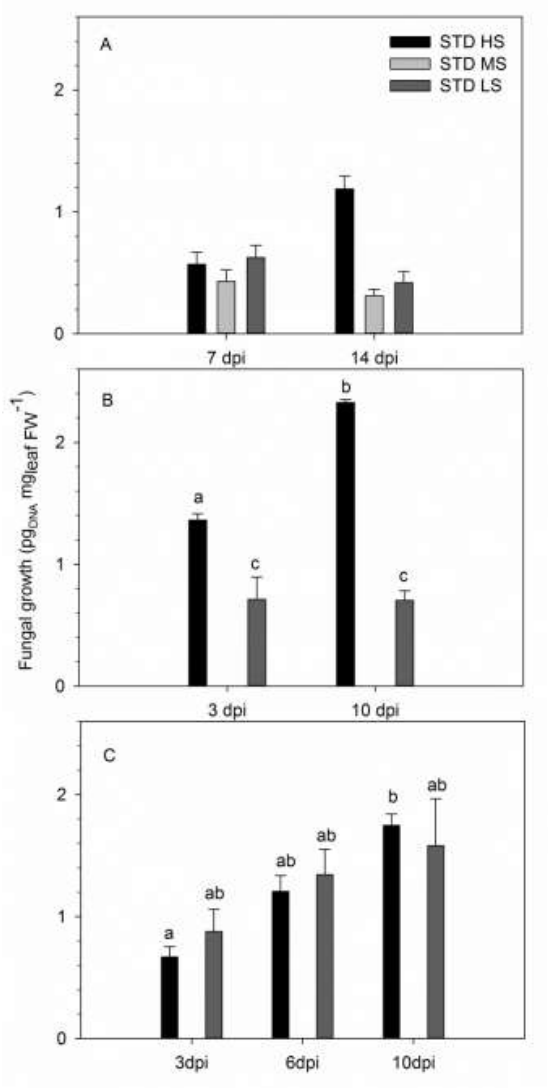

Fig. 21: Fungal amount of standard genotypes . Fungal amounts (pg_{DNA} $mg_{leaf\ FW}^{-1}$) of STD HS, MS and LS leaves were detected by qRT-PCR quantifying the *C. beticola* calmodulin gene. (A) In experiment 3, leaf discs were taken from leaf halves (n = 2 samples per genotype) at 7 and 14 dpi. Genotypes showed a disease severity between 0.5 to 10% (HS; MS) and 5% (LS) at 14 dpi. (B) In experiment 4, significant difference between leaf halves was detected (n = 4 per genotype) at 3 and 10 dpi (Two-Way ANOVA, Holm-Sidak, $P<0.001$). Genotypes showed a disease severity between 0.1 to 5% (HS) and 0.2% (LS) at 10 dpi. (C) In experiment 6, the HS genotype showed an significantly increased fungal amount from 3 to 10 dpi (n = 5 per genotype) estimated by One-Way ANOVA, Holm-Sidak, $P<0.05$. Genotypes showed a disease severity between 0.2 to 0.5% (HS; LS) at 10 dpi. Mean ± SE.

To quantify the fungal growth in the leaf tissue, non- and low symptomatic leaf disease stages were chosen to avoid an underestimation of fungal DNA. The necrosis of plant material could lead to fungal DNA loss in symptomatic leaves. Above 3% to 5% infected leaf area, fungal amount was underestimated (data not shown), as it had been described previously (De Coninck et al., 2011). In subsequent experiments, leaves of STD and BL genotypes were inoculated and fungal amount was quantified to analyze genotype-specific responses.

In experiment 3, 4 and 6, the three standard genotypes, STD HS, MS and LS, were compared in order to quantify fungal amount in inoculated leaves from 3 to 14 dpi at low-symptomatic disease stages. In experiment 3, genotypes showed a disease severity up to 10% (HS; MS) and 5% (LS) at 14 dpi, no symptoms were visible at 7 dpi. In the HS plants, a 50% increase of fungal amount was quantified from 7 to 14 dpi (Fig. 21 A), whereas the LS plants showed a slightly decreased fungal amount. In the MS plants, the fungal amount also slightly decreased. In experiment 4, genotypes showed a disease severity up to 5% (HS) and 0.2% (LS) at 10 dpi, at 3 dpi no symptoms were visible. From 3 to 10 dpi, a significantly increased fungal amount was measured in the HS plants, whereas the fungal amount in the LS plants did not change (t-test, $P<0.001$; Fig. 21 B). In experiment 6, genotypes showed an initial disease severity up to 0.5% (HS; LS) at 10 dpi. From 3 to 10 dpi, a significantly increased fungal amount was quantified in the HS plants (t-test, $P < 0.05$), whereas an non-significantly increasing fungal amount was measured in the LS plants (Fig. 21 C).

In experiment 9, 12, 14 and 15, the three breeding lines, BL 20, BL 18 and BL 8, were compared in order to quantify fungal amount in inoculated leaves from 1 to 10 dpi at low- and non-symptomatic disease stages. In experiment 9, genotypes showed no disease severity at 1, 4 and 6 dpi, whereas a significantly increasing fungal amount was quantified in the BL 20 and BL 8 plants (Fig. 22 A). In experiment 12, genotypes showed an initial disease severity up to 0.1% at 8 dpi (BL 20; BL 8). In the BL 20 plants an increase of fungal amount from 4 to 6 dpi and a decrease from 6 to 8 dpi was measured. This was similar in the BL 8 plants (Fig. 22 B). In experiment 13, genotypes showed no disease severity at 3 and 6 dpi, while an increase of fungal amount was quantified in the BL 20 plants. Such an increase was also measured in the BL 18 and in the BL 8 plants during the same period (Fig. 22 C). In experiment 14, genotypes showed a disease severity up to 0.2% (BL 20; BL 18; BL 8) at 10 dpi. In the BL 20 plants, a slight increase of fungal amount was measured from 3 to 10 dpi, whereas in the BL 8 plants a slight decrease was quantified and in the BL 18 plants no change was measured (Fig. 22 D). At 6 dpi, a slight decrease of fungal amount was measured in the BL 20 and BL 8 plants.

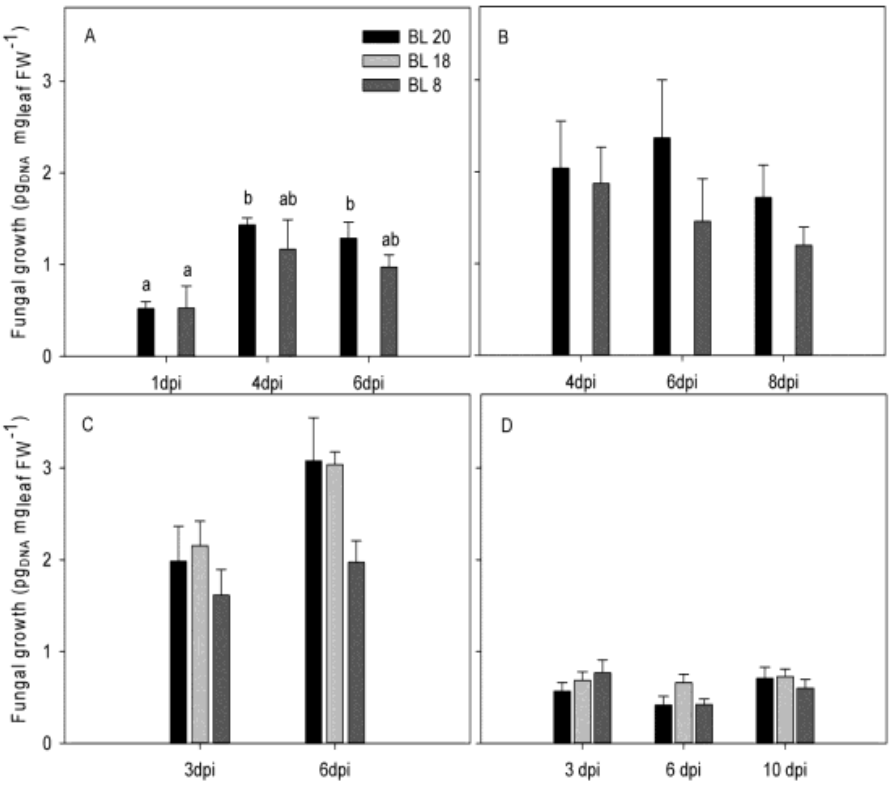

Fig. 22: Fungal amount of breeding lines. Fungal amounts (pg_{DNA} $mg_{leaf\ FW}^{-1}$) of BL 20, BL 18 and BL 8 leaves were detected by qRT-PCR quantifying the *C. beticola* calmodulin gene. (A) In experiment 9, the BL 20 leaves showed an significantly increasing fungal amount from 1 dpi to 4 and 6 dpi (One-Way ANOVA, Holm-Sidak, $P<0.05$). Genotypes showed no disease severity at 6 dpi. (B) In experiment 12, leaves were compared at 4, 6 and 8 dpi. Genotypes showed a disease severity between 0.01 to 0.1% (BL 20; BL 8) at 8 dpi. (C) In experiment 13, leaves were compared at 3 and 6 dpi. Genotypes showed no disease severity at 6 dpi. (D) In experiment 14, leaves were compared at 3, 6 and 10 dpi. Genotypes showed a disease severity between 0.01 to 0.2% (BL 20; BL 18, BL 8) at 10 dpi. Mean ± SE, n = 6 leaves per genotype.

In summary, CLS infection could be detected at an early, non-symptomatic disease stage of sugar beet leaves. The quantification of the fungal amount allowed to distinguish between genotypes and to verify their resistance classes. Overall, the HS plants (STD HS and BL 20) showed higher fungal amounts compared with LS ones (STD LS and BL 8). The MS plants (BL 18) showed similar or slightly higher fungal amounts compared with BL 20 plants. Based on their distinguishable responses, genotypes were used in further experiments in order to compare changes in photosynthesis, leaf signature and taproot growth dynamics.

3.5 Photosynthetic efficiency during foliar infestation

Foliar pathogens can cause the reduction of photosynthetic active leaf area, because of the leaf damage and the disturbance of photosynthesis in the remaining or surrounding leaf area (Berger et al., 2004; Robert et al., 2006). For *Cercospora* infection on sugar beet, it has been shown that photosynthesis was reduced, when a disease severity of 3-6% was reached using pulse-amplified modulation (PAM) fluorometer (Levall and Bornman, 2000). With the use of chlorophyll fluorescence imaging, the reduction of photosynthesis could be measured shortly before and after disease onset (Chaerle et al., 2007) under laboratory conditions. In order to investigate the impact of *Cercospora* infestation on sugar beets under greenhouse conditions, PAM measurements were conducted for the inoculated and non-inoculated BL 20 plants during the course of the day.

In experiment 17, the photosynthetic efficiency of inoculated and non-inoculated BL 20 sugar beet leaves were compared in regard to the apparent rate of photosynthetic electron transport (ETR) and the actual quantum yield Y(II) of photosystem (PS) II, depending on the photosynthetic active radiation (PAR). Dark adapted leaves were measured between 12 p.m and 1 a.m. to obtain the quantum yield of PSII as $Y(II)_{dark}$.

The electron transport rate (ETR) of the inoculated and non-inoculated leaves showed a high distribution. The relation of ETR to PAR for each leaf could be indicated by the use of curve fitting. Three days before inoculation, the ETR curves of the leaves of both treatments showed comparable values, while one non-inoculated leaf displayed higher ETR values compared with all other leaves (Fig. 23 A). At 14 dpi, the ETR curves of the inoculated leaves were slightly higher compared to the curves of the non-inoculated leaves (Fig. 23 B). At 24 dpi, the ETR curves lowered subsequently in leaves of both treatments, but only the inoculated leaf number #4 showed a reduced ETR (Fig. 23 C). However, also the ETR curves of the non-inoculated leaves decreased slightly from -3 dpi, to 14 and 24 dpi (Fig. 23 A, B, C).

While the ETR curves of the single leaves did not reveal a clear difference between the two treatments, the actual quantum yield of PSII Y(II) was just divided into the inoculated and non-inoculated treatment. The relation of Y(II) to PAR could be indicated by the use of curve fitting. At -3 dpi, the Y(II) curve of the inoculated treatment was similar compared with the non-inoculated leaves (Fig. 23 D). At 14 dpi, the Y(II) curve of the inoculated leaves was increased compared with the curve of the non-inoculated leaves and increased slightly until 24 dpi (Fig. 23 E, F). However, the Y(II) data points of the non-inoculated leaves also showed an increasing distribution at 24 dpi (Fig. 23 F).

The ETR and Y(II) curves did not reveal a clear difference between the inoculated and non-inoculated treatment at 14 and 24 dpi, while first visible leaf symptoms appeared at 14 dpi. At 14 dpi, all inoculated leaves showed first small necrotic spots

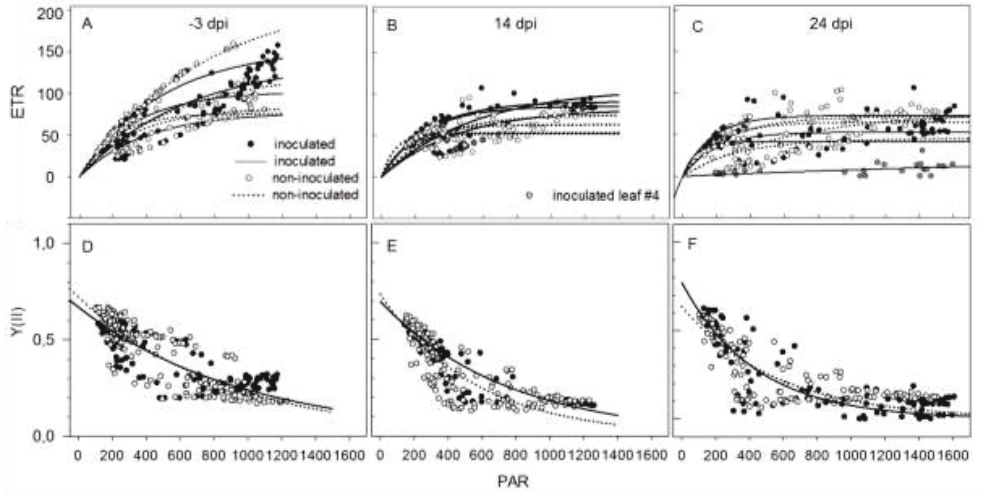

Fig. 23: Photosynthetic efficiency and electron transport rate of the HS breeding line. The efficiency of PSII (Y(II)) and the electron transport rate (ETR) of *C. beticola* inoculated and non-inoculated leaves of the BL 20 genotype at -3, 14 and 24 dpi. (A, B, C) ETR of each sugar beet leaf and (D, E, F) averaged Y(II) of the inoculated and non-inoculated treatment are shown depending on the photosynthetic active radiation (PAR). (B, C) The data of leaf sample #4, that showed a 60% infected measurement area at 24 dpi, were shown in gray (Fig. 24 I, J).The ETR data were fitted using a positive exponential function with a rise to maximum (single, two parameters) and the Y(II) data were fitted using a negative exponential function (single, two parameters) of light intensity by the Regression Wizard (SigmaPlot). Per treatment n = 4 leaves (one leaf per plant) were fixed in the leaf clips of monitoring PAM fluorometers and measured subsequently 24h per day, whereas data points were taken from 10 a.m. to 3 p.m. Measurement areas were inoculated with *C. beticola* conidia and single leaves were kept in plastic bags for three days to establish fungal infestation.

(<1%), while only one leaf had one and another leaf had two leaf spots in the leaf clip area. Compared to non-inoculated leaves (Fig. 24 A, B) at 24 dpi, leaf clip areas of inoculated leaves displayed disease severities of about 1% (Fig. 24 C, D), 3% (Fig. 24 E, F), 10% (Fig. 24 G, H) and 60% (Fig. 24 I, J). While visible leaf damage had already been occurred, it could not be distinguished between the inoculated and non-inoculated treatment in regard to ETR and Y(II). Just one leaf, leaf number #4, showed reduced ETR values (Fig. 23 C) that was referred to a 60% damage of the leaf clip area (Fig. 24 I, J). With the aim to highlight the difference in Y(II) between the two treatments, leaves were measured during the night to calculate the quantum yield of the relaxed PSII ($Y(II)_{dark}$). In both treatments, the $Y(II)_{dark}$ values were similar before and fourteen days after inoculation (Fig. 25). At 24 dpi, a difference between the treatments was measured (Table, Fig. 25). This reduction of photosynthetic efficiency was referred to the leaf number #4 showing a nearly completely destroyed leaf clip area (Fig. 24 I, J). The low disease severities up to 10% of the measurement area did not influenced $Y(II)_{dark}$.

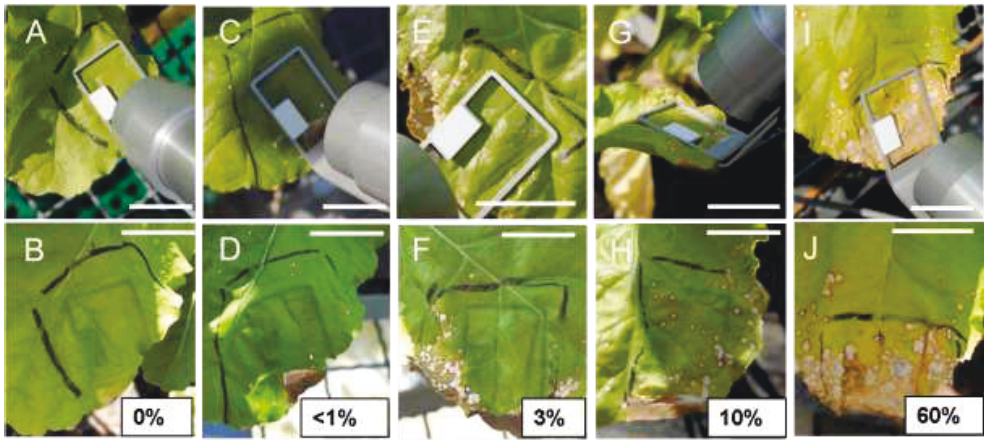

Fig. 24: Leaves of the HS breeding line fixed in leaf clips. Leaves of the BL 20 genotype were measured with Monitoring PAM fluorometers and were fixed in the leaf clips with an area of 2.2 cm x 3 cm, whose outline was visible at 24 dpi. To mark the measured leaf area before the inoculation, a rough black outline was drawn by hand. The non-inoculated leaf showed no disease severity (A, B), whereas the inoculated leaves showed a <1% (C, D), 3% (E, F), 10% (G, H) and 60% (I, J) infected area at 24 dpi of the leaf clip. Leaves are shown with fixed (A, C, E, G, I) and without leaf clips (B, D, F, H, J).

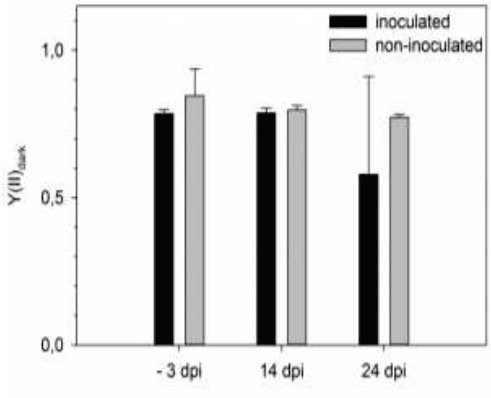

Treatment	$Y(II)_{dark}$	SD
Non-inoculated	0.77	0.01
Inoculated	0.77	0.01
Inoculated *	0.58	0.33

Fig. 25: Photosynthetic efficiency of the HS breeding line. The quantum yield of photosystem ($Y(II)_{dark}$) of inoculated and non-inoculated sugar beet leaves of the BL 20 genotype. (A) $Y(II)_{dark}$ at -3, 14 and 24 dpi. (B) Table of $Y(II)_{dark}$ at 24 dpi without (mean, n=3) and with (*) the leaf sample #4 that showed a 60% infected measurement area (See Fig. 26 I, J). Mean ± SD (n=4).

In summary, the ETR and Y(II) curves did not show differences between the inoculated and the non-inoculated treatment under greenhouse conditions. The reduction of ETR in both treatments from -3 to 24 dpi might be referred to leaf senescence. It might be possible that differences between inoculated and non-inoculated leaves become clear at higher light intensities beyond 1600 µmol cm^{-2} s^{-1} under laboratory conditions. A reduction of photosynthetic efficiency of PSII was detectable at an almost completely destroyed leaf clip area. Lower disease severity up to 10% did not affect $Y(II)_{dark}$. Plants seemed to be able to compensate the loss of photosynthetic active leaf according to fungal damage. Even though disease severity was already at a progressed stage, significant differences could not be detected using PAM fluorometers. Since only four leaves per treatment were measured in this experiment, these results should be interpreted with caution. Nonetheless, it would be valuable to investigate the impact of fungal infestation on photosynthesis using imaging fluorometer to distinguish between leaf spots and surrounding leaf area. Gas exchange measurements would enable to investigate early changes of plant respiration due to infestation. Comparing greenhouse, laboratory and field conditions might allow to evaluate the impact of light quality and amount on photosynthesis of *Cercospora*-infected plants.

3.6 Spectral measurements of sugar beet leaves during fungal infestation

The spectral leaf signature allows to evaluate the physiological leaf status (Buschmann and Nagel, 1993). Because *C. beticola* grows in the intercellular space of sugar beet leaves before inducing visible leaf damage (Steinkamp et al., 1979), it affects the leaf properties such as reflectance and transmittance by first microscopic cell destructions during foliar colonization. Therefore, the spectral signature can be changed already before visible symptoms occured (Rumpf et al., 2010). Spectral devices were used to figure out how early physiological changes of CLS infected leaves can be detected before visible symptoms appear. Experiments were first conducted on field plants infected with *Cercospora* leaf spot to refer all the obtained results to a sugar beet breeding scenario and evaluate the opportunity of establishing dedicated sensors and methodology. In a time series analysis, plants grown in the IBG-2 greenhouse were used to quantify spectral changes before and several days after inoculation.

3.6.1 *Cercospora*-induced changes of leaf reflectance in the field

In August 2012, an field experiment was conducted in cooperation with KWS SAAT AG (Einbeck, Germany). During this experiment conducted at the KWS field location in Plattling (Bavaria, Germany) four breeding lines (BL 20, 18, 17 and 8), previously inoculated by mixing field soil with infected leaf material were analyzed. According to fungal favorable growing conditions in August, plants were severely infected showing clear differences between genotypes. Under repeated infection cycles under these field conditions, progressive disease stages could be observed. The disease severity allowed a clear separation of genotypes depending on their resistance levels at the measurement time point. The LS genotype showed a nearly closed canopy (Fig. 27 A), whereas the MS and HS genotypes displayed increased leaf damage (Fig. 27 B and C). Using the KWS scale scoring protocol (Shane and Teng, 1992), non-infected sugar beets were scored with 1 (healthy canopy), the BL 8 plants with 5 (formation of leaf lesions), the BL 18 plants with 7 (larger lesions of outer leaves) and the BL 20 plants with 9 (dead outer leaves, severely damaged inner leaves). Such severe leaf damage was not observed under experimental greenhouse conditions. Here, only inoculated leaves developed leaf symptoms, probably because the low air humidity of about 60% in the greenhouse diminished conidia production, as it had been described for *C. beticola* (Khan et al., 2009; Wolf et al., 2001a). Therefore, disease did not spread from infected to regrown, non-inoculated leaves as observed under field conditions.

Fig. 27: *Cercospora*-infected breeding lines under field conditions. Sugar beet genotypes were grown under field condition in Platting, Bavaria in August 2012. (A) HS genotype (BL 20), (B) MS genotype (BL 18) and (C) LS genotype (BL 8) at a severely progressed disease stage after *in vitro* inoculation with dried infected leaf material which was mixed in field soil before sowing time point.

In the field experiment, the multispectral Tetracam and the hyperspectral FieldSpec were used to compare the breeding lines BL 20, 18 and 8. The multispectral and color-coded NDVI (Normalized Difference Vegetation Index) images allowed distinct differentiation between genotypes, as shown for other crops (Saberioon et al., 2013; Trout et al., 2008). The BL 8 plants showed less destroyed leaves compared with BL 20 plants (Fig. 28 A, B, C, D). The NDVI images were used to calculate absolute NDVI values of the genotypes allowing to distinguish significantly between vegetation (chlorophyll amount, leaf area or biomass) and soil reflectance at these wavelengths (Fig. 28 E). The BL 20 plants displayed the most severe leaf damage of 26% compared with BL 18 plants. BL 8 plants showed the lowest leaf area loss of 7%. The images of the non-infected sugar beets showed 98% leaf area and 2% soil area (Fig. 28 E). According to the progression of leaf damage, the field soil became visible between the leaves. This effect influenced the spectral signature of the measurement area leading to an overestimation of leaf area. This can be visualized in the color-coded NDVI images of the BL 20 plants (Fig. 28 C, D). Images revealed a clearly visible soil signature at certain spatial locations (Fig. 28 C) that were incorrectly detected as leaf area indicated by the color scale (Fig. 28 D). In this context, e.g. an NDVI value of 0.588 was referred to soil area that should have an NDVI value below 0.1, which represents the threshold between vegetation and soil.

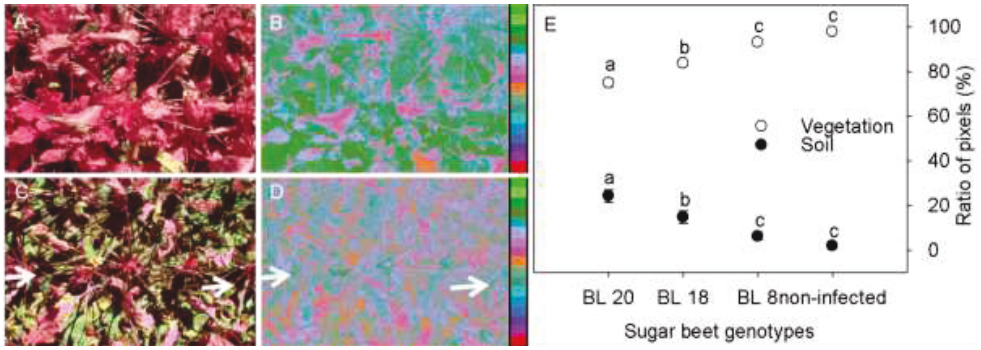

Fig. 28: Tetracam images of *Cercospora*-infected breeding lines. The BL 20, 18 and 8, and non-inoculated plants were imaged. Representative multispectral images of BL 8 plot (A, B) and BL 20 plot (C,D) with respective color-coded NDVI image calculated using Tetracam PixelWrench2. (E) Ratio of pixels with NDVI ≥0.1 (vegetation) and NDVI <0.1 (soil). The ratio correlated "vegetation pixel" and "soil pixels" with total pixel number of the image to calculate the percentage composition. Pixel ratios of the five genotypes differ significantly (One-Way ANOVA, $P<0.001$ (vegetation) and $P<0.005$ (soil)). Mean ± SD, n = 6 images per genotype.

The same genotypes were also measured with the FieldSpec device in order to verify NDVI values of the multispectral images and to investigate further vegetation indices that could be obtained by hyperspectral measurements. Based on the hyperspectral signatures, genotypes were compared regarding their leaf area (NDVI), their leaf water amount with the Leaf Water Index (LWI), and their disease severity with the *Cercospora* Leaf Spot Index (CLSI) and the *Cercospora* Detection Index (CDI). BL 8 plants showed significantly higher leaf area (NDVI = 0.84) compared with BL 18 and BL 20 plants, while significantly separating from non-infected plants (NDVI = 0.91; Fig. 29). BL 8 plants also displayed significantly higher leaf water amount (LWI = 6.1) compared with BL 18 and BL 20 plants, but showed a significant lower LWI value compared with non-infected plants (LWI = 8.3; Fig. 29). Regarding the CLSI, BL 8 plants showed significantly lower infected leaf area (CLSI = -0.23) compared with BL 18 (-0.01) and BL 20 plants showing the highest CLSI value of 0.03 (Fig. 29). The non-infected plants showed a CLSI value of -0.35. The CDI did not differ between the non-infected plants and the breeding lines.

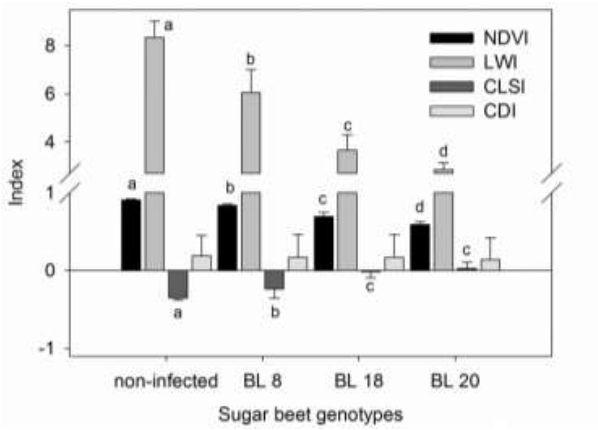

Fig. 29: Vegetation indices of *Cercospora*-infected breeding lines under field conditions. Indices were calculated for the BL 20, BL 18 and BL 8, and non-infected plants based on FieldSpec measurements. The NDVI, LWI and CLSI showed significant differences between genotypes (One-Way ANOVA, Holm-Sidak, $P<0.001$). Mean ± SD, n = 14 (non-infected) and n = 46 (BL 8, 18 and 20) images per genotype.

In summary, leaf area, leaf water content and disease severity differed significantly between the genotypes. BL 8 plants showed significantly higher NDVI and LWI values compared to the other three genotypes BL 20, 18 and 17, and the non-infected sugar beets, respectively. Moreover, BL 8 plants showed significantly reduced disease severity compared with the other breeding lines. Compared with multispectral images, hyperspectral data did not discriminate between vegetation and soil, since the FieldSpec has an integrated measurement area.

3.6.2 *Cercospora*-induced changes of leaf reflectance and transmittance during disease onset in controlled environment

Disease induced spectral changes were investigated with the new HyperART-system prototype allowing to calculate light absorbance of leaf properties due to simultaneous mapping of reflectance and transmittance. According to the mirror setup of the system (Fig. 9), a reflectance (left side) and transmittance image (right side) were obtained and a 3D data cube could be constructed with the spectrum of each leaf pixel as z component (Fig. 30 A). Obvious leaf symptoms, as visible in the habitus image (Fig. 30 B), were in contrast to the asymptomic leaf surrounding in the CLSI image (Fig. 30 C).

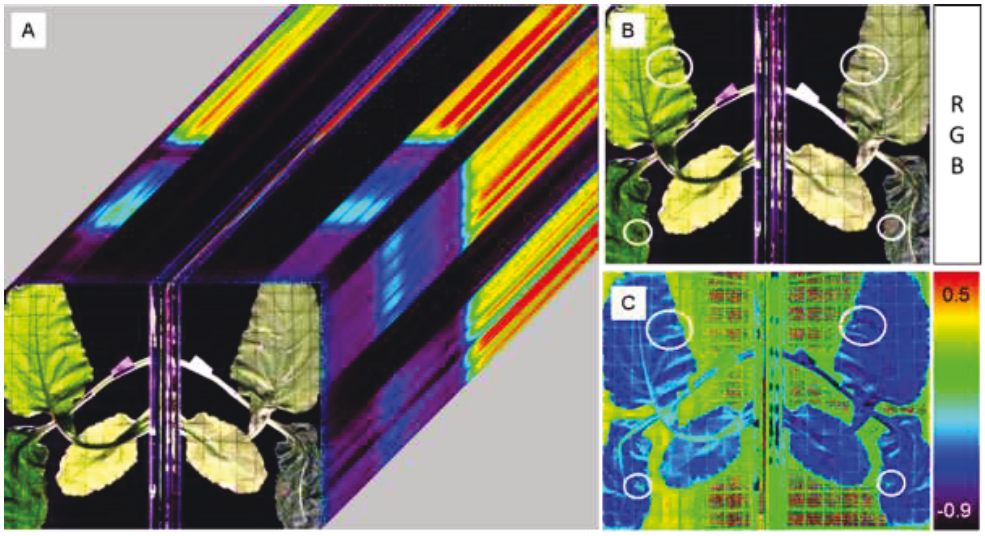

Fig. 30: Hyperspectral images of sugar beet leaves obtained by the HyperART-system. (A) 3D data cube with the spectrum of each leaf pixel as z component. (B) Habitus (RGB: red, green, blue) image of infected leaves with several single leaf spots. (C) *Cercospora* leaf spot (CLSI) map. Representative leaf spots are framed with white cycles, a change in CLSI is indicated by the color-coded scale. For each measurement, plants were moved carefully from the greenhouse to the laboratory. Plants were kept under laboratory conditions for approximately 2h, while the measurement took about 10 min per plant.

In a further step based on image analysis, the reflectance and transmittance signal of leaves were compared to evaluate if additional information can be provided by the transmittance spectrum. In this experiment 13, a time series was conducted to observe spectral changes of leaves before and after inoculation. Therefore, leaves were imaged in advance of the inoculation (0 dpi). After the measurement at 3 dpi, leaves were mounted in custom-made leaf clips and were again measured at 6 and 9 dpi (Fig. 31, RGB). At 6 dpi, the smaller, senescing primary leaf (leaf c) showed the first leaf spot. At 9 dpi, the larger, mature two leaves (leaf a and b) displayed first leaf symptoms. For each time point, the reflectance and transmittance spectra were used to calculate three vegetation indices in order to quantify chlorophyll loss (NDVI), as an indicator of necrosis, and disease progression (CLSI and CDI).

The NDVI of reflectance (ref) and transmittance (tra) differed between the three leaves. The $NDVI_{ref}$ map and in particular, the $NDVI_{tra}$ map revealed a clear difference in the chlorophyll content of the senescing primary leaf compared to the two mature leaves, which did not show symptoms of senescence (Fig. 31). The first leaf spot on the senescent leaf was clearly differentiated from the surrounding leaf area at 6 dpi. In addition, a developing leaf spot on one of the mature leaves (leaf b) was indicated at 6 dpi, while this spot was first visible by eye at 9 dpi.

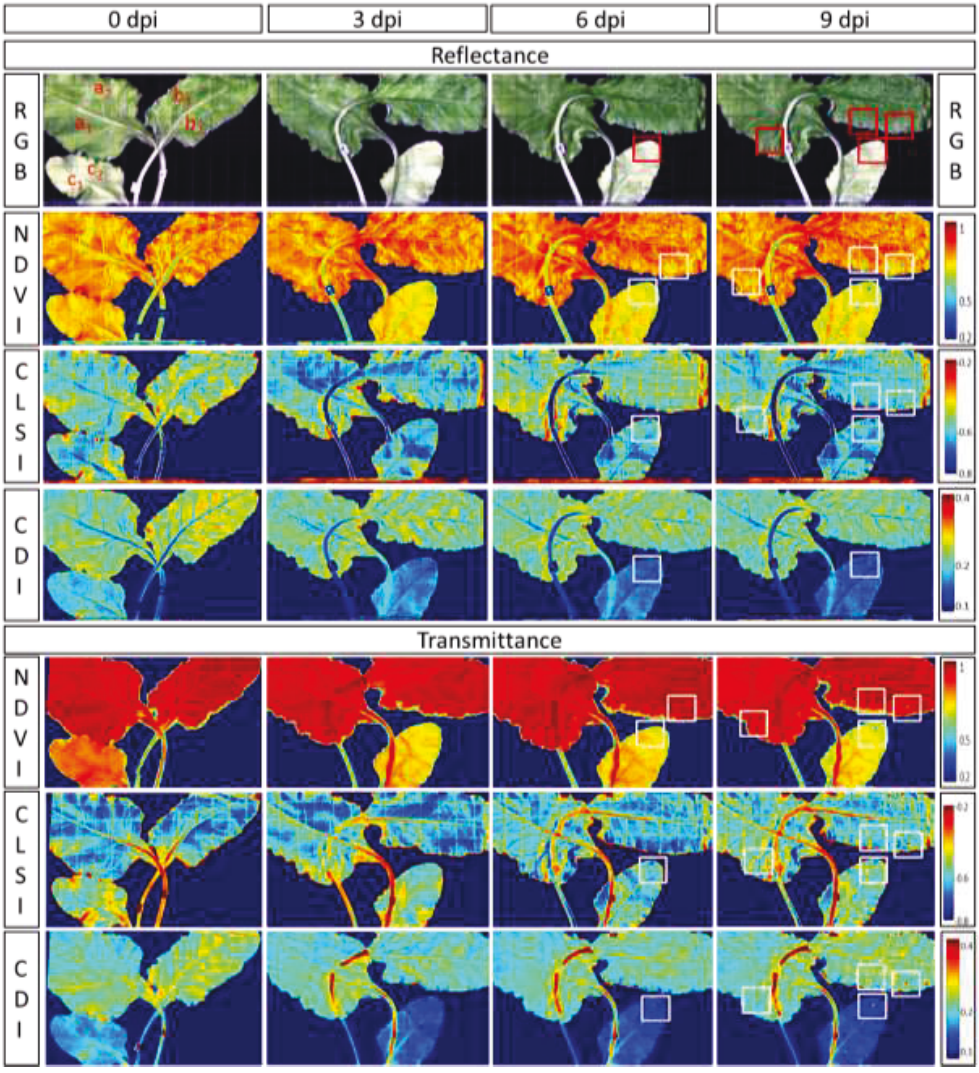

Fig. 31: Habitus and index maps of *Cercospora*-inoculated sugar beet leaves. Index maps of the reflected (A) and transmitted light (B) of leaves were obtained by the HyperART-system. Leaves were imaged in advance of the inoculation (0 dpi). After 3 dpi, leaves were then mounted in leaf clips until the following time points at 6 dpi and 9 dpi. The classification of leaf halves is given in red labeling. The color scales indicate increasing values for chlorophyll (NDVI) and *Cercospora* leaf spot (CLSI, CDI) from the bottom to the top. Leaf symptoms are framed by red (RGB) and white boxes (indices).

Compared with the NDVI, the CLS Index did not reveal developing symptoms at an earlier time point, neither in reflectance nor in transmittance. For the CDI the general trend of symptom indication remained the same.

In a further step of the image analysis, leaves were bisected and leaf halves a_1, a_2, b_1, b_2, c_1 and c_2 were analyzed (Fig. 31, RGB). The reflectance and transmittance spectrum of each leaf half was averaged to calculate the three vegetation indices of NDV, CLS and CD in order to adjust these values with the index maps.

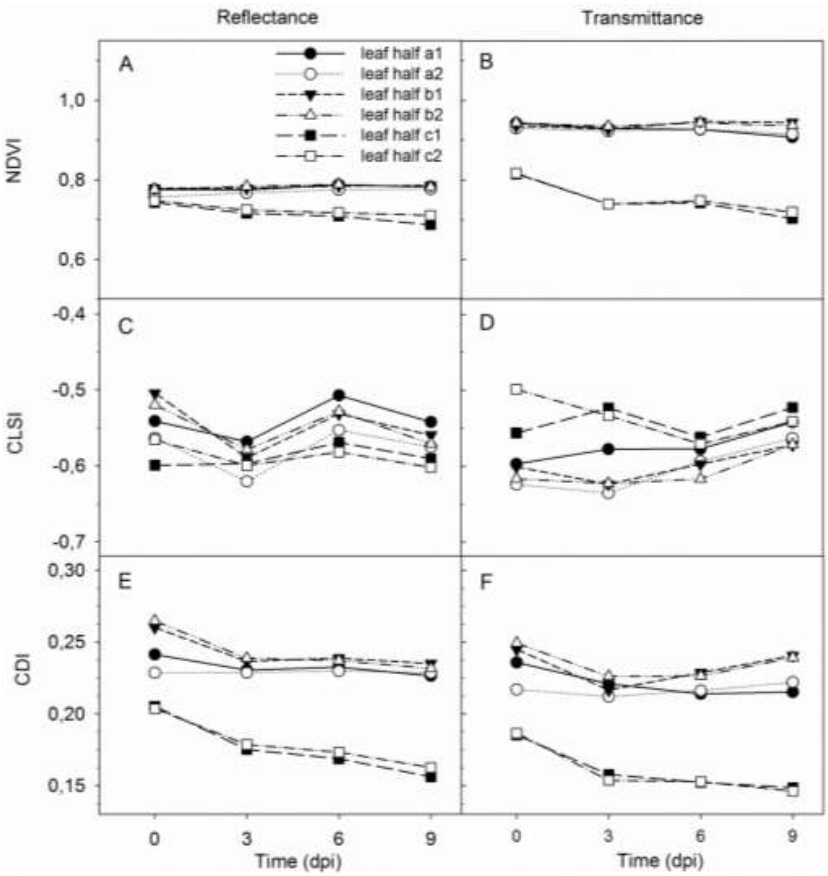

Fig. 32: Indices of *Cercospora*-inoculated sugar beet leaves. Vegetation indices were based on the reflectance and transmittance spectrum of leaves. The analyzed, hyperspectral data was obtained by the HyperART-system. Values of the (A, B) NDVI, (C-D) CLSI and (E, F) CDI shortly before and 3 to 9 days after inoculation. Indices were based on the spectra of reflectance (A, C, E) and transmittance (B, D, F).

The NDVI of reflectance (ref) and transmittance (tra) differed between the senescent leaf (leaf c; Fig. 31 A, B) and the other two mature leaves (leaf a and b; Fig. 31 A). The $NDVI_{ref/tra}$ decreased in the senescent leaf (Fig. 32 A, B). While the $NDVI_{ref}$ of the two mature leaves did not differ, the $NDVI_{tra}$ slightly decreased in one of the leaves at 6 and 9 dpi (Fig. 32 B). For both spectra, the $CLSI_{ref/tra}$ showed a similar pattern for all

leaves that did not reveal a relation to days after *Cercospora* inoculation (Fig. 32 C). The $CLSI_{tra}$ slightly increased from 3 to 9 dpi for the two mature leaves, whereas the senescent leaf showed no effect depending on time (Fig. 32 D). The CDI differed between the senescent leaf and the two mature leaves. While the CDI_{ref} slightly decreased for all leaves from 0 to 9 dpi (Fig. 32 E), the CDI_{tra} increased for one of the matures leaves from 6 to 9 dpi (Fig. 32 F).

In summary, the three indices NDVI, CLSI and CDI showed a clear difference between the senescent leaf and the two mature leaves, but failed to detect disease progression. The index maps of NDVI, CLSI and CDI revealed symptoms, when they were already visible. Compared with the index maps of the reflected light, the index maps of the transmitted light showed an increased contrast between leaf symptoms and the non-infected surrounding leaf area. This indicates a more simple classification between infected or non-infected tissue. In previous studies, the $NDVI_{ref}$ and the $CLSI_{ref}$ had been shown to be feasible for *Cercospora* detection (Mahlein et al., 2013; Rumpf et al., 2010). However, in this study, the analysis of only three leaves was presented that showed a low disease severity indicated by a few leaf spots at 9 dpi. Therefore, these results should be interpreted with caution. A detailed analysis of the obtained data of the HyperART system is underway in the scientific thesis of S. Bergsträsser. It is necessary to verify the usability and applicability of the transmittance spectrum of inoculated sugar beet leaves for earlier CLS disease detection.

3.7 Fungal effects on taproot growth

Cercospora leaf spot (CLS) is commonly thought to reduce taproot growth and yield (Shane and Teng, 1992), as described in Chapter 3.2.2. During disease progression, the foliar damage causes reduced leaf area for photosynthesis leading to a decreased amount of photoassimilates that can be stored in the taproot. Severe leaf loss is often accompanied by the formation of new leaves, however this response cannot compensate for both reduced root growth and yield loss. Although previous studies focused on effects of *Cercospora* leaf spot on sugar beet yield and gene expression (Weltmeier et al., 2011), yet very few findings exist about effects on the root system at disease onset and how internal taproot structures change morphologically following foliar disease progression. Different sugar beet genotypes were compared non-invasively to track fungal effects on taproot growth using MRI. For this reason, disease severity and shoot development (leaf area) were monitored and temporally compared with the growth response of taproots. In experiment 7, the highly (HS) and lowly susceptible (LS) standard genotypes were compared regarding both disease and shoot development influencing taproot growth (Table 13). To observe further morphological changes, we focused on the HS standard genotype during foliar disease progression in experiment 8. Experiment 16 was conducted with the three breeding lines, BL 20, BL 18 and BL 8.

3.7.1 Responses of the STD HS and LS genotypes during disease progression

In experiment 7, sugar beets grew in pots until harvest at 90 dpi showing phenotypic differences between genotypes with respect to the development of non-inoculated (Fig. 33 A, B) and inoculated shoots (Fig. 33 C, D). In the HS genotype, disease severity increased faster than in the LS genotype. The HS genotype showed 7% necrotic leaf area (n = 7 leaves per genotype) at 11 dpi increasing to 65% (n = 7 leaves) after the first inoculation at 52 dpi. Because disease did not spread from infected to non-infected leaves, a second inoculation was conducted to infect other leaves. Prior to an increased disease severity, freshly infected leaves reduced the average of disease severity for both genotypes. During 62 to 88 dpi, an increase of leaf damage from 52% (n = 7 leaves) to 67% (n = 20 leaves) was scored (Fig. 34 A). During the same periods, the LS genotype showed an increase of foliar damage from 2% (n = 1 leaf) to 38% (n = 6 leaves) and the second inoculation caused an increase from 37% (n = 6 leaves) to 52% (n = 16 leaves).

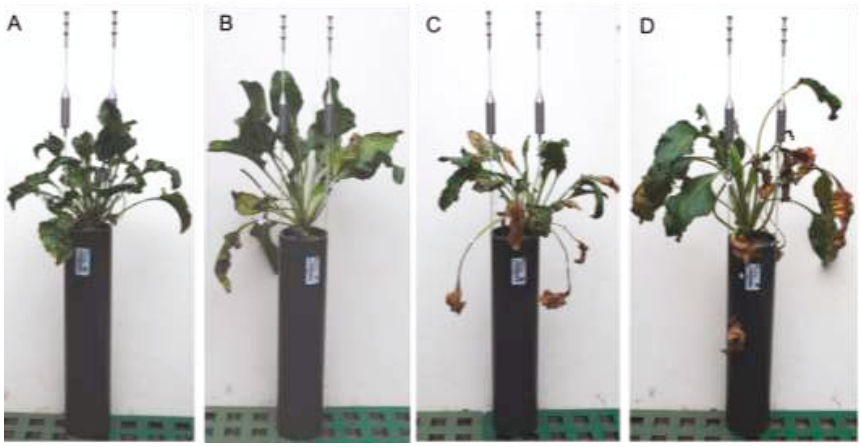

Fig. 33: Habitus of standard genotypes in MRI pots. The STD HS and LS sugar beet plants were inoculated or non-inoculated with *C. beticola*. Non-inoculated treatment of HS (A) and LS (B) genotype, and inoculated treatment of HS (C) and LS (D) genotype. Images were acquired shortly before harvest at 90 dpi.

Disease severity and leaf area were analyzed to compare shoot and taproot development of both genotypes during leaf infestation. The development of leaf area showed differences between genotypes and treatments. Leaf area developed similarly in all treatments until 14 days after inoculation (Fig. 34 B). During 14 to 42 dpi, all treatments decreased leaf area due to the onset and progressing disease severity, and extreme temperature conditions. The summer heat (day temperatures of maximal 38°C and average 33°C) interfered with leaf growth for all treatments. After greenhouse shading and readjustment of water supply to avoid severe water deficit, the non-inoculated treatments increased leaf area during 42 to 89 dpi, except for the HS genotype that started to increase leaf area after 56 dpi. The inoculated treatments increased leaf area during 42 to 62 dpi and decreased after the second inoculation at 62 dpi due to a progressively higher disease severity. Finally at 89 dpi, the LS genotype showed the highest leaf area for both treatments. Due to fungal infection, a significantly reduced leaf area was detected between the LS plants (t-test, $P<0.05$) and the HS plants (t-test, $P<0.05$) at 89 dpi (Fig. 34 B). The average leaf area (during -14 to 89 dpi) was similar in both treatments for each genotype (Table 17). In both treatments, the LS plants displayed an increased average leaf area of about 100 cm² compared with the HS ones (Table 17).

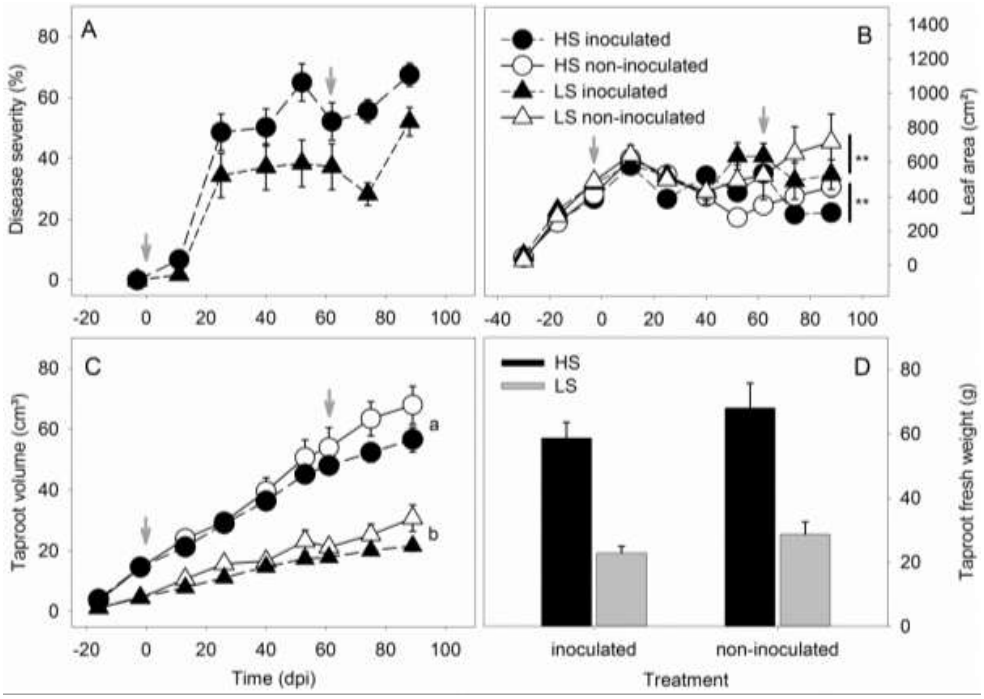

Fig. 34: Shoot and root development of standard genotypes. The STD HS and LS genotypes were analyzed In experiment 7. (A) Disease severity progression (mean ± SE) with increasing number of symptomatic leaves, 1-16 leaves for LS and 7-20 leaves for HS during 14 to 89 dpi. (B) Leaf area development during -28 to 89 dpi; asterisks indicate statistically significant differences between the inoculated and non-inoculated treatment of the HS and LS genotype at 89 dpi analyzed by a t-test, $P<0.05$. (C) Taproot volume measured non-invasively with MRI; different letters indicate statistically significant differences between HS and LS plants analyzed by a Two-Way ANOVA, $P<0.01$ during -14 to 89 dpi. (D) Taproot fresh weight after harvest at 90 dpi. (B, C, D) Mean of each plant was calculated during -14 dpi to 90 dpi (mean ± SE; n=5 per treatment). The two dates of inoculation with *C. beticola* are indicated by gray arrows.

During foliar disease progression, taproot development was reduced in the inoculated plants. In MRI measurements, it could be shown that taproots of HS plants grew significantly faster than roots of LS plants. Throughout the experiment, differences in the taproot volume of the two genotypes increased (Two-Way ANOVA with $P<0.01$; Fig. 34 C). For both treatments, the HS plants had a more than two-fold higher taproot volume than the LS ones at 90 dpi. These values are in line with the harvested taproot fresh weight, i.e. the HS plants had a 60% increased biomass (Fig. 34 D). When inoculated, the HS genotype lost 14% taproot volume and 17% fresh weight, while the LS genotype lost 30% taproot volume and 21% fresh weight (Fig. 34 C, D). However, the LS genotype had been expected to be less affected compared to the HS genotype.

Table 17: Average leaf area of standard genotypes. Leaf area (cm²) of the STD HS and the LS genotype during -28 and 89 dpi in experiment 7. Mean ±SE; n = 50 plants per treatment.

Treatment	Leaf area (cm²)	
	LS	HS
Inoculated	469 ± 30	374 ± 23
Non-inoculated	476 ± 40	374 ± 24

Based on the beet-specific secondary thickening, the taproot volume increased (Fig. 35 A - C). Besides the increasing taproot volume, the thickness of concentric cambial rings was measured in the cross-section of MRI images (Fig. 35 D - F). In these cross-sections darker zones were interpreted and identified as the xylem and phloem separated by a narrow bright ring, the cambium (Metzner et al., 2014, submitted). The broader light gray rings in between were identified as sugar-storing parenchyma. The thickness of a cambial ring consisted of the summed thicknesses of the respective cambium, xylem, phloem, and storage parenchyma. The outermost cambial ring, not showing a visible storage parenchyma at measurement time points, is marked with a white arrow. The thickness of the innermost cambial ring 1 is indicated with a black line (Fig. 35 D - F).

As previously described, the secondary thickening of the taproot starts with the growth of inner cambial rings, subsequently the outer rings enlarges (Artschwager, 1926; Zamski and Azenkot, 1981). In experiment 7, this effect of ring thickening could be observed, the inner cambial rings (ring 1 - 4) developed earlier compared with the outer cambial rings (ring 5 - 8). The inoculated and non-inoculated HS plants had a similar increase in the thickness of inner and outer cambial rings during -14 dpi to 89 dpi, whereas inner cambial rings were significantly larger than outer cambial rings (Fig. 36 A).

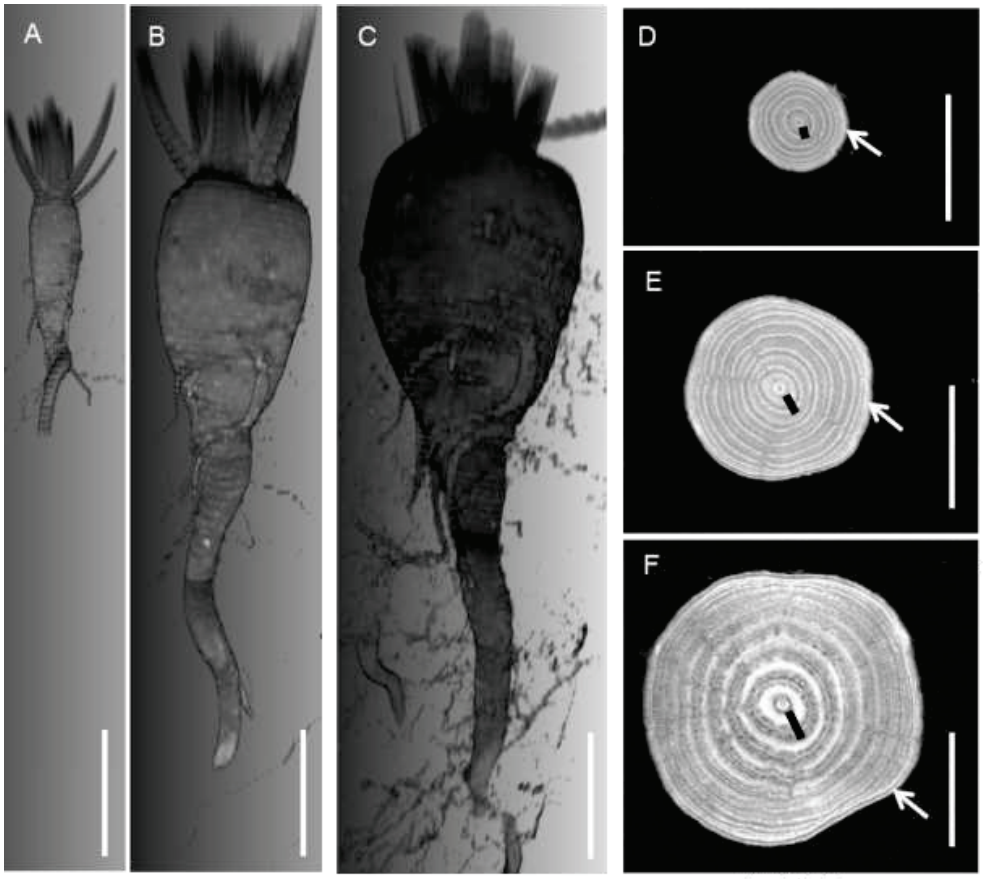

Fig. 35: MRI images of a representative HS plant during secondary thickening of the taproot. The taproot of the sugar beet is shown in isosurfaces and cross-sections at 11 weeks (A, D), 17 weeks (B, E) and 25 weeks after sowing (C, F). (D, E, F) In these cross-sections, the thickness of the innermost cambial ring (No. 1) is marked with a black line, the outermost ring with a white arrow. The scale of the isosurfaces and cross-sections is indicated by the white line (2 cm). Taproots grew out of the Field of View (70 x 70 mm²) after 16 weeks after sowing, therefore two measurements per taproot had to be conducted to capture the root system (B, C).

The inoculated and non-inoculated LS plants showed also a similar increased thickness of inner and other cambial rings during the same period, and a significantly larger thickness of inner cambial rings (Fig. 36 B). In this experiment 7, plants of both treatments enlarged the inner four and the outer four cambial rings similarly. However, compared to the LS plants, HS plants had about two-fold thicker cambial rings throughout the whole experiment during -14 dpi to 89 dpi (Fig. 36 A, B).

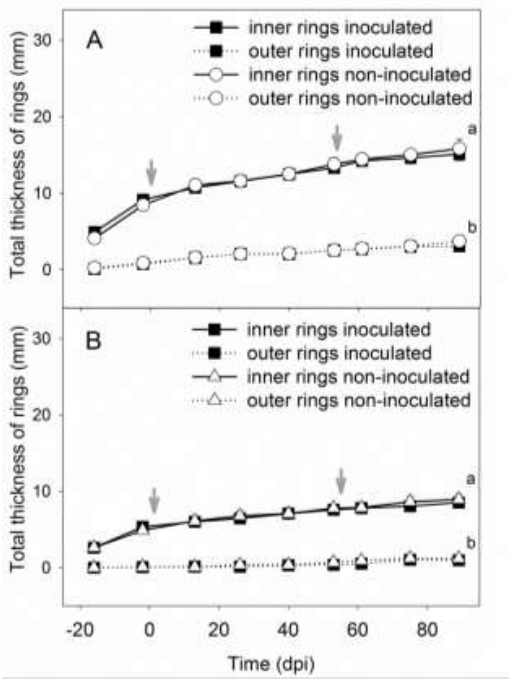

Fig. 36: Cambial ring growth of standard genotypes. Summed thickness of the inner (1 - 4) and outer (5 - 8) cambial rings of the STD HS. (A) and STD LS (B) genotypes with inoculated and non-inoculated treatment (mean ± SE, n=5 plants per treatment) between -14 dpi to 90 dpi, non-invasively measured with MRI. The significant differences between inner and outer cambial rings of both genotypes during -14 to 89 dpi were analyzed by a Two-Way ANOVA, $P<0.001$. The two dates of inoculation with *C. beticola* are indicated by gray arrows.

To summarize, compared with the STD LS genotype, the STD HS genotype showed higher disease severity and lower leaf area in both treatments as well as an increased taproot volume, a higher terminal biomass and a stronger growth of cambial rings. High temperatures in the greenhouse caused leaf wilting in the non-inoculated treatment, thus the genotypes showed a similar leaf area on average in both treatments. While plants of both treatments displayed a similar leaf area on average, the taproot growth was reduced in the inoculated plants. To reveal cambial ring changes during foliar disease development, the taproot development of the HS genotype was investigated in more detail in experiment 8.

3.7.2 Root response of the STD HS genotype during foliar disease

Disease severity and leaf area were analyzed to compare shoot and taproot development of the STD HS genotypes during leaf infestation. In the previous experiment 7, extreme summer day conditions (up to 38°C) led to leaf area loss of all treatments. It can be assumed that leaf area loss of the non-inoculated treatment was the reason for the small difference between treatments concerning taproot volume, fresh weight and ring thickness. To confirm the results of experiment 7, comparing the two genotypes, and to clarify foliar effects on the root system, experiment 8 was conducted under optimal water regime and moderate light conditions enabled by greenhouse shading that avoided heat-induced leaf loss. Referred to its reported higher sensitivity, stronger reaction to CLS and better growth development, the STD HS genotype was chosen to confirm and increase the accuracy of the results concerning taproot changes.

In experiment 8, disease severity and the taproot growth of the HS genotype were correlated in order to verify growth responses due to foliar infestation. The disease severity was comparable to the previous one in experiment 7. At 14 dpi the HS genotype showed <1% necrotic leaf area (n = 5 leaves per genotype) increasing to 63% (n = 8 leaves) at 56 dpi after the first inoculation, the second inoculation caused an increase of leaf damage from 56% (n = 8 leaves) to 69% (n = 19 leaves) at 97 dpi (Fig. 37 A).

For the MRI taproot measurements, the inoculated plants showed a significantly reduced growth already at 14 dpi compared with the non-inoculated plants (Fig. 37 A; t-test with $P<0.05$), even though the disease severity was below <1% infected leaf area. The second inoculation, 56 days after the first one, resulted in a further reduction of the taproot growth and significant differences between the inoculated and non-inoculated treatment were measured (t-test with $P<0.05$; Fig. 37 A). To quantify growth reduction, the relative growth rates (RGR) of the taproots were compared within 14 days after inoculation. The inoculated plants showed a reduced RGR of 11% (first inoculation) and 13% (second inoculation) compared with the non-inoculated plants (Table 18). At 98 dpi, the inoculated plants had a 28% lower taproot volume (Fig. 37 A) that correlates with the 26% lower taproot fresh weight compared with the inoculated plants (Table 18).

Table 18: Relative taproot growth rates of the HS standard genotype. Relative growth rates of taproots (RGR; % day^{-1}) within 14 days after inoculation, and taproot fresh weight (FW; g) of the STD HS genotype in experiment 8. Significant differences in taproot fresh weight were measured between treatments at harvest 98 dpi (t-test, P<0.05). Mean ±SE; n = 4 plants.

Treatment	RGR of taproots (% d^{-1})		taproot FW (g)
	HS		
	1st inoculation	2nd inoculation	
	At 0 dpi	At 56 dpi	At 98 dpi
Inoculated	6.05 ± 0.31	2.53 ± 0.27	69.7 ± 4.8
Non-inoculated	6.79 ± 0.41	2.90 ± 0.28	97.8 ± 8.7

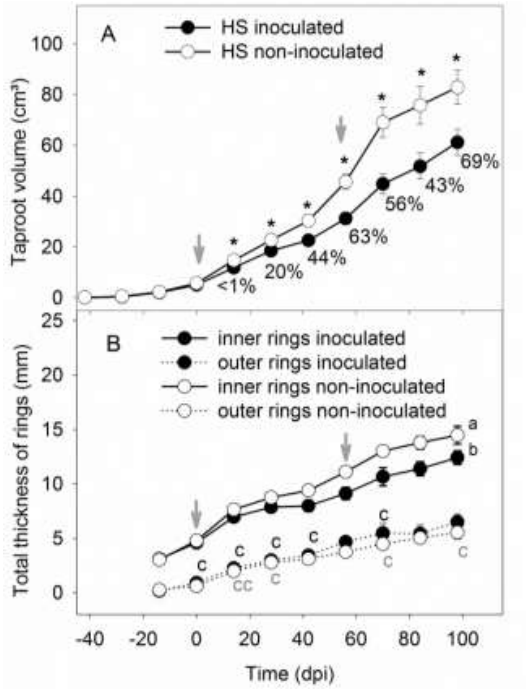

Fig. 37: Root and cambial ring growth of the HS standard genotype. Root development, measured with MRI, and disease severity of the STD HS genotype scored visually in experiment 8. (A) Taproot volume and percentage of disease severity with increasing number of symptomatic leaves, 5 - 19 leaves during 14 to 98 dpi. The significant differences between treatments is indicated by asterisks and estimated by a t-test, P<0.05. (B) Summed thickness of inner (1 - 4) and outer (5 - 10) cambial rings between inoculated and non-inoculated treatment. The appearance of further outer cambial rings is indicated by "c" (gray = non-inoculated and black = inoculated). Significant differences in inner cambial rings of inoculated and non-inoculated plants were analyzed by Two-Way ANOVA, P<0.05 during -14 to 98 dpi. Mean values (± SE, n=4 per treatment) were calculated during -14 dpi to 98 dpi (A, B). The two dates of inoculation are indicated by gray arrows.

In the secondary thickening of taproot, the inner (ring 1 - 4) and the outer (ring 5 - 10) cambial rings developed differently. The inoculated HS plants showed a significantly reduced thickness of inner cambial rings during -14 to 98 dpi compared with the non-inoculated plants (Fig. 37 B). During 56 to 98 dpi, the inoculated plants showed a 15% decrease in thickness of the inner cambial rings and a 15% increase in thickness of outer rings compared with non-inoculated plants. Furthermore, inner and outer cambial rings differed in the onset of thickening. The outer cambial rings of the inoculated plants were detectable earlier (Table 19; Fig. 37 B; the appearance of an additional cambial ring was marked with a “c”).

Table 19: Cambial ring growth of the HS standard genotype. The number of cambial rings of the inoculated and non-inoculated STD HS genotype after fungal inoculation.

Appearance of cambial rings (dpi)	**Cambial ring number Treatment**	
	Inoculated	**Non-inoculated**
0	6	-
14	7	6 and 7
28	8	8
42	9	-
56	-	-
70	10	9
84	-	-
98	-	10

To summarize, the STD HS genotype showed a significantly reduced taproot growth already 14 dpi, when a very low disease severity below 1% was scored. The inoculated plants showed a significantly reduced thickness of inner cambial rings, but an increased thickness of outer cambial rings indicating a compensatory growth of outer cambial rings that were provided by new, non-inoculated leaves.

3.7.3 Responses of breeding lines to foliar disease

In experiment 16, the breeding lines BL 20, BL 18 and BL 8 were compared in order to quantify plant responses to CLS. Each treatment consisted of five plants, except the BL 18 treatments. Two of the ten BL 18 plants were massively reduced in shoot and root growth, therefore they were excluded and the treatment number had to be limited to four plants per treatment. The disease severity and leaf area of breeding lines were analyzed to compare responses in the shoot with the responses of the taproot.

Disease severity of breeding lines was scored visually. The BL 20 and BL 8 plants showed a more severely disease severity compared with the BL 18 ones. The BL 20 plants reached a disease severity of 64% (n = 24 leaves) at 38 dpi after the first inoculation (Fig. 38 A). During the same period, the BL 8 plants reached 73% (n = 28 leaves) and the BL 18 plants 40% disease severity (n = 27 leaves). At 102 dpi, four weeks after the second inoculation, all genotypes showed a similar disease severity about 25 % infected leaf area (Fig. 38 A).

Leaf area was measured to compare the shoot development of the inoculated treatment with the non-inoculated treatment of each genotype. The development of leaf area showed differences between genotypes and treatments. Leaf area developed similarly in all treatments until 14 dpi (Fig. 38 B). During 14 to 38 dpi, the inoculated treatments displayed leaf area loss of about 40% due to the progressively higher disease severity. Due to the observed wilting of older leaves also the non-inoculated plants lost leaf area, even though, there were no extreme temperature conditions recorded for the growing period (≤ 23°C) compared with experiment 7 (up to 38°C). In general, the daily amount of water-nutrient solution was restricted to avoid root rot due to waterlogging and reduced aeration in the specific soil-filled MRI pots. Therefore, plants were closely monitored in regard to symptoms of water stress, e.g. reduced leaf turgor, but such symptoms had not been observed. It can be assumed that the leaf wilting effect might be traced back to the lack of nutrients. Older, mature leaves wilted in order to supply young, immature leaves with mineral nutrients (Marschner et al., 1996). Referred to these assumptions, the daily supply of water and nutrients was increased reducing, but not completely eliminating this wilting effect. At 102 dpi, a significant difference between the inoculated and non-inoculated treatment of each genotype was measured (Two-Way ANOVA, Holm-Sidak, $P<0.05$). Compared to the respective non-inoculated plants, the inoculated plants showed a 26% (BL 20), 24% (BL 8) and 22% (BL 18) reduced leaf area. The average leaf area (during -16 to 102 dpi) of the inoculated treatments was also reduced for each genotype (Table 20). Due to the leaf infestation, the BL 20 plants lost 22% leaf area on average, and the BL 8 and BL 18 plants lost 12%. For both treatments, the BL 8 plants displayed an increased average leaf area compared with the BL 20 and 18 ones (Table 20).

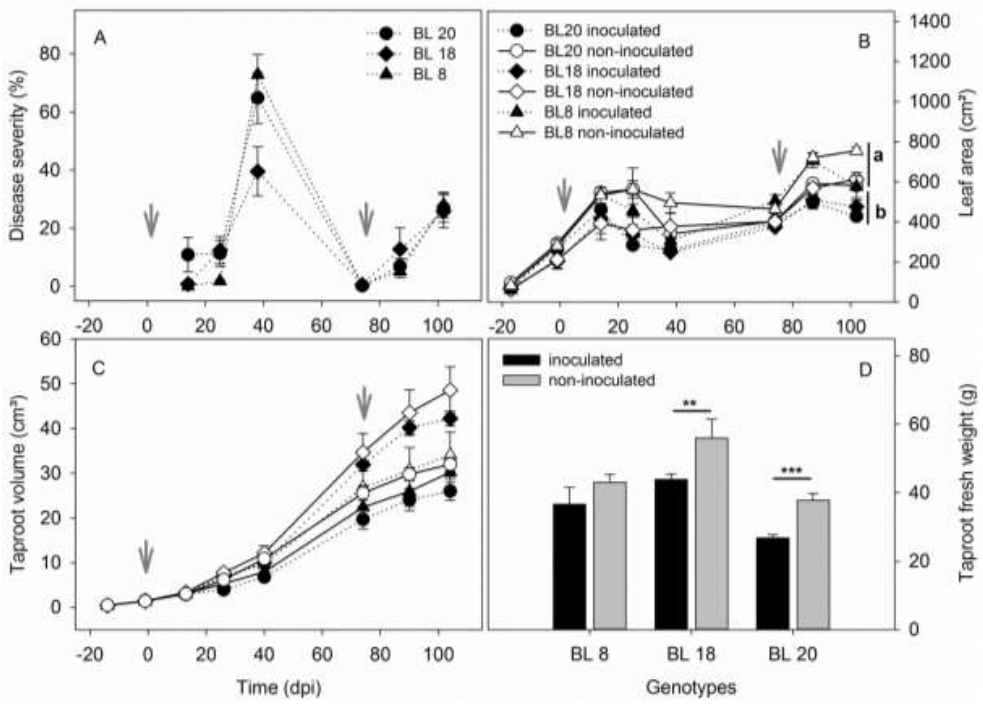

Fig. 38: Shoot and root development of breeding lines. The BL 20, BL 18 and BL 8 plants were analyzed in experiment 16. (A) Disease severity progression (mean ± SE) with increasing number of symptomatic leaves, 23 - 53 leaves for BL 20, 11 – 40 leaves for BL 18 and 12 - 79 leaves for BL 8 during 14 to 102 dpi. (B) Leaf area development during -16 to 102 dpi; At 102 dpi, the significant difference between the inoculated and non-inoculated treatments of each genotype was estimated by Two-Way ANOVA, Holm-Sidak ($P<0.05$). The significant dfference of the BL 8 genotype compared with the other two genotypes is indicated by letters and was estimated by Two-Way ANOVA, Holm-Sidak ($P<0.05$). (C) Taproot volume measured non-invasively with MRI. (D) Taproot fresh weight after harvest at 105 dpi. The significant differences between the treatments of BL 18 and BL 20 plants is indicated by asterisks and analyzed by a t-test, ** $P<0.05$ and *** $P<0.001$. (B, C, D) Mean of each plant was calculated during -16 dpi to 103 dpi (mean ± SE; $n_{BL20/8}$ =5 and n_{BL18}=4 per treatment). The two dates of *Cercospora* inoculation are indicated by gray arrows.

During the foliar disease progression, taproot development was reduced in the inoculated treatments of the three genotypes (Fig. 38 C). At 104 dpi, the BL 20 plants showed the smallest and the BL 18 plants had the largest taproot volume in both treatments. These values are in line with the harvested taproot fresh weight, the BL 20 plants showed the smallest biomass production, whereas the BL 18 plants had the highest biomass compared with the other genotypes at harvest (Fig. 38 D). Compared with the respective non-inoculated plants, the fresh weight of the inoculated plants was significantly reduced by 29% in the BL 20 plants, 21% in the BL 18 and 15% in the BL 8 plants (Fig. 38 D).

Table 20: Average leaf area of breeding lines. Leaf area (cm²) of BL 8, BL 18 and BL 20 plants during -16 to 102 dpi. Mean ±SE; $n_{BL20/8}$ = 40 and n_{BL18} = 32.

Treatment	Leaf area (cm²)		
	BL 8	**BL 18**	**BL 20**
Inoculated	428 ± 32	355 ± 26	334 ± 21
Non-inoculated	487 ± 35	403 ± 29	427 ± 30
Leaf area loss	12%	12%	22%

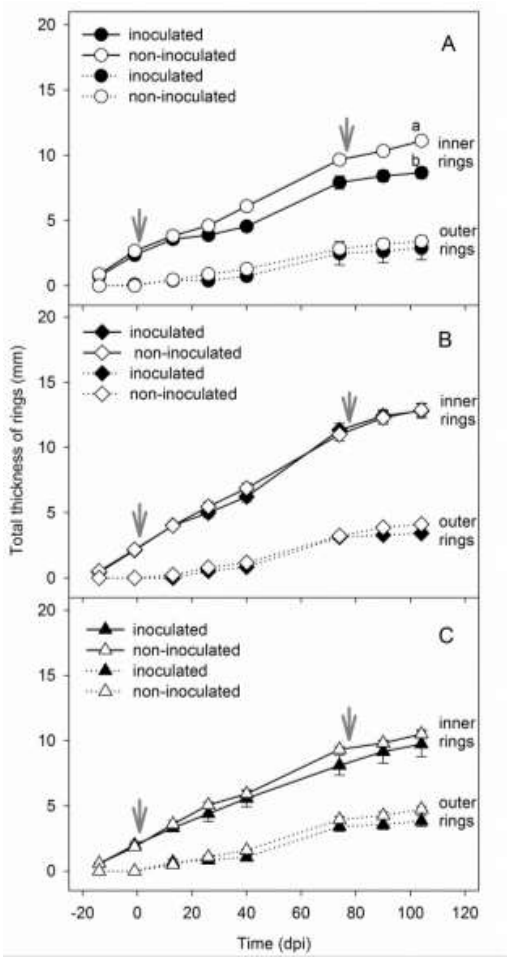

Fig. 39: Cambial ring growth of breeding lines. Summed thickness of the inner (1 - 4) and outer (5 - 10) cambial rings of the inoculated and non-inoculated treatment of breeding lines between -14 dpi to 104 dpi, non-invasively measured with MRI. (A) The BL 20. Significant differences during -14 to 104 dpi were analyzed between inner cambial rings of inoculated and non-inoculated plants by Two-Way ANOVA, $P<0.05$. (B) The BL 18. (C) the BL 8. Mean ± SE, $n_{BL20/8}$= 5 and n_{BL18}= 4 plants per treatment. The two dates of *Cercospora* inoculation are indicated by gray arrows.

The inner cambial rings (1 - 4) developed earlier compared with the outer ones (5 - 10). During -14 to 104 dpi, the inoculated BL 20 plants had a reduced thickness of inner cambial rings and a similar thickness of outer cambial rings compared to the non-inoculated plants (Fig. 39 A). During the same period, the BL 18 plants showed an increasing thickness of inner and outer cambial rings for both treatments (Fig. 39 B). The inoculated BL 8 plants showed a similar growth of inner and outer cambial rings as the BL 20 plants (Fig. 39 C).

To summarize, the largest leaf area was produced by the BL 8 plants and the lowest leaf area by the BL 20 plants. The BL 20 genotype was more severely affected by the fungal infestation compared with the two other genotypes. The BL 18 plants showed the lowest disease severity and the lowest taproot growth reduction as well as an increased thickness of inner and outer cambial rings in both treatments. In the BL 8 and BL 20 plants, the fungal infestation caused a reduced thickness of cambial rings.

3.7.4 Effects of disease severity on taproot growth

An early effect of fungal infestation on taproot growth was investigated using MRI. The breeding lines displayed reduced growth eight weeks after inoculation. The BL 18 plants showed an increased taproot growth in both treatments compared with the BL 20 and BL 8 plants. The STD LS genotype displayed a reduced taproot growth in both treatments compared with the STD HS genotype that showed a significantly reduced taproot growth already 14 dpi, while a very low disease severity was scored below 1% infected leaf area. In particular, the STD HS genotype revealed fungal induced growth changes in cambial ring structure. Inoculated plants displayed an increased thickness of outer cambial rings and a reduced thickness of inner cambial rings.

4 Discussion

Cercospora leaf spot (CLS) results in economically important yield losses in sugar beet (Malandrakis et al., 2006; Skaracis et al., 2010; Weiland and Koch, 2004). To ensure yield gain under reduced pesticide treatment, breeding efforts aim at sugar beet lines with reduced susceptibility as well as high productivity (Holtschulte et al., 2010; Märländer et al., 2003; Wolf et al., 2001b). In regard to their natural ability, sugar beets can defend against pathogens at different stages of infestation from the initial contact, during invasion, all the way to the final disease effects on shoot and root. First of all, the cuticle has to be overcome by the pathogen (Agrios, 1997; Carver and Gurr, 2008). Secondly, the fungal ramification in the leaf tissue can be limited by specifically expressed pathogenesis-related (PR) proteins (Gottschalk et al., 1998; Nielsen et al., 1994). In the following, this leads to reduced disease severity as well as to a reduced loss of shoot and root biomass (Weiland and Koch, 2004). In the following sections of this thesis, the genotype responses were discussed in regard to i) the rapid effect on taproot growth, ii) the development of disease severity and fungal ramification in the leaf tissue, iii) the impact of leaf waxes, and iv) the disease detection by the spectrometry of leaves.

4.1 Taproot response of sugar beets to CLS

Although previous studies focused on effects of *Cercospora* leaf spot on sugar beet yield and gene expression (Shane and Teng, 1992; Weltmeier et al., 2011), less is known about effects on the root system at disease onset and how internal taproot morphology changes during foliar disease progression. This non-invasive MRI study of sugar beets grown in soil revealed taproot growth reduction and morphological changes at the beginning of foliar *Cercospora beticola* infestation showing low levels of disease severity. Measurements over several weeks revealed changes in taproot volume and cambial ring development due to fungal infection. In this context, sugar beets could be classified based on their genotype-specific responses regarding root growth and reduced structural root alterations during foliar infestation by CLS.

4.1.1 Sugar beets reacted to CLS inoculation with a rapid response in taproot growth

The taproot growth of different genotypes with high (HS) and low susceptibility (LS) was reduced within 14 days after foliar inoculation with *C. beticola*. This effect was investigated for the STD HS and LS genotypes as well as for the breeding lines BL 20, BL 18 and BL 8 obtained from KWS SAAT AG. Additional inoculation at 62 dpi and 74 dpi caused further growth reductions, amplifying the differences between the

inoculated and non-inoculated treatments. Compared with the HS genotype, LS plants showed significantly reduced taproot growth for both treatments during the whole experiment and a greater loss of fresh weight at harvest 90 dpi. These results are in agreement with the findings of Smith and Campbell (1996) reporting a negative correlation between disease resistance and sucrose yield, and describing higher productivity of HS plants under low infection pressure. In regard to the comparison of the STD HS and LS genotype, the findings indicate a relatively low disease pressure under experimental greenhouse conditions. The LS genotype could not benefit from its genetic background. Expressing defense genes under these conditions may consume much more in terms of effort and resources than it could provide considerable advantages. Defense activation may have a high energy cost and conflict with energy storage in the taproot. The expression of defense genes that act directly against pathogens or improve signal perception compete with the expression of genes that regulate the carbon metabolism (Berger et al., 2004; Weltmeier et al., 2011).

Compared with the STD HS and LS genotype, the breeding lines displayed minor differences in taproot volume and biomass. However, comparing the breeding lines, the BL 20 plants were more strongly affected showing the highest loss in taproot volume and fresh weight, whereas the BL 8 plants displayed the lowest loss. Compared with these genotypes, the BL 18 plants produced the highest biomass and showed a moderately reduced yield due to fungal infestation. According to Smith and Campbell (1996), these response features would describe a moderately susceptible genotype that shows a high productivity combined with a potentially reduced yield loss during infection. Germplasm displaying similar growth responses would meet the demand of sugar beet breeders and sugar producers (Holtschulte et al., 2010). However, to be introduced into breeding programs, genotypes have to be tested under field condition to verify plant responses and productivity under various disease pressures.

Under experimental greenhouse conditions, the LS genotypes turned out to have not as much biomass production as the other genotypes. It can be assumed, that the genetic advantage of the STD LS and BL 8 plants becomes beneficial at a later disease stage under field conditions that offer optimal requirements for fungal infestation. The initial time point of severe disease progression is reached after leaf covering of plant rows that triggers an increase of air humidity and leaf wetting (Wolf et al., 2001a; Wolf et al., 2001b). Thus, on the field, BL 8 plants might be more productive than BL 18 plants, which may have yield penalties at a higher disease pressure.

Besides a smaller and lighter taproot, the STD LS genotype had also reduced thickness of cambial rings compared with the STD HS genotype. The inner cambial rings of the STD HS genotype were almost two-fold and the outer rings three-fold thicker compared with the STD LS plants, even though both genotypes were at a

similar developmental stage with eight mature leaves at the time point of inoculation. In the STD HS genotype, inner cambial rings were significantly thicker than the outer rings, because the secondary thickening of the taproot started with the storage of sugars in the inner cambial rings and then widened to the outer cambial rings (Artschwager, 1926). The fungal infection of leaves led to a reduction in thickness of inner cambial rings. This response indicated that inner cambial rings were provided by leaves that could only supply low amounts of photoassimilates. The outer cambial rings were slightly increased in thickness indicating that they were provided with higher amounts of sugars by leaves displaying an increased photosynthetic activity. This indicated compensatory effects to CLS-caused growth reduction of the inner cambial rings by increasing growth of outer cambial rings. These findings point to a primary vascular connection of fungal-infected leaves (first six mature) to the inner four cambial rings, as Zamski and Azenkot (1981) concluded about the vascular system of sugar beet. The observation of leaf-dependent ring growth is also in agreement with the study of sectorial sugar accumulation in taproots (Jahnke et al., 2009). In this combined study using MRI and positron emission tomography (PET) co-localization, sugar beet leaves were exposed to $^{11}CO_2$ revealing photoassimilate transport along defined routes to vascular rings in the taproot. Depending on the leaf labeled with $^{11}CO_2$ different taproot regions were supplied with photoassimilates. While the growth of outer cambial rings was reduced in the inoculated STD HS plants, this effect was not found among the breeding lines. Here, the growth of both inner and outer cambial rings was reduced in the inoculated plants. Nonetheless, growth reduction of the inner four cambial rings of BL 20 and BL 8 plants was caused by the inoculation of the first six mature leaves. The growth reduction of these cambial rings strengthens the argument that the fungal infestation of the respective vascularly connected leaves was responsible for this reduction. In contrast to these genotypes, the BL 18 showed a similar thickening of rings connected to both inoculated and non-inoculated leaves. Referring to the growth response of the BL 18 plants, this genotype was less severely affected by fungal infestation indicating that this germplasm seems to be appropriate for resistance breeding. Disease-induced morphological changes of taproots, such as volume, cambial ring thickness, ring number and the respective growth rates, could contribute to a better understanding of disease effects of the canopy affecting the root system. The interrelation of taproot traits with the percentage of sucrose had been discussed by Artschwager (1930) trying to correlate sucrose content with cambial ring numbers, ring width, ring density and parenchymal cell size. However, a structural regularity could not be found for sugar beets that displayed an increased sucrose content (Artschwager, 1930). Based on MRI images, which allow non-invasive observation of specific regions, it is possible to intervene invasively at particular growing stages in order to analyze tissue samples i.e. inner and outer cambial rings regarding their gene expressional or metabolic status. In a comparable study using populus leaves, the genetic and metabolic differences of the growing zones were investigated that were previously chosen by digital imaging (Matsubara et al., 2006). Due to the alteration during the

secondary thickening of sugar beets, morphological traits could be the taproot diameter and the overall proportion of different root parts such as hypercotyl, taproot body or taproot tail (Fig. 35). The general shape of the taproot body can also be considered a selection factor, since a smooth body lowers the amount of adhering soil that can cause problems during factory processing (Theurer, 1993).

Hence, disease effects at the whole plant level can be analyzed to select candidates for breeding programs. Insights into important developmental stages of taproot growth might support plant protection aiming at the optimization of fungicide application for more vulnerable plant stages. MRI might contribute to breakthroughs in understanding complex regulatory plant performance mechanisms and their functionality also regarding other crops to fulfill future needs in food and energy (Van As and van Duynhoven, 2013).

4.1.2 What factors triggered the rapid response in taproot growth?

Sugar beets showed altered taproot growth within two weeks after inoculation, while only a few leaf spots were observed. This growth effect could be referred to the beginning of extensive fungal colonization and subsequent ramification in the intercellular space of leaves. Although there were only a few macroscopic necrosis visible, it is likely that many cells were already damaged, as described previously (Steinkamp et al., 1979). Consequently, the content of destroyed cells represented the nutrient reservoir of the pathogen and photoassimilates were withdrawn by the pathogen instead of being stored in the plant (Berger et al., 2004; Berger et al., 2007; Leal and Lastra, 1984).

There is increasing evidence that pathogens do not only induce direct defense responses, but also alter primary carbohydrate metabolism. Particularly, the induction of cell wall-bound invertase, belonging to the key regulators of carbohydrate partitioning, was reported several times (Berger et al., 2004; Berger et al., 2007; Bonfig et al., 2010; Chou et al., 2000; Essmann et al., 2008; Kocal et al., 2008; Swarbrick et al., 2006). Based on the sugar degradation of source leaves and the changes in source-sink metabolism, the carbon transport to sink organs such as roots is reduced (Bonfig et al., 2010; Van As and van Duynhoven, 2013). Furthermore, fungi often cause yield loss of their host crops by reducing photosynthesis within the infected leaf (Berger et al., 2004; Swarbrick et al., 2006). For example, the infection of barley leaves with *Blumeria graminis* and tomato leaves with *Botrytis cinerea* resulted in lower rates of photosynthesis associated with increased invertase activity and down-regulated photosynthesis gene expression (Berger et al., 2004; Swarbrick et al., 2006). Levall and Bornman (2000) showed a decrease of photosynthetic efficiency of young sugar beets due to *Cercospora* infection. At 16 day post inoculation (dpi), leaves with 3 to 6% infected area showed significant reduced chlorophyll fluorescence investigated by Pulse Amplitude

Modulation (PAM) measurements (Levall and Bornman, 2000). However, in this dissertation, disease severity up to 10% of the measurement area had no clear impact on the electron transport rate and the actual quantum yield of PSII until, while both were first reduced when 60% infected area had been reached. It might be assumed that differences between inoculated and non-inoculated leaves become clearer at higher light intensities, as the ones that prevailed during the experiment in the greenhouse. Further investigations are needed to verify the photosynthesis reduction of sugar beet during CLS infection. However, in accordance with several other studies, it still might be assumed that *Cercospora beticola,* as a hemibiotropic fungus, induces metabolic changes and carbohydrate withdraw in sugar beet, as other fungal pathogens (Berger et al., 2004; Chaerle et al., 2007). Such *Cercospora*-induced changes in the carbon metabolism and photosynthesis as well as minor cell damage may lead to taproot growth reduction at pre- and low-symptomatic infections sites.

4.2 Shoot response of sugar beets depends on plant susceptibility

Several studies used conventional methods such as visual disease scoring and taproot weighing in order to quantify yield loss caused by CLS (De Coninck et al., 2011; Rossi and Battilani, 1989; Shane and Teng, 1992). These efficient and usually low-cost methods permit a first way to screen for putative plant defense ability, but implicate that genotypes have to show a progressed foliar damage and yield loss prior to an evaluation of their resistance class. Otherwise, few studies focused on disease tracking in infected leaves before visible leaf symptoms appear with the aim to identify disease-causing pathogen and to describe fungal spreading in the host tissue (De Coninck et al., 2011; Lartey et al., 2003; Weltmeier et al., 2011). In this thesis, quantitative real-time PCR amplification of the *C. beticola* calmodulin gene was used to detect the disease prior to major symptom development. The defense ability of sugar beet genotypes correlated with fungal colonization levels in the leaf tissue as well as with foliar disease progression and taproot biomass loss following inoculation.

4.2.1 How did the fungus develop in the leaf tissue of contrasting sugar beet genotypes?

After invading through the stomata fungal hyphae start to grow in the intercellular space of the leaf tissue (Steinkamp et al., 1979). Depending on their resistance level, plants are able to inhibit fungal spreading (Feindt et al., 1981b). In greenhouse experiments, the STD HS and BL 20 plants showed a tendency towards increased fungal growth compared with the STD LS and BL 8 plants.

Schmidt et al. (2008) determined a fungal growing period of 1 to 5 dpi for conidia adhesion, extensive growth on the leaf surface, and the first growth through stomata for colonization. Extensive colonization in the host tissue was observed between 5 to 9 dpi. The first necrotic spots appeared after another 6 days, between 10 to 15 dpi. A two-fold faster fungal development was detected when plants were grown on agar containers in climate chambers instead of greenhouse cultivation in soil-filled pots. In line with the results of Schmidt et al. (2008), in this thesis, a similar fungal amount was quantified in genotypes with high and low susceptibility at 1 dpi. At 3 dpi, the first differences in fungal growth between genotypes could be found. While the STD HS plants showed slightly higher fungal growth than the STD LS plants at 4 dpi, the BL 20 and BL 8 plants differed at 10 dpi. These results are consistent with the histopathological examination of Solel and Minz (1970) concluding that sugar beet resistance determined the speed of leaf colonization as well as the frequency of penetration. They concluded that plant's intervention in the fungal infection process of *C. beticola* can be referred to resistance mechanisms (Solel and Minz, 1971). An example for a resistance mechanism is the plant ability to reduce the growth of germ tubes towards stomata by suppressing the stimulus of hydrotropism. The smaller the

percentage of penetrating germ tubes, the lower was the number of infection spots. The stomatal density of the genotypes and the fungal penetration of stomata were not investigated in this thesis. However, Solel and Minz (1970) showed that the percentage of stomata penetration was independent from stomata density. It is likely that the LS genotypes could limit fungal ramification thanks to increased defense gene expression. Weltmeier et al. (2011) showed that fungal infestation was reduced in a polygenic resistant cultivar according to a two-fold higher defense gene expression compared with a susceptible cultivar. The resistant cultivar also displayed a significantly broader gene pool activation fifteen days after inoculation. Especially genes were expressed directly acting against pathogens and also important for signal perception and signaling. For example, receptor-like proteins (cell-surface receptors) and ubiquitin ligase improve pathogen recognition or signal transduction concerning defense reaction, thus decreasing fungal disease development (Weltmeier et al., 2011).

The differences in fungal growth between the experiments could result from seasonal changes in environmental conditions. While in August significantly higher fungal amounts were detected for the STD HS genotype compared with the STD LS genotype, the clear difference was hardly measurable in January. A similar effect could be observed for the breeding lines that showed an increased fungal growth in May and June compared with the experiments in April. Temperature and light have been shown to affect CLS development regarding conidia germination, fungal colonization in the leaves, sporulation and toxin production (Bleiholder and Weltzien, 1972; Calpouzos and Stallknecht, 1965; Khan et al., 2009; Levall and Bornman, 2000; Lynch and Geoghegan, 1979; Skaracis et al., 2010; Wolf et al., 2001a). Higher light intensity and illuminance can increase fungal aggressiveness, since the fungal toxin cercosporin requires light for toxicity in order to produce reactive oxygen species (ROS) damaging host cells (Daub and Ehrenshaft, 2000). The applied inoculation conditions in this thesis correspond with the known favorable conditions for *Cercospora* growth (Schmidt et al., 2004; Schmidt et al., 2008; Weltmeier et al., 2011). An optimal temperature of 25-30°C and relative humidity of 98% for 7 days were applied for conidia germination and good hyphal spreading in the leaf tissue (Wolf et al., 2001a). Prior to inoculation, the fungus was grown under stable and controlled conditions in a climate chamber that should ensure only minor differences in fungal cultivation. The most likely cause for the differing absolute and relative fungal amounts is that the seasonal changes in light intensity and temperature had an impact on the developmental cycle of *C. beticola* in sugar beets. Future experiments testing the influence of light and temperature on disease progression in sugar beets are necessary to verify the seasonal effects observed in this study.

4.2.2 How did the environment affect defense ability of sugar beets?

Sugar beet growth can be enhanced by environmental factors that are within an optimal range. Terry (1968) showed that the highest yield in dry matter of sugar beets was found at 24°C for the shoot and 17 to 24°C for the root which could be increased by additionally applied light. With increasing light intensity, the photosynthetic net assimilation increased almost proportionally, but was not significantly affected by increased temperatures. Due to the predisposition of plants (disease disposition), plant defense can be reduced and pathogens are enabled to infect them more easily and with increasing severity (Agrios, 1997; Hallmann et al., 2009; Wolf et al., 2001a). For example, high temperature induce leaf wilting which lowers plant resistance and increases strength of disease (Schmidt, 1928). Another important factor is the availability of nutrients. Li et al. (2011) investigated improved sugar beet resistance to *C. beticola* after balanced fertilizing, whereas low levels of resistance were measured under low nitrogen supply.

In this study, the genotype susceptibilities were verified, but the difference among the genotypes was not as clear as in the field experiment. On the field, it is likely that another factor of plant growth can be taken into account. It was shown that the extensive leaf production of sugar beet during rosette filling has an beneficial effect on disease development. The so-called row closure, occurring in the third and fourth week of June (Wolf et al., 2001a), leads to a 90% leaf covering of plant rows usually causing increased self-shading and reduced drying of leaves after nighttime dewfall in the plant stand. Compared with microclimate conditions before row closure, this leads to a 10% increase in relative humidity and a 35% increase in leaf wetting that are requirements for plant epidemics of facultative pathogens, e.g. *Cercospora beticola* and *Ramularia beticola* (Wolf et al., 2001a). This problem may worsen in the future due to global climate changes[5] that would likely be beneficial for pathogens (Levall and Bornman, 2000). Under greenhouse cultivation, plants were grown in single pots, leaf covering was generally prevented and the air humidity did not exceed 60%. Therefore, the main reasons for the variable defense ability of sugar beet genotypes under greenhouse and field conditions seemed to be the two factors light and temperature, which may have influenced the disposition of sugar beet genotypes. However, such experiments can be sufficient for pre-selection, but cannot replace field evaluations needed to verify resistance level under “natural” disease pressure over a full growing season. Nevertheless, MRI experiments might be designed to choose soil compositions and probably bigger pot sizes in order to slightly reduce the gap between field and greenhouse conditions for further analysis of the root system in differently composed environment.

[5] http://www.umwelt.nrw.de/klima/klimawandel/klimaentwicklung_nrw/index.php

4.2.3 How strongly can selected sugar beet germplasm tolerate *Cercospora* infections?

Disease severity was investigated from the leaf to the canopy level. A comparatively low susceptibility led to a delayed and less severe leaf damage reflecting both a lower disease severity and a lower number of symptomatic leaves. Low susceptibility was associated with low biomass loss and reduction of fungal growth in the leaf tissue.

Apart from this, plants with high susceptibility consistently showed a more severe disease progression in changing environmental conditions, as measured by a lower coefficient of variation (Table 21). The generally higher disease severity of these plants is in good agreement with several studies (Feindt et al., 1981a; Shane and Teng, 1992; Weltmeier et al., 2011), but in contradiction to the results of Rossi et al. (1999). Plants did not show a significantly earlier appearance of leaf symptoms, 5 to 12 days in advance, compared with lowly susceptible plants. This can be explained by the selection of different genotypes that varied in their genetic background and therefore in their defense ability.

Table 21: Coefficient of variation of disease severity for sugar beet genotypes. Coefficient of variation (CV) was calculated of disease severity for the standard genotypes (STD) and breeding lines (BL). Disease severity was summarized from leaves of all experiments (Table 13). Mean values of disease severity, leaf number (n) and standard deviation (SD) were compared at comparative time points after inoculation (dpi) of experiments 1 to 4 and 9 to 11.

Genotype	CV (%)	Disease severity (Mean)	Leaves (n)	SD	Exp.	Dpi
STD HS	**1.06**	36.0	132	38.3	1, 2,	28, 27,
STD MS	**1.11**	35.0	110	39.0	3, 4	31
STD LS	**1.20**	36.0	107	43.0		
BL 20	**1.34**	25.3	120	33.9	9, 10,	29, 28,
BL 8	**1.98**	14.5	118	28.7	11	28
BL 18	**1.50**	11.0	77	16.4		
BL 17	**1.59**	20.1	37	31.9		

In this dissertation, several genotypes with similar susceptibilities to CLS were analyzed. In contrast to the STD HS plants, the BL 20 plants were strongly affected by CLS causing a greater biomass loss in comparison with the other breeding lines.

The STD HS plants, which should be affected more severely by CLS, showed higher taproot biomass and lower disease-induced losses compared with the STD LS plants. These effect was not observed in the breeding lines, the BL 8 plants were only slightly less affected compared with the BL 20 plants. Because it is known that under high disease pressure lowly susceptible plants are more productive than highly susceptible plants (Smith and Campbell 1996), it is possible that a low disease pressure prevailed in the greenhouse experiments. The MS genotypes showed a variable reaction in disease development compared with the more reproducible HS plants. These genotypes seemed to be able to adjust better to a changing disease pressure leading to low disease severity and low yield loss, as well as to higher leaf damage under high disease pressure. Based on this effect, these MS genotypes might be more appropriate for yield gain under low-to-moderate disease pressure. While HS plants would be comparatively more strongly infected, and LS plants would not yet be comparatively more productive. It was shown that the shoot response allowed to classify genotypes regarding their susceptibility against CLS by conventional disease scoring. Nonetheless, investigating plant defense at different levels of disease progression, e.g. by the analysis of fungal spreading in leaves and taproot growth, strengthens a meaningful classification of genotype susceptibility.

4.3 Importance of cuticular waxes on plant susceptibility

Less information is available about the role of leaf waxes on the interaction of sugar beet and *Cercospora beticola*. This study revealed an increased amount of leaf waxes on the leaf surface of a LS genotype compared with a HS genotype.

In this study, it could be shown that BL 8 plants had higher wax amounts than the BL 20 plants and mature leaves higher amounts than immature, still expanding leaves. This leads to the conclusion that the amount of leaf waxes might be a factor of plant resistance, also in agreement with the prior observation that an increased susceptibility to CLS was also detected for immature leaves (Feindt et al., 1981b; Rossi et al., 1999). Baker and Hunt (1980) have shown that primary alcohols are the main compounds of sugar beet wax. The detected total wax amounts of sugar beet leaves are consistent with the results of the aforementioned study (Baker and Hunt, 1981). Leaves of different developmental stages are known to differ in total wax amounts. However, contradictory studies reported about species-related increased wax amounts at the leaf senescence stage (Rich, 1994 using *Sorghum*, and Jenks et al. 1996 using *Arabidopsis*) or at leaf immaturity (Baker, 1982 using *Brassica oleraceae*, and Beattie and Marcell, 2002 using *Zea mays*). Comparing sugar beet leaf sizes from 20 to 60 cm², Baker and Hunt (1981) measured decreasing epicuticular wax amounts from 7 to 2.5 µg cm^{-2}. In contradiction to these results, an increase in total wax amount was measured from immature to mature sugar beet leaves in this thesis. These contrasting results might be explained by different cultivars and leaf ages that were analyzed. Separating between adaxial and abaxial leaf surface, Baker and Hunt (1980) showed lower wax amounts for the abaxial side that also differed in its chemical composition compared with the adaxial leaf surface (Carver and Gurr, 2008). In general agreement with this study, an higher total wax amount was detected when waxes of both the adaxial and abaxial leaf side of BL 20 and BL 8 plants were analyzed.

Mature and immature leaves of both genotypes were inoculated to correlate fungal growth with the total amount of leaf waxes. In contrast to the immature leaves, the total wax amount of mature leaves decreased for both genotypes from 1 to 3 dpi. For fungal inoculation, leaves were kept one week under relative humidity between 90 and 100%. According to Koch et al. (2006), these inoculation conditions could have led to the reduction of total wax amounts of mature leaves. These authors found that wax amounts of *Brassica oleracea* (kohlrabi) decreased by half at 98% relative humidity. Also Baker et al. (1974) showed that both wax production and accumulation were influenced by air humidity and temperature. Furthermore, Koch et al. (2006) reported an altered wax composition within a 6 week period of cultivation under high humidity. The period of one week under high humidity, that was applied here, might have been too short of a time to lead to a change in wax composition.

A wax reduction is expected to cause either increased conidia attachment on the leaf surface, or reduced conidia germination due to the loss of signals for host-recognition

(Carver and Thomas, 1990). As it had been indicated for the plant-pathogen system mulberry and *Cercospora moricola*, resistant genotypes displayed more waxes, thicker surface layers and less number of stomata per unit area resistant against (Philip and Govindaiah, 1996). However, in this study, a similar total wax amount was measured for both the stripped and the untreated leaf surface. Since the amount of waxes removed by cellulose acetate strips was not analyzed, it is possible that the leaves were not properly stripped of waxes, or that new wax recovered within a day. The second possibility would be in line with the rapid formation of wax crystals of *Galanthus nivalis* (Koch et al., 2004). Via atomic force microscopy (AFM) it could be shown that 20 min after wax removal a first visible layer and after 74 min an almost completely reorganized layer of wax crystals was produced. This confirms a dynamically changing structure and chemistry of epicuticular waxes (Koch et al., 2006b). In several studies, the impact of wax components as a signaling factor in plant-pathogen systems had been described (Carver and Gurr, 2008; Mendoza-Mendoza et al., 2009). For the plant-pathogen system *Puccinia sorghi* and *Zea mays*, it could be shown that conidia failed to germinate on leaves of 'waxless' mutants having a reduced epicuticular wax layer (Wynn and Staples, 1981). As indicated by several other studies (Tsuba et al., 2002; Wright et al., 2000), the wax layer of plants plays an increasing important role and should be carefully investigated as a barrier not only to pathogens, but also to abiotic and chemical stresses. For example, the pre-emergence application of ethofumesate, an herbicide, severely decreases the epicuticular wax composition on sugar beet leaf surfaces (Duncan et al., 1980) pointing to the investigations of pesticide effects on the cuticle. Regarding the depletion of stratospheric ozone and climate changes, the UV-B radiation increasingly affects plant surfaces as well (Levall and Bornman, 2000). Therefore, further studies should be conducted to verify the correlation between the total amount of leaf waxes and plant susceptibility to both biotic and abiotic stresses. Furthermore, the variation in wax composition and in the structure of wax crystals might be correlated with infections rates of *C. beticola* on sugar beet. Non-invasive spectrophotometry was shown to be feasible to detect differences between leaf layers (Pfündel et al., 2008). Accompanied by microscopic studies and spectrometric analyses of wax quantity and quality, the spectral features of leaves might improve the selection process for specific leaf properties.

4.4 *Cercospora* altered the spectral signature of sugar beet leaves

Vegetation indices are widely-used to describe the plant status by the correlation of specific wavelengths of the reflectance spectrum with optical remote sensing. Leaf properties such as biomass, chlorophyll and leaf water can be investigated according to their specific wavelengths absorbance and reflectance of the incoming light (Tucker, 1977; Tucker, 1978). Recently the quantification of nitrogen (Mutanga and Skidmore, 2004; Ollinger et al., 2002), proteins and polyphenols (Skidmore et al., 2010) were included as well as the detection of biotic stresses including important diseases (Bock et al., 2010). Spectral sensors are the interface between field and greenhouse that enable non-invasively the quantification of plant responses to biotic and abiotic stresses.

Mahlein et al. (2013) proved that the *Cercospora* leaf spot index (CLSI) allowed to detect CLS accurately after 6-9% disease severity. In agreement with this result, this thesis shows that besides the Normalized Difference Vegetation Index (NDVI), the CLSI can complement visual disease scoring. The LS genotype (BL 8) showed significantly higher leaf biomass (NDVI), higher leaf water content (LWI) and lower *Cercospora* infestation (CLSI) compared with the other breeding lines and the non-infected plants.

At a given disease stage in the field, spectral measurements can be influenced by changes in the plant stand such as the uncovering of soil due to canopy damage that an be induced by both biotic and abiotic factors. It was shown that the multispectral data were influenced by the soil reflectance visualized in the color-coded NDVI images, introducing spectral disturbances. It can be assumed that the FieldSpec instrument also included soil signals in its integrated measurement area. Nonetheless under natural conditions, soil is visible between young sugar beets at the beginning of the growing period. Field measurements were conducted at a growth stage after row closure that means the soil was mostly covered by canopy. Therefore at this developmental stage, open soil can be referred either to cultivar-specific shoot property or foliar damage due to biotic or abiotic stresses. Robust shoot architecture is a criterion for genotype selection[6]. Lush foliage that is resistant to mechanical stresses leads to increased biomass and sugar accumulation in the taproot. Therefore, the uncovering of soil between plants might be considered as indicator for stunted plant development. The soil effect might be mitigated when using indices that are based on wavelengths independent of soil signals, e.g. the CLSI.

The challenge is to detect the disease at its onset and prior to the appearance of visible symptoms. In several studies, photosynthetic reduction was reported due to pathogen infestation using fluorescence imaging (Balachandran et al., 1994; Berger et al., 2004; Chaerle et al., 2007; Kocal et al., 2008; Scholes and Rolfe, 1996; Swarbrick et al., 2006). Also pre-symptomatic thermal and fluorescence changes of

[6] www.baes.gv.at/pflanzensorten/oesterreichische-beschreibende-sortenliste/beta-rueben/zuckerruebe

Cercospora infection sites on sugar beet leaves were investigated. Chaerle et al. (2007) measured a local decrease in temperature, and thus an increase in transpiration seven days after inoculation, indicating toxin-induced mesophyll cell damage and evaporation of cellular fluids. The detection of *Cercospora* leaf spot was achieved even before first symptoms appeared by the evaluation of spectroradiometric measurements combined with the classification of support vector machines (Rumpf et al., 2010). All these studies provided evidence that this fungal infestation is detectable before visible symptoms appear. However, in this study, it was shown that the index maps and indices of the transmittance and reflectance spectrum did not indicate leaf symptoms prior to visible development. It had to be noted that only three leaves have been analyzed so far that had only a few visible leaf symptoms at 9 dpi illustrated in the index maps. Therefore, these results should be interpreted with caution. Nonetheless, according to the induced changes in the leaf reflectance properties, due to either cell damage and/or metabolic changes, this remains a promising approach to investigate the very beginning of disease onset starting with the initial ramification of mycelia in the intercellular space. The additional signature of leaf transmittance might provide complementary data that also increase detection sensitivity. As it was shown in the index maps of the transmitted light, the difference between leaf symptoms and the non-infected surrounding leaf area was increased. This might allow to detect spectral changes at earlier time points. Using the new HyperART-system, slight modification of leaf properties should be detectable by imaging simultaneously the reflectance and transmittance signal. Consequently, the derived absorbance function might provide new aspects for disease detection in order to select and quantify sugar beets with increased resistance to CLS.

5 Conclusions

5.1 Taproot response

The taproot response and growth effect was investigated during foliar disease development using MRI. An early growth reduction within two weeks after inoculation at a very low disease severity was detected according to the first occurring cell damage of the leaf tissue. The reduced growth of cambial rings connected to inoculated leaves contrasted the increased growth of rings that were connected to newly formed, non-inoculated leaves. The sugar beet genotypes showed different responses in the taproot growth due to CLS inoculation. The STD HS genotype showed a significantly increased taproot growth for both treatments compared with the STD LS genotype indicating a relatively low disease pressure, since LS genotypes are generally described to be more productive under more severely increased disease severity. The BL 18 plants showed an increased taproot growth for both treatments compared with the BL 8 and BL 20 plants indicating that this seems to be a promising germplasm for resistance breeding to CLS combined with an increased yield production. The analysis of further genotypes with MRI would open the possibility to investigate complex regulatory plant performance mechanisms and their functionality. In order to obtain a full picture of how the plant responds to CLS, more detailed observations of shoot and taproot are necessary. Further experiments combining MRI and PAM measurements would reveal how early photosynthesis is reduced triggering the rapid response in taproot growth, and the analysis of photoassimilate supply to the taproot from source leaves could be analyzed by $^{11}CO_2$ supply using PET.

5.2 Shoot response

Different strengths of disease response could be investigated, depending on the active plant defense ability. Based on the molecular analysis, it could be shown that plants with high susceptibility allowed a stronger fungal colonization in the leaf tissue than ones with low susceptibility correlating with the respective disease severity. The HS genotypes displayed a more stable and reproductive response in disease severity compared with the LS plants. In particular, the moderately susceptible (MS) genotype seemed to be promising according to its variable response indicating a more adaptable reaction to changing environmental conditions. Based on this effect, this MS genotype might be more appropriate for yield gain under a low-to-moderate disease pressure, when HS plants would be comparatively more strongly infected, and LS ones would not yet be comparatively more productive. The combination of visual disease scoring and the molecular analysis of fungal colonization allowed to verify plant resistance classes. Therefore, the combination of these methods might

open the opportunity to select genotypes from sugar beet populations and to classify them in regard to their resistance level. Following the selection, candidate genotypes can be used for new crosses in order to enrich germplasm for the breeding of sugar beet with increased resistance as well as increased sugar yield.

5.3 The impact of cuticular waxes

A higher amount of leaf waxes was investigated in sugar beet genotypes with low susceptibility and in mature leaves of both the HS and LS genotypes compared with immature, still expanding leaves. An impact of leaf waxes on fungal growth could not be shown. Further improved stripping studies, focusing on a time series within hours or even minutes after removal, would open the possibility to determine the speed of wax re-deposition in sugar beet. In combination with the quantification of fungal growth, the importance of leaf waxes for plant defense ability and the recognition between plant-pathogen might be revealed. An overview of the total wax amount and its composition in a large genotype selection would reveal the variation among cultivars and might allow the correlation with sugar beet tolerance to both biotic and abiotic stresses. A screening of sugar beet populations might then accelerate the selection of genotypes with increased resistance to CLS and other stress factors such as chemicals and UV radiation. Accompanied by microscopic studies and spectrometric analyses of wax quantity and quality, the spectral features of leaves might represent a non-invasive approach to screen for the variation between sugar beet genotypes in order to select plants with specific properties that are important for pathogen resistance.

5.4 Spectral signature changes

The vegetation indices NDVI, LWI and CLSI correlated significantly with the visual scored resistance classes and therefore allowed to quantify foliar damage and disease strength at a progressed stage. The new HyperART-system might allow the detection of *Cercospora* leaf spot at the very beginning. Based on the leaf absorbance it might be possible to evaluate fungal colonization in the leaf tissue before symptoms appear. Besides the detection of further biotic stresses, also abiotic stress responses might be detectable allowing the selection of host plants with specific defense abilities. Furthermore, the quantity and quality of leaf waxes might be analyzed by this hyperspectral system that might allow to distinguish sugar beet genotypes in regard to specific optical leaf properties that are important for stress responses.

5.5 Potential assistance for breeding approaches

A combination of invasive and non-invasive methods revealed plant responses above and below the ground during foliar infection at different disease stages. Plant resistance was quantified by the use of the well-established visual disease scoring and with novel detection systems, revealing more detailed insight into disease progression. In particular, the early and progressively reduced taproot growth opens the possibility to track potential traits for resistance breeding using MRI. In the terms of applicability, pre-selection of candidate genotypes might be very useful to achieve valuable information about the plant performance in regard to taproot traits that change during the secondary thickening such as shape, volume, cambial ring thickness, and the overall ratio between hypocotyl and the main body. The molecular analysis allowed to detect an increased fungal growth in plants with high susceptibility. Therefore, this method helps to give an overview, but seems to be less appropriate for a strict genotype separation for breeding aims when resistance is developed at a later stage of disease progression. The spectral imaging with the HyperART-system seems to be a promising method for disease detection. In this study, the combined approach of detection methods provided a total picture of disease effects on shoot and root. Plants could be classified regarding their resistance level and yield losses. These might allow new aspects beneficial for sugar beet resistance breeding. Combining, MRI and spectral analysis might facilitate the quantification of plant responses to other biotic or abiotic stresses interfering with plant root or shoot development.

6 Publications and Posters

Manuscripts

Jansen, M., Bergsträsser, S., Schmittgen, S., Müller-Linow, M. and Rascher, U. (2014). Non-Invasive Spectral Phenotyping Methods can Improve and Accelerate *Cercospora* Disease Scoring in Sugar Beet Breeding. *Agriculture* **4**, 147-158.

Schmittgen, S., Metzner, R., Van Dusschoten, D., Jansen, M., Fiorani, F., Jahnke, S., Rascher, U. and Schurr, U. (2014). Magnetic resonance imaging of sugar beet taproots in soil reveals growth reduction and morphological changes during *Cercospora beticola* foliar infestation *Journal of Experimental Botany* (in progress)

Conferences

Schmittgen, S., Bergsträsser, S., Fiorani F., Jansen, M., Rascher, U., Scharr, H. Identification of sugar beets resistant against the fungal pathogen *Cercospora* beticola using non-invasive and invasive detection systems. Arbeitskreistreffen Mykologie der Deutschen Phytopathologischen Gesellschaft, Göttingen, Germany, 03/03/2013 - 03/04/2013 (2013)

Schmittgen, S., Bergsträsser, S., Jansen, M.
Phenotyping of pathogen disease dynamic with noninvasive sensor system. Status Seminar Cropsense.net. Siebeldingen, 2011-09-28 (2011)

Posters

Schmittgen, S., Metzner, R., Van Dusschoten, D., Jansen, M., Fiorani, F., Jahnke, S., Rascher, U. and Schurr, U.
Quantification of sugar beet resistance to fungal *Cercospora* infestation using Magnetic Resonance Imaging and quantitative real-time PCR. International Plant Phenotyping Symposium, Chennai, Indien 17/02/2014 – 19/02/2014

Schmittgen, S., Bergsträsser, S., Jansen, M., Fiorani, F., Jahnke, S., Rascher, U. Identification of *Cercospora*-resistant sugar beet lines using multi-sensory and molecular detection systems. American Phytopathological Society, Austin / Texas, USA, 08/10/2013 - 08/14/2013 (2013)/ Cropsense.net Status Seminar, Bonn, Germany, 10/10/2013 - 10/11/2013 (2013)

7 List of Figures

8 List of Tables

9 References

Agrios, G. N. (1997). Plant pathology. San Diego,CA: Academic Press.

Allen, E. A., Hoch, H. C., Steadman, J. R. and Stavely, R. J. (1991). Influence of Leaf Surface Features on Spore Deposition and the Epiphytic Growth of Phytopathogenic Fungi. In *Microbial Ecology of Leaves*, eds. J. Andrews and S. Hirano), pp. 87-110: Springer New York.

Artschwager, E. (1926). Anatomy of the vegetative organs of the sugar beet. *Journal of Agricultural Research, Washington D. C.* **33** 143- 176.

Artschwager, E. (1930). A study of the structure of sugar beets in relation to sugar content and type. *Journal of Agricultural Research, Washington D. C.* **40**, 867-915.

Baker, E. (1982). Chemistry and morphology of plant epicuticular waxes. In *Linnean Society symposium series*, vol. 1982.

Baker, E. A. (1974). The influence of environment on leaf wax development in *Brassica oleracea var. gemmifera*. *New Phytologist* **73**, 955-966.

Baker, E. A. and Hunt, G. M. (1981). Developmental changes in leaf epicuticular waxes in relation to foliar penetration. *New Phytologist* **88**, 731-747.

Balachandran, S., Osmond, C. B. and Daley, P. F. (1994). Diagnosis of the Earliest Strain-Specific Interactions between Tobacco Mosaic Virus and Chloroplasts of Tobacco Leaves in Vivo by Means of Chlorophyll Fluorescence Imaging. *Plant Physiology* **104**, 1059-1065.

Bargel, H., Koch, K., Cerman, Z. and Neinhuis, C. (2006). Evans Review No. 3: Structure–function relationships of the plant cuticle and cuticular waxes — a smart material? *Functional Plant Biology* **33**, 893-910.

Barlow, R. J. (1989). Statistics: a guide to the use of statistical methods in the physical sciences: John Wiley & Sons.

Barthlott, W. and Neinhuis, C. (1997). Purity of the sacred lotus, or escape from contamination in biological surfaces. *Planta* **202**, 1-8.

Beattie, G. A. and Marcell, L. M. (2002). Effect of alterations in cuticular wax biosynthesis on the physicochemical properties and topography of maize leaf surfaces. *Plant, Cell & Environment* **25**, 1-16.

Berger, S., Papadopoulos, M., Schreiber, U., Kaiser, W. and Roitsch, T. (2004). Complex regulation of gene expression, photosynthesis and sugar levels by pathogen infection in tomato. *Physiologia Plantarum* **122**, 419-428.

Berger, S., Sinha, A. K. and Roitsch, T. (2007). Plant physiology meets phytopathology: plant primary metabolism and plant–pathogen interactions. *Journal of Experimental Botany* **58**, 4019-4026.

Bleiholder, H. and Weltzien, H. C. (1972). Contribution to epidemiology of *Cercospora beticola* on sugar beets Part 2 Conidia formation in relation to the environmental factors temerature, relative humidity and light. Beitrage zur Epidemiologie von *Cercospora beticola Sacc.*an Zuckerrübe II. Die Konidienbildung in Abhangigkeit von den UmweltbedingungcnTemperatur, relative Luftfeuchtigkeit und Licht. *Phytopathologische Zeitschrift* **73**, 46-48.

Bock, C. H., Poole, G. H., Parker, P. E. and Gottwald, T. R. (2010). Plant Disease Severity Estimated Visually, by Digital Photography and Image Analysis, and by Hyperspectral Imaging. *Critical Reviews in Plant Sciences* **29**, 59-107.

Bonfig, K. B., Gabler, A., Simon, U. K., Luschin-Ebengreuth, N., Hatz, M., Berger, S., Muhammad, N., Zeier, J., Sinha, A. K. and Roitsch, T. (2010). Post-Translational Derepression of Invertase Activity in Source Leaves via Down-Regulation of Invertase Inhibitor Expression Is Part of the Plant Defense Response. *Molecular Plant* **3**, 1037-1048.

Borisjuk, L., Rolletschek, H. and Neuberger, T. (2012). Surveying the plant's world by magnetic resonance imaging. *The Plant Journal* **70**, 129-146.

Boudry, P., Wieber, R., Saumitou-Laprade, P., Pillen, K., Dijk, H. and Jung, C. (1994). Identification of RFLP markers closely linked to the bolting gene B and their significance for the study of the annual habit in beets (Beta vulgaris L.). *Theoretical and Applied Genetics* **88**, 852-858.

Box, J. E. and Ramsuer, E. L. (1993). Minirhizotron Wheat Root Data: Comparisons to Soil Core Root Data. *Agron. J.* **85**, 1058-1060.

Bradshaw, J. E., Biancardi, E., McGrath, J. M., Panella, L. W., Lewellen, R. T. and Stevanato, P. (2010). Sugar Beet. In *Root and Tuber Crops*, vol. 7, pp. 173-219: Springer New York.

Buschmann, C. and Nagel, E. (1993). *In vivo* spectroscopy and internal optics of leaves as basis for remote-sensing of vegetation. *International Journal of Remote Sensing* **14**, 711-722.

Calpouzos, L. and Stallknecht, G. F. (1965). Sporulation of *Cercospora beticola* affected by an interaction between light and temperature. *Phytopathology* **55**, 1370-1371.

Campbell, C. L., Huang, J.-S. and Payne, G. A. (1980). Defense at the perimeter: the outer walls and the gates. *JF Horsfall and EB Cowling*, 103-120.

Carver, T. L. and Gurr, S. J. (2008). Filamentous fungi on plant surfaces. *Annual Plant Reviews, Biology of the Plant Cuticle* **23**, 368.

Carver, T. L. W. and Thomas, B. J. (1990). Normal germling development by *Erysiphe graminis* on cereal leaves freed of epicuticular wax. *Plant Pathology* **39**, 367-375.

Chaerle, L., Hagenbeek, D., De Bruyne, E. and Van Der Straeten, D. (2007). Chlorophyll fluorescence imaging for disease-resistance screening of sugar beet. *Plant Cell Tissue and Organ Culture* **91**, 97-106.

Chou, H.-M., Bundock, N., Rolfe, S. A. and Scholes, J. D. (2000). Infection of *Arabidopsis thaliana* leaves with *Albugo candida* (white blister rust) causes a reprogramming of host metabolism. *Molecular Plant Pathology* **1**, 99-113.

Coons, G. H., Owen, F. V. and Stewart, D. (1955). Improvement of the Sugar Beet in the United States. In *Advances in Agronomy*, vol. 7 (ed. A. G. Norman), pp. 89-139: Academic Press.

Daub, M. E. and Ehrenshaft, M. (2000). The Photoactivated *Cercospora* Toxin Cercosporin: Contributions to Plant Disease and Fundamental Biology. *Annual Review of Phytopathology* **38**, 461 -490.

De Coninck, B. M. A., Amand, O., Delauré, S. L., Lucas, S., Hias, N., Weyens, G., Mathys, J., De Bruyne, E. and Cammue, B. P. A. (2011). The use of digital image analysis and real-time PCR fine-tunes bioassays for quantification of *Cercospora* leaf spot disease in sugar beet breeding. *Plant Pathology*, no-no.

De Wit, P. (2007). How plants recognize pathogens and defend themselves. *Cellular and Molecular Life Sciences* **64**, 2726-2732.

Draycott, A. P. (2008). Sugar beet: John Wiley & Sons.

Duffus, J. E. and Ruppel, E. G. (1993). Diseases. In *The Sugar Beet Crop*, eds. D. A. Cooke and R. K. Scott), pp. 347-427: Springer Netherlands.

Duncan, D. N., Meggitt, W. F. and Penner, D. (1980). Basis for increased activity from herbicide combinations with ethofumesate applied on sugarbeet (Beta vulgaris). *Weed Science* **30**, 195-200.

Essmann, J., Schmitz-Thom, I., Schön, H., Sonnewald, S., Weis, E. and Scharte, J. (2008). RNA Interference-Mediated Repression of Cell Wall Invertase Impairs Defense in Source Leaves of Tobacco. *Plant Physiology* **147**, 1288-1299.

Fajola, A. O. (1978). Cercosporin, a phytotoxin from *Cercospora spp*. *Physiological Plant Pathology* **13**, 157-164.

Feindt, F., Mendgen, K. and Heitefuss, R. (1981a). Der Einfluß der Spaltöffnungsweite und des Blattalters auf den Infektionserfolg von *Cercospora beticola* bei Zuckerrüben (*Beta vulgaris L.*) unterschiedlicher Anfälligkeit. *Journal of Phytopathology* **101**, 281-297.

Feindt, F., Mendgen, K. and Heitefuss, R. (1981b). Feinstruktur unterschiedlicher Zellwandreaktionen im Blattparenchym anfälliger und resistenter Rüben (*Beta vulgaris* L.) nach Infektion durch *Cercospora beticola* Sacc. *Journal of Phytopathology* **101** 248-264.

Fieuw, S. and Willenbrink, J. (1990). Sugar-transport and sugar-metabolizing enzymes in sugar-beet storage roots (*Beta vulgaris ssp. altissima*). *Journal of Plant Physiology* **137**, 216-223.

Fiorani, F., Rascher, U., Jahnke, S. and Schurr, U. (2012). Imaging plants dynamics in heterogenic environments. *Current Opinion in Biotechnology* **23**, 227-235.

Fiorani, F. and Schurr, U. (2013). Future scenarios for plant phenotyping. *Annu Rev Plant Biol* **64**, 267-91.

Freytag, S. and Hahlbrock, K. (1992). Abwehrreaktionen von Pflanzen gegen Pilzbefall. *Biologie in unserer Zeit* **22**, 135-142.

Gamon, J. A., Peñuelas, J. and Field, C. B. (1992). A narrow-waveband spectral index that tracks diurnal changes in photosynthetic efficiency. *Remote Sensing of Environment* **41**, 35-44.

Gamon, J. A. and Surfus, J. S. (1999). Assessing leaf pigment content and activity with a reflectometer. *New Phytologist* **143**, 105-117.

Gapillout, I., Mikes, V., Milat, M. L., SimonPlas, F., Pugin, A. and Blein, J. P. (1996). *Cercospora beticola* toxins. Use of fluorescent cyanine dye to study their effects on tobacco cell suspensions. *Phytochemistry* **43**, 387-392.

Gardes, M., White, T. J., Fortin, J. A., Bruns, T. D. and Taylor, J. W. (1991). Identification of indigenous and introduced symbiotic fungi in ectomycorrhizae by amplification of nuclear and mitochondrial ribosomal DNA. *Canadian Journal of Botany* **69**, 180-190.

Glidewell, S. M. (2006). NMR imaging of developing barley grains. *Journal of Cereal Science* **43**, 70-78.

Gniwotta, F., Vogg, G., Gartmann, V., Carver, T. L. W., Riederer, M. and Jetter, R. (2005). What Do Microbes Encounter at the Plant Surface? Chemical Composition of Pea Leaf Cuticular Waxes. *Plant Physiology* **139**, 519-530.

Gottschalk, T. E., Mikkelsen, J. D., Nielsen, J. E., Nielsen, K. K. and Brunstedt, J. (1998). Immunolocalization and characterization of a [beta]-1,3-glucanase from sugar beet, deduction of its primary structure and nucleotide sequence by cDNA and genomic cloning. *Plant Science* **132**, 153-167.

Goudet, C., Milat, M.-L., Sentenac, H. and Thibaud, J.-B. (2000). Beticolins, Nonpeptidic, Polycyclic Molecules Produced by the Phytopathogenic Fungus *Cercospora beticola*,

as a New Family of Ion Channel-Forming Toxins. *Molecular Plant-Microbe Interactions* **13**, 203-209.

Groenewald, M., Groenewald, J. Z., Braun, U. and Crous, P. W. (2006). Host range of *Cercospora apii* and *C. beticola* and description of *C. apiicola*, a novel species from celery. *Mycologia* **98**, 275-285.

Hallmann, J., Quadt-Hallmann, A. and von Tiedemann, A. (2009). Phytomedizin: Grundwissen Bachelor. Stutttgart (Hohenheim): Verlag Eugen Ulmer Stuttgart.

Hauke, V. and Schreiber, L. (1998). Ontogenetic and seasonal development of wax composition and cuticular transpiration of ivy (Hedera helix L.) sun and shade leaves. *Planta* **207**, 67-75.

Heath, M. C. (1991). Evolution of resistance to fungal parasitism in natural ecosystems. *New Phytologist* **119**, 331-343.

Helback, H. (1959). Domestication of Food Plants in the Old World: Joint efforts by botanists and archeologists illuminate the obscure history of plant domestication. *Science* **130**, 365-372.

Hess, M., Barralis, G., Bleiholder, H., Buhr, L., Eggers, T., Hack, H. and Stauss, R. (1997). Use of the extended BBCH scale—general for the descriptions of the growth stages of mono- and dicotyledonous weed species. *Weed Research* **37**, 433-441.

Hillnhütter, C. and Mahlein, A.-K. (2008). Neue Ansätze zur frühzeitigen Erkennung und Lokalisierung von Zuckerrübenkrankheiten. *Gesunde Pflanzen* **60**, 143-149.

Hillnhütter, C., Sikora, R. A., Oerke, E.-C. and van Dusschoten, D. (2011). Nuclear magnetic resonance: a tool for imaging belowground damage caused by *Heterodera schachtii* and *Rhizoctonia solani* on sugar beet. *Journal of Experimental Botany*.

Holtschulte, B., Mechelke, W. and Stahl, J. D. (2010). Coventional and Novel Approaches in Cercospora Resistance Breeding in Sugar Beets. In *Cercospora Leaf Spot of Sugar Beet and Related Species*, eds. R. T. Lartey J. Weiland J. L. Panella P. W. Crous and C. E. Windels): The American Phytopathological Society.

Hornak, J. P. (1996). The Basics of MRI: Interactive Learning Software 2008.

Huete, A. R. (1988). A soil-adjusted vegetation index (SAVI). *Remote Sensing of Environment* **25**, 295-309.

Jahnke, S., Menzel, M. I., Van Dusschoten, D., Roeb, G. W., Bühler, J., Minwuyelet, S., Blümler, P., Temperton, V. M., Hombach, T., Streun, M. et al. (2009). Combined MRI–PET dissects dynamic changes in plant structures and functions. *The Plant Journal* **59**, 634-644.

Jansen, M., Pinto, F., Nagel, K. A., Dusschoten, D., Fiorani, F., Rascher, U., Schneider, H. U., Walter, A. and Schurr, U. (2014). Non-invasive Phenotyping Methodologies Enable the Accurate Characterization of Growth and Performance of Shoots and Roots. In *Genomics of Plant Genetic Resources*, eds. R. Tuberosa A. Graner and E. Frison), pp. 173-206: Springer Netherlands.

Jenks, M. A., Rashotte, A. M., Tuttle, H. A. and Feldmann, K. A. (1996). Mutants in *Arabidopsis thaliana* Altered in Epicuticular Wax and Leaf Morphology. *Plant Physiology* **110**, 377-385.

Jetter, R., Kunst, L. and Samuels, A. L. (2008). 4 Composition of plant cuticular waxes. *Annual Plant Reviews, Biology of the Plant Cuticle* **23**, 145.

Johnson, G., Nolan, T. and Bustin, S. (2013). Real-Time Quantitative PCR, Pathogen Detection and MIQE. In *PCR Detection of Microbial Pathogens*, vol. 943 (ed. M. Wilks), pp. 1-16: Humana Press.

Jones, M. G. K., Outlaw, W. H. and Lowry, O. H. (1977). Enzymic Assay of 10^{-7} to 10^{-14} Moles of Sucrose in Plant Tissues. *Plant Physiology* **60**, 379-383.

Jones, R. K. and Windels, C. E. (1991). A management model for Cercospora leaf spot of sugarbeets: University of MinnesotaExtension Service AG-FO-5643-E.

Jung, I.-C., Jeong, I. S. and Kim, C.-S. (2012). Distinction of Internal Tissue of Raw Ginseng Root Using a Computed Tomography Scanner. *Journal of ginseng research* **36**, 469-476.

Karaoglanidis, G. S., Ioannidis, P. M. and Thanassoulopoulos, C. C. (2000). Reduced sensitivity of *Cercospora beticola* isolates to sterol-demethylation-inhibiting fungicides. *Plant Pathology* **49**, 567-572.

Khan, J., Qi, A. and Khan, M. F. R. (2009). Fluctuations in Number of *Cercospora beticola* Conidia in Relationship to Environment and Disease Severity in Sugar Beet. *Phytopathology* **99**, 796-801.

King, R. W. and von Wettstein-Knowles, P. (2000). Epicuticular waxes and regulation of ear wetting and pre-harvest sprouting in barley and wheat. *Euphytica* **112**, 157-166.

Kocal, N., Sonnewald, U. and Sonnewald, S. (2008). Cell Wall-Bound Invertase Limits Sucrose Export and Is Involved in Symptom Development and Inhibition of Photosynthesis during Compatible Interaction between Tomato and Xanthomonas campestris pv vesicatoria. *Plant Physiology* **148**, 1523-1536.

Koch, K., Barthlott, W., Koch, S., Hommes, A., Wandelt, K., Mamdouh, W., De-Feyter, S. and Broekmann, P. (2006a). Structural analysis of wheat wax (Triticum aestivum, c.v. 'Naturastar' L.): from the molecular level to three dimensional crystals. *Planta* **223**, 258-270.

Koch, K. and Ensikat, H.-J. (2008). The hydrophobic coatings of plant surfaces: Epicuticular wax crystals and their morphologies, crystallinity and molecular self-assembly. *Micron* **39**, 759-772.

Koch, K., Hartmann, K. D., Schreiber, L., Barthlott, W. and Neinhuis, C. (2006b). Influences of air humidity during the cultivation of plants on wax chemical composition, morphology and leaf surface wettability. *Environmental and Experimental Botany* **56**, 1-9.

Koch, K., Neinhuis, C., Ensikat, H. J. and Barthlott, W. (2004). Self assembly of epicuticular waxes on living plant surfaces imaged by atomic force microscopy (AFM). *Journal of Experimental Botany* **55**, 711-718.

Kolattukudy, P. (1970). Plant waxes. *Lipids* **5**, 259-275.

Kristensen, A. K., Brunstedt, J., Nielsen, K. K., Roepstorff, P. and Mikkelsen, J. D. (2000). Characterization of a new antifungal non-specific lipid transfer protein (nsLTP) from sugar beet leaves. *Plant Science* **155**, 31-40.

Kunst, L. and Samuels, A. L. (2003). Biosynthesis and secretion of plant cuticular wax. *Progress in Lipid Research* **42**, 51-80.

Lartey, R. T., Weiland, J. J., Caesar-TonThat, T. and Bucklin-Comiskey, S. (2003). A PCR Protocol for Rapid Detection of *Cercospora beticola* in Sugarbeet Tissues. *Journal of Sugar Beet Research* **40**, 1-10.

Lartey, R. T., Weiland, J. J., Panella, L., Crous, P. W. and E., W. C. (2010). *Cercospora* Leaf Spot of Sugar Beet and Related Species, pp. 304. Minnesota: The American Phytopathological Society.

Leal, N. and Lastra, R. (1984). Altered metabolism of tomato plants infected with tomato yellow mosaic virus. *Physiological Plant Pathology* **24**, 1-7.

Levall, M. W. and Bornman, J. F. (2000). Differential response of a sensitive and tolerant sugarbeet line to *Cercospora beticola* infection and UV-B radiation. *Physiologia Plantarum* **109**, 21-27.

Lexander, K. (1980). Present knowledge of sugar-beet bolting mechanisms. In *Proceedings 43rd Winter Congress of the Institut International de Recherches Betteravieres, Brussels.*, pp. 245-258.

Li, Y.-G., Zhang, L. and Mang, F.-M. (2011). Response of *Cercospora beticola* in sugar beet at different cultivars and fertilization level. *African Journal of Microbiology Research* **5**, 5985-5989.

Longden, P. and Goddard, V. (1987). Effects of weed beet on crop yield and processabililty. *Br Sugar Beet Rev* **55**, 10-11.

Lynch, F. J. and Geoghegan, M. J. (1979). Regulation of growth and cercosporin photoinduction in *Cercospora beticola*. *Transactions of the British Mycological Society* **73**, 311-327.

Macri, F., Dellantone, P. and Vianello, A. (1983). Atp-Dependent Proton Uptake Inhibited by *Cercospora-Beticola* Toxin in Pea Stem Microsomal Vesicles. *Plant Cell and Environment* **6**, 555-558.

Mahlein, A. K., Rumpf, T., Welke, P., Dehne, H. W., Plümer, L., Steiner, U. and Oerke, E. C. (2013). Development of spectral indices for detecting and identifying plant diseases. *Remote Sensing of Environment* **128**, 21-30.

Malandrakis, A., Markoglou, A., Nikou, D., Vontas, J. and Ziogas, B. (2006). Biological and molecular characterization of laboratory mutants of *Cercospora beticola* resistant to Qo inhibitors. *European Journal of Plant Pathology* **116**, 155-166.

Märländer, B., Hoffmann, C., Koch, H. J., Ladewig, E., Merkes, R., Petersen, J. and Stockfisch, N. (2003). Environmental Situation and Yield Performance of the Sugar Beet Crop in Germany: Heading for Sustainable Development. In *Journal of Agronomy & Crop Science*, vol. 189, pp. 201-226: Wiley-Blackwell.

Marschner, H., Kirkby, E. A. and Cakmak, I. (1996). Effect of mineral nutritional status on shoot-root partitioning of photoassimilates and cycling of mineral nutrients. *Journal of Experimental Botany* **47**, 1255-1263.

Matsubara, S., Hurry, V., Druart, N., Benedict, C., Janzik, I., Chavarría-Krauser, A., Walter, A. and Schurr, U. (2006). Nocturnal changes in leaf growth of *Populus deltoides* are controlled by cytoplasmic growth. *Planta* **223**, 1315-1328.

McFarlane, J. (1971). Variety development. *Advances in sugarbeet production: principles and practices. The Iowa State University Press, Ames, IA*, 402-435.

Meier, U. (2001). Growth stages of mono-and dicotyledonous plants BBCH Monograph: Federal Biological Research Centre for Agriculture and Forestry.

Mendoza-Mendoza, A., Berndt, P., Djamei, A., Weise, C., Linne, U., Marahiel, M., Vraneš, M., Kämper, J. and Kahmann, R. (2009). Physical-chemical plant-derived signals induce differentiation in *Ustilago maydis*. *Molecular Microbiology* **71**, 895-911.

Metzner, R., van Dusschoten, D., Bühler, J., Schurr, U. and Jahnke, S. (2014). Belowground development of sugar beet measured with Magnetic Resonance Imaging (MRI) *New Phytologist*.

Milford, G. F. J. (1973). The growth and development of storage root of sugar beet. *Annals of Applied Biology* **75**, 427-438.

Mutanga, O. and Skidmore, A. K. (2004). Integrating imaging spectroscopy and neural networks to map grass quality in the Kruger National Park, South Africa. *Remote Sensing of Environment* **90**, 104-115.

Neinhuis, C. and Barthlott, W. (1997). Characterization and Distribution of Water-repellent, Self-cleaning Plant Surfaces. *Annals of Botany* **79**, 667-677.

Nielsen, K., Nielsen, J., Madrid, S. and Mikkelsen, J. (1996). New antifungal proteins from sugar beet (Beta vulgaris L.) showing homology to non-specific lipid transfer proteins. *Plant Molecular Biology* **31**, 539-552.

Nielsen, K. A., Nicholson, R. L., Carver, T. L. W., Kunoh, H. and Oliver, R. P. (2000). First touch: An immediate response to surface recognition in conidia of *Blumeria graminis*. *Physiological and Molecular Plant Pathology* **56**, 63-70.

Nielsen, K. K., Bojsen, K., Collinge, D. B. and Mikkelsen, J. D. (1994). Induced Resistance in Sugar-Beet against *Cercospora-Beticola* - Induction by Dichloroisonicotinic Acid Is Independent of Chitinase and Beta-1,3-Glucanase Transcript Accumulation. *Physiological and Molecular Plant Pathology* **45**, 89-99.

Nilsson, N. O., Hansen, M., Panagopoulos, A. H., Tuvesson, S., Ehlde, M., Christiansson, M., Rading, I. M., Rissler, M. and Kraft, T. (1999). QTL analysis of *Cercospora* leaf spot resistance in sugar beet. *Plant Breeding* **118**, 327-334.

Ollinger, S. V., Smith, M. L., Martin, M. E., Hallett, R. A., Goodale, C. L. and Aber, J. D. (2002). Regional Variation in Foliar Chemistry and N Cycling among Forests of diverse History and Composition. *Ecology* **83**, 339-355.

Pfündel, E. E., Agati, G. and Cerovic, Z. G. (2008). Optical properties of plant surfaces. *Biology of the plant cuticle. Annual Plant Reviews* **23**, 216-249.

Philip, T. and Govindaiah. (1996). Studies on the factors contributing for disease resistance in mulberry against *Cercospora moricola*. *Indian Journal of Sericulture* **35**, 39-42.

Pin, Pierre A., Zhang, W., Vogt, Sebastian H., Dally, N., Büttner, B., Schulze-Buxloh, G., Jelly, Noémie S., Chia, Tansy Y. P., Mutasa-Göttgens, Effie S., Dohm, Juliane C. et al. (2012). The Role of a Pseudo-Response Regulator Gene in Life Cycle Adaptation and Domestication of Beet. *Current Biology* **22**, 1095-1101.

Plaza, A., Valencia, D., Plaza, J. and Martinez, P. (2006). Commodity cluster-based parallel processing of hyperspectral imagery. *Journal of Parallel and Distributed Computing* **66**, 345-358.

Pohlmeier, A., Oros-Peusquens, A., Javaux, M., Menzel, M. I., Vanderborght, J., Kaffanke, J., Romanzetti, S., Lindenmair, J., Vereecken, H. and Shah, N. J. (2008). Changes in Soil Water Content Resulting from Ricinus Root Uptake Monitored by Magnetic Resonance Imaging. *Vadose Zone J.* **7**, 1010-1017.

Pool, V. W. and McKay, M. (1916). Relation of stomatal movement to infection by *Cercospora beticola*. *Journal of Agricultural Research* **5**, 1011-1038.

Powell, G., Maniar, S., Pickett, J. and Hardie, J. (1999). Aphid responses to non-host epicuticular lipids. In *Proceedings of the 10th International Symposium on Insect-Plant Relationships*, vol. 56 eds. S. Simpson A. J. Mordue and J. Hardie), pp. 115-123: Springer Netherlands.

Prell, H. H. (1996). Interaktion von Pflanzen und phytopathogenen Pilzen: Gustav Fischer Verlag Jena, Stuttgart.

Rabbinge, R., Jorritsma, I. T. M. and Schans, J. (1985). Damage components of powdery mildew in winter wheat. *Netherlands Journal of Plant Pathology* **91**, 235-247.

Rascher, U., Agati, G., Alonso, L., Cecchi, G., Champagne, S., Colombo, R., Damm, A., Daumard, F., de Miguel, E., Fernandez, G. et al. (2009). CEFLES2: the remote sensing component to quantify photosynthetic efficiency from the leaf to the region by measuring sun-induced fluorescence in the oxygen absorption bands. *Biogeosciences* **6**, 1181-1198.

Rascher, U., Blossfeld, S., Fiorani, F., Jahnke, S., Jansen, M., Kuhn, A. J., Matsubara, S., Märtin, L. L. A., Merchant, A., Metzner, R. et al. (2011). Non-invasive approaches for phenotyping of enhanced performance traits in bean. *Functional Plant Biology* **38**, 968-983.

Rascher, U., Lüttge, U. and Freiberg, M. (2012). Functional diversity of photosynthetic light use of sixteen vascular epiphyte species under fluctuating irradiance in the canopy of a giant Virola michelii (Myristicaceae) tree in the tropical lowland forest of French Guyana. *Frontiers in Plant Science* **2**.

Rathaiah, Y. (1976). Infection of Sugarbeet by *Cercospora beticola* in Relation to Stornatal Condition. *Phytopathology* **66**, 737-740.

Raven, P. H., Evert, R. F. and Eichhorn, S. E. (2006). Biologie der Pflanze: de Gruyter.

Rich, P. (1994). Quantitative and qualitative characterization of epicuticular wax from chemically induced bloomless and sparse bloom mutants of Sorghum bicolor: PhD thesis. Purdue University, West Lafayette, IN.

Robert, C., Bancal, M.-O., Lannou, C. and Ney, B. (2006). Quantification of the effects of Septoria tritici blotch on wheat leaf gas exchange with respect to lesion age, leaf number, and leaf nitrogen status. *Journal of Experimental Botany* **57**, 225-234.

Rossi, V. (1995). Effect of host resistance in decreasing infection rate of *Cercospora* leaf spot epidemics on sugarbeet. *Phytopathologia Mediterranea* **34**, 149-156.

Rossi, V. and Battilani, P. (1989). Assessment of Intensity of *Cercospora* Disease on Sugarbeet. I. In *Einschätzung der Cercospora-Befallsintensität in Zuckerrüben. I.*, vol. 124, pp. 63-66: Wiley-Blackwell.

Rossi, V., Battilani, P., Chiusa, G., Giosue, S., Languasco, L. and Racca, P. (1999). Components of rate-reducing resistance to *Cercospora* leaf spot in sugar beet: Incubation length, infection efficiency, lesion size. *Journal of Plant Pathology* **81**, 25-35.

Rossi, V., Battilani, P., Chiusa, G., Giosue, S., Languasco, L. and Racca, P. (2000). Components of rate-reducing resistance to *Cercospora* leaf spot in sugar beet: Conidiation length, spore yield. *Journal of Plant Pathology* **82**, 125-131.

Rouse, J. W., R.H. Haas, J.A. Schell, and D.W. Deering. (1973). Monitoring Vegetation Systems in the Great Plains with ERTS. *Third ERTS Symposium, NASA SP-351*, 309-317.

Rumpf, T., Mahlein, A. K., Steiner, U., Oerke, E. C., Dehne, H. W. and Pluemer, L. (2010). Early detection and classification of plant diseases with Support Vector Machines based on hyperspectral reflectance. *Computers and Electronics in Agriculture* **74**, 91-99.

Saberioon, M., Amin, M., Aimrun, W., Anuar, A. and Gholizadeh, A. (2013). Multi-Spectral Images Tetracam Agriculture Digital Camera to Estimate Nitrogen and Grain Yield of Rice at Different Growth Stages. *The Philippine Agricultural Scientist* **96**.

Saito, K.-I. (1966). Studies on the *Cercospora* Leaf Spot Resistance in Sugar Beet Breeding. *Memoirs of the Research Faculty of Agriculture, Hokkaido University* **6**, 113-179.

Samson, B. and Sinclair, T. (1994). Soil core and minirhizotron comparison for the determination of root length density. *Plant and Soil* **161**, 225-232.

Schäfer-Pregl, R., Borchardt, D. C., Barzen, E., Glass, C., Mechelke, W., Seitzer, J. F. and Salamini, F. (1999). Localization of QTLs for tolerance to *Cercospora beticola* on sugar beet linkage groups. *Theoretical and Applied Genetics* **99**, 829-836.

Schmidt, E. W. (1928). Untersuchungen über die *Cercospora*-Blattfleckenkrankheit der Zuckerrübe. *Parasitology Research* **1**, 100-137.

Schmidt, K., Heberle, B., Kurrasch, J., Nehls, R. and Stahl, D. J. (2004). Suppression of phenylalanine ammonia lyase expression in sugar beet by the fungal pathogen *Cercospora beticola* is mediated at the core promoter of the gene. *Plant Molecular Biology* **55**, 835-852.

Schmidt, K., Pflugmacher, M., Klages, S., Maser, A., Mock, A. and Stahl, D. J. (2008). Accumulation of the hormone abscisic acid (ABA) at the infection site of the fungus *Cercospora beticola* supports the role of ABA as a repressor of plant defence in sugar beet. *Molecular Plant Pathology* **9**, 661-673.

Schmittgen, S., Jansen, M., Walter, A. and Westhoff, P. (2011). Einfluss des Nährstoffangebots auf Biomasse-Allokation in Spross bzw. Wurzel in ausgewählten Energie- und Kulturpflanzen: Heinrich-Heine-Universität, Düsseldorf.

Schneider, K., Schafer-Pregl, R., Borchardt, D. C. and Salamini, F. (2002). Mapping QTLs for sucrose content, yield and quality in a sugar beet population fingerprinted by EST-related markers. *Theoretical and Applied Genetics* **104**, 1107-1113.

Scholes, J. (1992). Photosynthesis: cellular and tissue aspects in diseased leaves. *Envionmental Plant Biology Series*, 85-106.

Scholes, J. D. and Rolfe, S. A. (1996). Photosynthesis in localised regions of oat leaves infected with crown rust (*Puccinia coronata*): quantitative imaging of chlorophyll fluorescence. *Planta* **199**, 573-582.

Seelig, H.-D., Hoehn, A., Stodieck, L. S., Klaus, D. M., Adams, W. W. I. and Emery, W. J. (2008). Relations of remote sensing leaf water indices to leaf water thickness in cowpea, bean, and sugarbeet plants. *Remote Sensing of Environment* **112**, 445-455.

Setiawan, A., Koch, G., Barnes, S. R. and Jung, C. (2000). Mapping quantitative trait loci (QTLs) for resistance to *Cercospora* leaf spot disease (*Cercospora beticola Sacc.*) in sugar beet (*Beta vulgaris L.*). *Theoretical and Applied Genetics* **100**, 1176-1182.

Shane, W. W. and Teng, P. S. (1992). Impact of *Cercospora* Leaf Spot on Root Weight, Sugar Yield and Purity of *Beta Vulgaris*. *Plant Disease* **76**, 812-820.

Singh, D. P. (2005). Disease and insect resistance in plants.

Skaracis, G., Pavli, O. and Biancardi, E. (2010). *Cercospora* Leaf Spot Disease of Sugar Beet. *Sugar Tech* **12**, 220-228.

Skaracis, G. N. and Biancardi, E. (2000). Breeding for *Cercospora* resistance in sugarbeet - *Cercospora beticola Sacc.* biology, agronomic influence and control measures in sugar beet.

Skidmore, A. K., Ferwerda, J. G., Mutanga, O., Van Wieren, S. E., Peel, M., Grant, R. C., Prins, H. H. T., Balcik, F. B. and Venus, V. (2010). Forage quality of savannas — Simultaneously mapping foliar protein and polyphenols for trees and grass using hyperspectral imagery. *Remote Sensing of Environment* **114**, 64-72.

Smith, G. A. and Campbell, L. G. (1996). Association between resistance to *Cercospora* and yield in commercial sugarbeet hybrids. *Plant Breeding* **115**, 28-32.

Smith, G. A. and Ruppel, E. G. (1974). Herability of Resistance to *Cercospora* Leaf Spot in Sugarbeet1. *Crop Science* **14**, 113-115.

Solel, Z. and Minz, G. (1971). Infection process of *Cercospora beticola* in sugarbeet in relation to susceptibility. *Phytopathology* **61**, 463-466.

Steinkamp, M. P., Martin, S. S., Hoefert, L. L. and Ruppel, E. G. (1979). Ultrastructure of lesions produced by *Cercospora beticola* in leaves of *Beta vulgaris*. *Physiological Plant Pathology* **15**, 13-26.

Swarbrick, P. J., Schulze-Lefert, P. and Scholes, J. D. (2006). Metabolic consequences of susceptibility and resistance (race-specific and broad-spectrum) in barley leaves challenged with powdery mildew. *Plant, Cell & Environment* **29**, 1061-1076.

Taguchi, K., Kubo, T., Takahashi, H. and Abe, H. (2011). Identification and Precise Mapping of Resistant QTLs of *Cercospora* Leaf Spot Resistance in Sugar Beet (*Beta vulgaris L.*). *G3 Genes Genomes Genetics* **1**, 283-91.

Terry, N. (1968). Developmental Physiology of Sugar Beet I. Influence of Light and Temperature on Growth. *Journal of Experimental Botany* **19**, 795-&.

Theurer, J. (1993). Pre-breeding to change sugarbeet root architecture. *J. Sugar Beet Res* **30**, 221-239.

Trebbi, D. and McGrath, J. M. (2009). Functional differentiation of the sugar beet root system as indicator of developmental phase change. In *Physiologia Plantarum*, vol. 135, pp. 84-97.

Trout, T. J., Johnson, L. F. and Gartung, J. (2008). Remote Sensing of Canopy Cover in Horticultural Crops. *HortScience* **43**, 333-337.

Tsuba, M., Katagiri, C., Takeuchi, Y., Takada, Y. and Yamaoka, N. (2002). Chemical factors of the leaf surface involved in the morphogenesis of *Blumeria graminis*. *Physiological and Molecular Plant Pathology* **60**, 51-57.

Tucker, C. J. (1977). Asymptotic nature of grass canopy spectral reflectance. *Applied Optics* **16**, 1151-1156.

Tucker, C. J. (1978). A comparison of satellite sensor bands for vegetation monitoring. *Photogrammetric Engineering and Remote Sensing*.

Van As, H. (2007). Intact plant MRI for the study of cell water relations, membrane permeability, cell-to-cell and long distance water transport. *Journal of Experimental Botany* **58**, 743-756.

Van As, H., Homan, N., Vergeldt, F. J. and Windt, C. W. (2007). Soil–Plant–Atmosphere Continuum Studied by MRI. In *eMagRes*: John Wiley & Sons, Ltd.

Van As, H. and van Duynhoven, J. (2013). MRI of plants and foods. *Journal of Magnetic Resonance* **229**, 25-34.

Van Oijen, M. (1990). Photosynthesis is not impaired in healthy tissue of blighted potato plants. *Netherlands Journal of Plant Pathology* **96**, 55-63.

Von Thümen, F. (1886). Die Bekämpfung der Pilzkrankheiten unserer Culturgewächse: Versuch einer Pflanzentherapie zum praktischen Gebrauche für Land-und Forstwirthe, Gärtner, Obst-und Weinzüchter: Faesy.

Von Wettstein-Knowles, P. (1974). Ultrastructure and origin of epicuticular wax tubes. *Journal of Ultrastructure Research* **46**, 483-498.

Waggoner, P. E. and Berger, R. D. (1987). Defoliation, disease, and growth. *Phytopathology* **77**, 393-398.

Walter, A., Feil, R. and Schurr, U. (2002). Restriction of nyctinastic movements and application of tensile forces to leaves affects diurnal patterns of expansion growth. *Functional Plant Biology* **29**, 1247-1258.

Walter, A. and Schurr, U. (1999). The modular character of growth in *Nicotiana tabacum* plants under steady-state nutrition. *Journal of Experimental Botany* **50**, 1169-1177.

Weiland, J. and Koch, G. (2004). Sugarbeet leaf spot disease (*Cercospora beticola Sacc.*). *Molecular Plant Pathology* **5**, 157-166.

Weiland, J. J. and Sundsbak, J. L. (2000). Differentiation and Detection of Sugar Beet Fungal Pathogens Using PCR Amplification of Actin Coding Sequences and the ITS Region of the rRNA Gene. *Plant Disease* **84**, 475-482.

Weishaupt, D., Koechli, V. D. and Marincek, B. (2009). Wie funktioniert MRI?: Springer Berlin.

Weltmeier, F., Maser, A., Menze, A., Hennig, S., Schad, M., Breuer, F., Schulz, B., Holtschulte, B., Nehls, R. and Stahl, D. J. (2011). Transcript Profiles in Sugar Beet Genotypes Uncover Timing and Strength of Defense Reactions to *Cercospora beticola* Infection. *Molecular Plant Microbe Interaction* **24**, 758-72.

West, J. S., Bravo, C., Oberti, R., Lemaire, D., Moshou, D. and McCartney, H. A. (2003). The potential of optical canopy measurement for targeted control of field crop diseases. *Annual Review of Phytopathology* **41**, 593-614.

Whitney, E. D. and Lewellen, R. T. (1976). Identification and distribution of race C1 and C2 of *Cercospora beticola* from sugarbeet. *Phytopathology* **66**, 1158-1160.

Wicke, G., Vollhardt, D. and Richter, L. (1993). Beeinflussung der Benetzung von Blattoberflächen durch Tenside. *Archives Of Phytopathology And Plant Protection* **28**, 365-370.

Wolf, P., Heindl, M. and Verreet, J. (2001a). Zum Einfluss des Bestandesklimas auf die Prädisposition der Zuckerrübe gegenüber Infektionen von *Cercospora beticola* (Sacc.). *Zeitschrift für Pflanzenkrankheiten und Pflanzenschutz* **108**, 578-592.

Wolf, P., Weis, F. and Verreet, J. (2001b). Bekämpfungsschwellen als Indikatoren des Fungizideinsatzes zur Kontrolle des Blattbefalls von *Cercospora beticola* (Sacc.) in Zuckerrüben. *Journal of Plant Diseases and Protection* **108**, 244-257.

Wolf, P. F. J., Kraft, R. and Verreet, J. A. (1998). Characteristics of damage caused by *Cercospora beticola* (Sacc.) in sugar beet as a base of yield loss forecast. *Journal of Plant Diseases and Protection* **105**, 462-474.

Wright, A. J., Carver, T. L. W., Thomas, B. J., Fenwick, N. I. D., Kunoh, H. and Nicholson, R. L. (2000). The rapid and accurate determination of germ tube emergence site by Blumeria graminis conidia. *Physiological and Molecular Plant Pathology* **57**, 281-301.

Wynn, W. and Staples, R. (1981). Tropisms of fungi in host recognition. *Plant disease control: Resistance and susceptibility*, 45-69.

Zamski, E. and Azenkot, A. (1981). Surgarbeet Vasculature. 1. Cambial Development and the 3-Dimensional Structure of the Vascular System. *Botanical Gazette* **142**, 334-343.

Zhang, J., Stewart, J. and Mac. (2000). Economical and rapid method for extracting cotton genomic DNA. *J. Cotton Sci* **4**, 193-201.

Zhu, J., Ingram, P. A., Benfey, P. N. and Elich, T. (2011). From lab to field, new approaches to phenotyping root system architecture. *Current Opinion in Plant Biology* **14**, 310-317.

10 Attachment

10.1 BLAST analysis

A BLAST analysis[7] was used to to compare the calmodulin genes of *C. beticola* (EMBL-EBI, DQ026493) and C. *apii* (EMBL-EBI, AY840414.1).

```
>gb|AY840414.1|  Cercospora apii strain CBS 114416 calmodulin (cmdA) gene, partial

Cds Length=301

         Score      =            484      bits      (262),            Expect      =      2e-138
         Identities       =       287/299       (96%),       Gaps       =       2/299       (1%)
         Strand=Plus/Plus

Query  1    TTCAAGGAGGCCTTCTCTCTCTTCGTACGTACAGTTTTCTGAAACAATCAGGCAGCCGCG  60    C.beticola

            ||||||||||||||||||||||||||||||||||||||||||||||||||||||||||||

Sbjct  4    TTCAAGGAGGCCTTCTCTCTCTTCGTACGTACAGTTTTCTGAAACAATCAGGCAGCCGCG  63    C.apii


Query  61   AGGCAGAGCTAACGACAGCAACACAGGACAAGGACGGCGATGGTATGATGTGCGCCCACC  120

            ||||||||||||||| |||| ||||||||||||||||||||||||| ||||| |||||

Sbjct  64   AGGCAGAGCTAACGAGAGCACCACAGGACAAGGACGGCGATGGTATGAAGTGCGACCACC  123

               F
Query  121  CTCTGCGAA-TGTACTGAACTAACCTCGACCGAAGGACAAATCACCACCAAGGAGCTCGG  179

            |||||| || ||  ||||||||| ||| ||||||||||||||||||||||||||||||

Sbjct  124  CTCTGC-AACTGCGCTGAACTAATCTCAACCGAAGGACAAATCACCACCAAGGAGCTCGG  182


Query  180  CACTGTCATGCGCTCCCTCGGCCAGAACCCCAGCGAGTCTGAGCTGCAGGACATGATCAA  239

            ||||||||||||||||||||||||||||||||||||||||||||||||||||||||||||

Sbjct  183  CACTGTCATGCGCTCCCTCGGCCAGAACCCCAGCGAGTCTGAGCTGCAGGACATGATCAA  242

                                                                    R
Query  240  CGAAGTCGACGCCGACAACAACGGCACAATCGATTTCCCCGAATTCCTCACCATGATGG  298

             || ||||||||||||||||||||||||||||||||||||||||||||||||||||||||

Sbjct  243  TGAGGTCGACGCCGACAACAACGGCACAATCGATTTCCCCGAATTCCTCACCATGATGG  301
```

[7] http://blast.ncbi.nlm.nih.gov

Acknowledgements

I would like to thank all the people who have supported me during my PhD. Thank you for the pleasant working environment, the good collegial banter and all your help.

In particular, I would like to thank my supervisor team, Dr. Fabio Fiorani, Dr. Marcus Jansen and Prof. Dr. Uwe Rascher for giving me continual support, endless patience, valuable advice and scientific discussions during the last three years.

I would like to thank Prof. Dr. Ulrich Schurr for allowing me to perform my experiments at the institute of plant sciences (IBG-2) as part of the Forschungszentrum Jülich. I am also very grateful to Prof. Dr. Peter Westhoff at the Heinrich Heine University of Düsseldorf, who kindly agreed to act as referee of my work.

I would like to thank Dr. Werner Beyer and Dr. Madlaina Peter for providing sugar beet genotypes for the experimental work and the possibility to conduct the field experiment as well as for the pleasant email correspondence and chats.

I would like to thank Sergej Bergsträsser for his work and analyses in our joint project.

I appreciate the kind welcome at the department of Ecophysiology (IZMB, University of Bonn, Germany) and would like to thank Prof. Dr. Lukas Schreiber for the opportunity to perform my experiments. Thanks to Friedrich Waßmann for his help and explanations about GC.

Dr. Jessica Knüfer and Dr. Carmen Müllenborn deserve very special thanks for enticing me into the world of pathogens.

I am very grateful to Dr. Michaela Ernst for showing me that statistics can be fascinating. I enjoyed our lunch breaks and trips back home.

I would like to thank Dr. Ralf Metzner, Dr. Dagmar van Dusschoten and Dr. Siegfried Jahnke for all the MRI-related advice and discussions.

I would also like to thank Dr. Gerd Roeb for all the information and discussions about sugar beet.

I would like to thank Dr. Tobias Wojciechowski for his contribution to the wax analysis.

I am very grateful to Dr. Walter Schröder, who invited me to amazing SEM imaging.

Special thanks go to Prof. Dr. Ingar Janzik, Sabine Preiskowski and Esther Breuer for helping me out with all my questions related to molecular biology. I would also like to thank Dr. Shizue Matzubara and Dr. Anika Wiese-Klingenberg for providing valuable questions and thoughts.

I would like to thank Catalin Voiniciuc for his kindly offer to proof-read my thesis.

I would like to thank Dr. Onno Muller for his spontaneous readiness to help me with photosynthesis measurements.

I would like to thank Isabell Meuser, Thomas Hombach, Dr. Christina Schreiber, Lothar Pieta and Sven Süßmilch for hosting me in their cars, while having pleasant talks.

I would like to thank Christoph Briese, Olaf Gardeick, Dr. Adi Kesseler, Dr. Roland Pieruschka and Dr. Heike Schneider for introducing me to the Indian side.

I would like to thank Niels Banek, Thomas Bodewein, Dr. Regina Braun, Vera Lisa Hecht, Dr. Tom Ruts, Marcel Schneider and Beate Uhlig for their support and the nice breaks from work.

Finally, I would like to thank my family for their patient ears, helpful discussions, encouragement and love. In particular, I appreciate my mother's strength.

Thank you, Michael Röhlen, for your encouragement, your never-ending ideas and for picking me up when something did not go according to plan. I am so glad to have met you in Jülich.

Band / Volume 230
Data Processing and Trace Gas Retrievals for the GLORIA Limb Sounder
T. Guggenmoser (2014), xi, 111, XXVI
ISBN: 978-3-89336-993-5

Band / Volume 231
Assessment of Laser Induced Ablation Spectroscopy (LIAS) as a method for quantitative in situ surface diagnostic in plasma environments
N. Gierse (2014), 199 pp
ISBN: 978-3-89336-994-2

Band / Volume 232
Lattice-Boltzmann-Simulation in faserbasierten Mikrostrukturen
J. P. Brinkmann (2014), viii, 129 pp
ISBN: 978-3-89336-995-9

Band / Volume 233
Numerische Simulationen von Abfallgebinden aus der Wiederaufarbeitung von Kernbrennstoffen
S. Schneider (2014), 201 pp
ISBN: 978-3-89336-998-0

Band / Volume 234
Materials for Advanced Power Engineering 2014
J. Lecomte-Beckers, O. Dedry, J. Oakey, B. Kuhn (Ed.)
(2014), xxi, 930, viii pp
ISBN: 978-3-95806-000-5

Band / Volume 235
Untersuchungen zur Abtrennung, Konversion und Transmutation von langlebigen Radionukliden
Ein Beitrag zur fortschrittlichen Entsorgung von hochradioaktiven Abfällen
G. Modolo (2014), 291 pp
ISBN: 978-3-95806-005-0

Band / Volume 236
Keramische Membranen für die H_2-Abtrennung in CO-Shift-Reaktoren
D. van Holt (2014), IV, 169 pp
ISBN: 978-3-95806-007-4

Band / Volume 237
Entwicklung von porösen Silica-Membranen zur CO_2-Abtrennung aus dem Rauchgas fossil befeuerter Kraftwerke
J. S. Eiberger (2014), II, 163 pp
ISBN: 978-3-95806-008-1

Schriften des Forschungszentrums Jülich
Reihe Energie & Umwelt / Energy & Environment

Band / Volume 238
Development of a highly sensitive and versatile mass spectrometer system for laboratory and atmospheric measurements
S. Albrecht (2014), iv, 171 pp
ISBN: 978-3-95806-009-8

Band / Volume 239
High Temperature Corrosion of Alloys and Coatings in Gas-Turbines Fired with Hydrogen-Rich Syngas Fuels
W. Nowak (2014), 201 pp
ISBN: 978-3-95806-012-8

Band / Volume 240
Einfluss neuer Membranmaterialien auf Herstellung und Betrieb von Direktmethanol-Brennstoffzellen
S. Hürter (2014), V, 164 pp
ISBN: 978-3-95806-013-5

Band / Volume 241
Spannungsinduziertes Versagen in Hochtemperaturschichtsystemen
C. Nordhorn (2014), v, 118 pp
ISBN: 978-3-95806-016-6

Band / Volume 242
Änderungsdetektion digitaler Fernerkundungsdaten mittels objekt-basierter Bildanalyse
C. Listner (2014), 176 pp
ISBN: 978-3-95806-017-3

Band / Volume 243
Räumlich hoch aufgelöste Modellierung des Spaltprodukt-verhaltens in einem HTR-Core mit kugelförmigen oder prismatischen Brennelementen
A. Xhonneux (2014), viii, 239 pp
ISBN: 978-3-95806-020-3

Band / Volume 244
Effects of *Cercospora* leaf spot disease on sugar beet genotypes with contrasting disease susceptibility

Energie & Umwelt /
Energy & Environment
Band / Volume 244
ISBN 978-3-95806-021-0